REFERENCES

Adachi, K., Nakamoto, T., and Kotaka, T. (1989) Swelling equilibrium of solution cross-linked polybutadiene networks in polyisoprene solutions. Macromolecules, 22(7), 3106-3111.

Al Minnath, M., Unnikrishnan, G., and Purushothaman, E. (2011) Transport studies of thermoplastic polyurethane/natural rubber (TPU/NR) blends. Journal of Membrane Science, 379(1-2), 361-369.

Anonymous (1990) Drug releases. Geriatric Nursing, 11(4), 206.

Anonymous (2003) Conductive polymers. Plastics Engineering, 59(7), 84.

Ansari, M., Kazemipour, M., and Aklamli, M. (2006) The study of drug permeation through natural membranes. International Journal of Pharmaceutics, 327(1-2), 6-11.

Bagheri, H., Ayazi, Z., and Naderi, M. (2013) Conductive polymer-based microextraction methods: A review. Analytica Chimica Acta, 767(0), 1-13.

Bailly, N., Thomas, M., and Klumperman, B. (2012) Poly(N-vinylpyrrolidone)-block-poly(vinyl acetate) as a drug delivery vehicle for hydrophobic drugs. Biomacromolecules, 13(12), 4109-4117.

Bussière, P.O., Gardette, J.L., Lacoste, J., and Baba, M. (2005) Characterization of photodegradation of polybutadiene and polyisoprene: chronology of crosslinking and chain-scission. Polymer Degradation and Stability, 88(2), 182-188.

Cabaniss, S.E. and McVey, I.F. (1995) Aqueous infrared carboxylate absorbances: aliphatic monocarboxylates. Spectrochimica Acta Part A: Molecular and Biomolecular Spectroscopy, 51(13), 2385-2395.

Chansai, P., Sirivat, A., Niamlang, S., Chotpattananont, D., and Viravaidya-Pasuwat, K. (2009) Controlled transdermal iontophoresis of sulfosalicylic acid from polypyrrole/poly(acrylic acid) hydrogel. International Journal of Pharmaceutics, 381(1), 25-33.

Choi, S.S., Hong, J.P., Seo, Y.S., Chung, S.M., and Nah, C. (2006) Fabrication and characterization of electrospun polybutadiene fibers crosslinked by UV irradiation. Journal of Applied Polymer Science, 101(4), 2333-2337.

Chou, H.-W. and Huang, J.-S. (2008) Effects of ultraviolet irradiation on the static and dynamic properties of neoprene rubbers. Journal of Applied Polymer Science, 110(5), 2907-2913.

Debjit Bhowmik, C., Chiranjib ,Chandira, M., Jayakar, B., and Sampath, K.P. (2010) Recent advances in transdermal drug delivery system. International Journal of PharmTech Research, 2(1), 68-77

Decker, C. (1998) The use of UV irradiation in polymerization. Polymer International, 45(2), 133-141.

Deng, J., Wang, L., Liu, L., and Yang, W. (2009) Developments and new applications of UV-induced surface graft polymerizations. Progress in Polymer Science, 34(2), 156-193.

Di Colo, G., Carelli, V., Nannipieri, E., Serafini, M.F., and Vitale, D. (1986) Effect of water-soluble additives on drug release from silicone rubber matrices. II. Sustained release of prednisolone from non-swelling devices. International Journal of Pharmaceutics, 30(1), 1-7.

Dupeyron, D., Kawakami, M., Ferreira, A.M., Caceres-Velez, P.R., Rieumont, J., Azevedo, R.B., and Carvalho, J.C. (2013) Design of indomethacin-loaded nanoparticles: effect of polymer matrix and surfactant. International Journal of Nanomedicine, 8, 3467-3477.

Durmaz, S., Fank, S., and Okay, O. (2002) Swelling and mechanical properties of solution-crosslinked poly(isobutylene) gels. Macromolecular Chemistry and Physics, 203(4), 663-672.

Fan, Q., Sirkar, K.K., and Michniak, B. (2008) Iontophoretic transdermal drug delivery system using a conducting polymeric membrane. Journal of Membrane Science, 321(2), 240-249.

Fanning, R. and Bekkedahl, N. (1951) Quantitative determination of natural rubber hydrocarbon by refractive index measurements. Analytical Chemistry, 23(11), 1653-1656.

Ge, J., Neofytou, E., Cahill, T.J., Beygui, R.E., and Zare, R.N. (2011) Drug release from electric-field-responsive nanoparticles. ACS Nano, 6(1), 227-233.

Geer, W.C. (1922) Recent developments in the chemistry of rubber. Journal of Industrial & Engineering Chemistry, 14(5), 369-374.

George, S.C. and Thomas, S. (2001) Transport phenomena through polymeric systems. Progress in Polymer Science, 26(6), 985-1017.

Georgoulis, L.B., Morgan, M.S., Andrianopoulos, N., and Seferis, J.C. (2005) Swelling of polymeric glove materials during permeation by solvent mixtures. Journal of Applied Polymer Science, 97(3), 775-783.

González, L., Rodríguez, A., del Campo, A., and Marcos-Fernández, A. (2000) Some aspects on the crosslink reaction of natural rubber with dipentamethylene thiuram tetrasulfide. Rubber Chemistry and Technology, 73(1), 89-100.

Grazulevicius, J.V., Strohriegl, P., Pielichowski, J., and Pielichowski, K. (2003) Carbazole-containing polymers: synthesis, properties and applications. Progress in Polymer Science, 28(9), 1297-1353.

Grenquist, E.A. (1930) Structural changes during the processing of rubber1. Industrial & Engineering Chemistry, 22(7), 759-765.

Gupta, B. and Prakash, R. (2010) Interfacial polymerization of carbazole: Morphology controlled synthesis. Synthetic Metals, 160(5-6), 523-528.

Herculano, R.D., Alencar de Queiroz, A.A., Kinoshita, A., Oliveira Jr, O.N., and Graeff, C.F.O. (2011) On the release of metronidazole from natural rubber latex membranes. Materials Science and Engineering: C, 31(2), 272-275.

Herculano, R.D., Guimarães, S.A.C., Belmonte, G.C., Duarte, M.A.H., Oliveira Júnior, O.N.d., Kinoshita, A., and Graeff, C.F.d.O. (2010) Metronidazole release using natural rubber latex as matrix. Materials Research, 13, 57-61.

Herculano, R.D., Silva, C.P., Ereno, C., Guimaraes, S.A.C., Kinoshita, A., and Graeff, C.F.d.O. (2009) Natural rubber latex used as drug delivery system in guided bone regeneration (GBR). Materials Research, 12, 253-256.

Higuchi, T. (1961) Rate of release of medicaments from ointment bases containing drugs in suspension. Journal of Pharmaceutical Sciences, 50(10), 874-875.

Huang, X., Li, C., Zhu, W., Zhang, D., Guan G., and Xiao, Y. (2011) Ultraviolet-induced crosslinking of poly(butylene succinate) and its thermal property, dynamic mechanical property, and biodegradability. Polymers for Advanced Technologies, 22(5), 648-656.

Hungaro Oliveira Júnior, O.N., Kinoshita, A., and Graeff, C.F.O. (2010) Metronidazole release using natural rubber latex as matrix. Materials Research, 13, 57-61.

Ick Chan, K., You Han, B., and Sung Wan, K. (1991) Electrically erodible polymer gel for controlled release of drugs. Nature, 354(6351), 291-293.

Iraqi, A. and Wataru, I. (2004) 3,6-linked 9-alkyl-9H-carbazole main-chain polymers: Preparation and properties. Journal of Polymer Science Part A: Polymer Chemistry, 42(23), 6041-6051.

Jayasuriya, M.M., Makuuchi, K., and Yoshi, F. (2001) Radiation vulcanization of natural rubber latex using TMPTMA and PEA. European Polymer Journal, 37(1), 93-98.

Jiang, S., Sun, Y., Cui, X., Huang, X., He, Y., Ji, S., Shi, W., and Ge, D. (2013) Enhanced drug loading capacity of polypyrrole nanowire network for controlled drug release. Synthetic Metals, 163(0), 19-23.

Juntanon, K., Niamlang, S., Rujiravanit, R., and Sirivat, A. (2008) Electrically controlled release of sulfosalicylic acid from crosslinked poly(vinyl alcohol) hydrogel. International Journal of Pharmaceutics, 356(1-2), 1-11.

Kalia, Y.N. and Guy, R.H. (2001) Modeling transdermal drug release. Advanced Drug Delivery Reviews, 48(2-3), 159-172.

Korsmeyer, R. W., Gurny, R., Doelker, E., Buri, P., and Peppas, N.A. (1983) Mechanisms of solute release from porous hydrophilic polymers. International Journal of Pharmaceutics, 15(1), 25-35.

Kumar, D. and Sharma, R.C. (1998) Advances in conductive polymers. European Polymer Journal, 34(8), 1053-1060.

Li Yan, Q. and You Han, B. (2006) Polymer architecture and drug delivery. Pharmaceutical Research, 23(1), 1-30.

Lowman, A.M. and Peppas, N.A. (1999) Hydrogels. Encyclopedia of controlled drug delivery, 1, 397-418.

Luo, X. and Cui, X.T. (2009) Sponge-like nanostructured conducting polymers for electrically controlled drug release. Electrochemistry Communications, 11(10), 1956-1959.

Miller, L.L., Zinger, B., and Zhou, Q.X. (1987) Electrically controlled release of hexacyanoferrate(4-) from polypyrrole. Journal of the American Chemical Society, 109(8), 2267-2272.

Morin, J.-F., Leclerc, M., Adès, D., and Siove, A. (2005) Polycarbazoles: 25 years of progress. Macromolecular Rapid Communications, 26(10), 761-778.

Mwangi, J.W. and Ofner Iii, C.M. (2004) Crosslinked gelatin matrices: release of a random coil macromolecular solute. International Journal of Pharmaceutics, 278(2), 319-327.

Naddaka, M., Mondal, E., and Lellouche, J.-P. (2011) Oxidative fabrication of spherical polycarbazole-based microparticles. Materials Letters, 65(8), 1165-1167.

Niamlang, S. and Sirivat, A. (2009) Electrically controlled release of salicylic acid from poly(p-phenylene vinylene)/polyacrylamide hydrogels. International Journal of Pharmaceutics, 371(1-2), 126-133.

Paradee, N., Sirivat, A., Niamlang, S., and Prissanaroon-Ouajai, W. (2012) Effects of crosslinking ratio, model drugs, and electric field strength on electrically controlled release for alginate-based hydrogel. Journal of Materials Science, 23, 999-1010.

Peppas, N.A. and Merrill, E.W. (1977) Crosslinked poly(vinyl alcohol) hydrogels as swollen elastic networks. Journal of Applied Polymer Science, 21(7), 1763-1770.

Phinyocheep, P. and Duangthong, S. (2000) Ultraviolet-curable liquid natural rubber. Journal of Applied Polymer Science, 78(8), 1478-1485.

Phumman, P., Niamlang, S., and Sirivat, A. (2009) Fabrication of poly(*p* Phenylene)/ zeolite composites and their responses towards ammonia. Sensors, 9, 8031-8046.

Pichayakorn, W., Suksaeree, J., Boonme, P., Amnuaikit, T., Taweepreda, W., and Ritthidej, G.C. (2012) Deproteinized natural rubber latex/hydroxylpropyl methyl cellulose blending polymers for nicotine Matrix films. Industrial & Engineering Chemistry Research, 51(25), 8442-8452.

Pichayakorn, W., Suksaeree, J., Boonme, P., Amnuaikit, T., Taweepreda, W., and Ritthidej, G.C. (2012) Nicotine transdermal patches using polymeric natural rubber as the matrix controlling system: Effect of polymer and plasticizer blends. Journal of Membrane Science, 411-412(0), 81-90.

Pongjanyakul, T., Prakongpan, S., and Priprem, A. (2003) Acrylic matrix type nicotine transdermal patches: in vitro evaluations and batch-to-batch uniformity. Drug Development and Industrial Pharmacy, 29(8), 843-853.

Prausnitz, M.R. and Langer, R. (2008) Transdermal drug delivery. Nature Biotechnology, 26(11), 1261-1268.

Qin, R. and Bo, Z. (2012) Synthesis and characterization of 2,7-linked carbazole oligomers. Macromolecular Rapid Communications, 33(1), 87-91.

Raj, V., Madheswari, D., and Mubarak Ali, M. (2010) Chemical formation, characterization and properties of polycarbazole. Journal of Applied Polymer Science, 116(1), 147-154.

Rettler, E.F.J., Rudolph, T., Hanisch, A., Hoeppener, S., Retsch, M., Schubert, U.S., and Schacher, F.H. (2012) UV-induced crosslinking of the polybutadiene domains in lamellar polystyrene-block-polybutadiene block copolymer films – an in-depth study. Polymer, 53(25), 5641-5648.

Riyajan, S.-A., Sasithornsonti, Y., and Phinyocheep, P. (2012) Green natural rubber-g-modified starch for controlling urea release. Carbohydrate Polymers, 89(1), 251-258.

Sakota, K., Okuno, K., Okaya, T., and Tsuchiya, S. (1976) Oxidation behavior of isoprene/styrene copolymer and butadiene/styrene copolymer. Journal of Applied Polymer Science, 20(10), 2811-2819.

Sawahata, K., Hara, M., Yasunaga, H., and Osada, Y. (1990) Electrically controlled drug delivery system using polyelectrolyte gels. Journal of Controlled Release, 14(3), 253-262.

Sharma, M., Waterhouse, G.I.N., Loader, S.W.C., Garg, S., and Svirskis, D. (2013) High surface area polypyrrole scaffolds for tunable drug delivery. International Journal of Pharmaceutics, 443(1-2), 163-168.

Sittiwong, J., Niamlang, S., Paradee, N., and Sirivat, A. (2012) Electric field-controlled benzoic acid and sulphanilamide delivery from poly(vinyl alcohol) hydrogel. Journal of the American Association of Pharmaceutical Scientists, 13(4), 1407-1415.

Soulas, D.N. and Papadokostaki, K.G. (2011) Regulation of proxyphylline's release from silicone rubber matrices by the use of osmotically active excipients and a multi-layer system. International Journal of Pharmaceutics, 408(1–2), 120-129.

Soulas, D.N., Papadokostaki, K.G., and Sanopoulou, M. (2013) Silicone rubber films modified by ethylenoxy moieties:Characterization and drug delivery properties. Journal of Applied Polymer Science, 129(2), 874-883.

Soulas, D.N., Sanopoulou, M., and Papadokostaki, K.G. (2012) Proxyphylline release kinetics from symmetrical three-layer silicone rubber matrices: effect of different excipients in the outer rate-controlling layers. International Journal of Pharmaceutics, 427(2), 192-200.

Sriamornsak, P., Thirawong, N., and Korkerd, K. (2007) Swelling, erosion and release behavior of alginate-based matrix tablets. European Journal of Pharmaceutics and Biopharmaceutics, 66(3), 435-450.

Suksaeree, J., Boonme, P., Taweepreda, W., Ritthidej, G.C., and Pichayakorn, W. (2012) Characterization, in vitro release and permeation studies of nicotine transdermal patches prepared from deproteinized natural rubber latex blends. Chemical Engineering Research and Design, 90(7), 906-914.

Syed Abthagir, P., Dhanalakshmi, K., and Saraswathi, R. (1998) Thermal studies on polyindole and polycarbazole. Synthetic Metals, 93(1), 1-7.

Tamura, K., Shiotsuki, M., Kobayashi, N., Masuda, T., and Sanda, F. (2009) Synthesis and properties of conjugated polymers containing 3,9- and 2,9-linked carbazole units in the main chain. Journal of Polymer Science Part A: Polymer Chemistry, 47(14), 3506-3517.

Taoudi, H., Bernede, J.C., Bonnet, A., Morsli, M., and Godoy, A. (1997) Comparison of polycarbazole obtained by oxidation of carbazole either in solution or in thin film form. Thin Solid Films, 304(1–2), 48-55.

Taoudi, H., Bernede, J.C., Del Valle, M.A., Bonnet, A., Molinie, P., Morsli, M., Diaz, F., Tregouet, Y., and Bareau. A. (2000) Polycarbazole obtained by electrochemical polymerization of monomers either in solution or in thin film form. Journal of Applied Polymer Science, 75(13), 1561-1568.

Uhrich, K.E., Cannizzaro, S.M., Langer, R.S., and Shakesheff, K.M. (1999) Polymeric systems for controlled drug release. Chemical Reviews, 99(11), 3181-3198.

Verghese, M.M., Basu, T., and Malhotra, B.D. (1995) Influence of pH on the electroactivity of polycarbazole. Materials Science and Engineering: C, 3(3-4), 215-218.

Verghese, M.M., Ram, M.K., Vardhan, H., Malhotra, B.D., and Ashraf, S.M. (1997) Electrochromic properties of polycarbazole films. Polymer, 38(7), 1625-1629.

Weaver, J.C., Vaughan, T.E., and Chizmadzhev, Y. (1999) Theory of electrical creation of aqueous pathways across skin transport barriers. Advanced Drug Delivery Reviews, 35(1), 21-39.

APPENDICES

Appendix A Functional Groups of PCz Investigation

Oxidation polymerization of Cz monomer with $(NH_4)_2S_2O_8$ in aqueous HCl (Gupta and Prakash, 2010) provided olive-green PCz. The synthesized PCz was neutralized by NaOH followed with the doping of IN into the dedoped PCz. All of products were investigated for the functional groups using the FTIR spectrometer (Thermo Nicolet, Nexus 670) in the transmission mode with optical grade KBr as the background material and 64 scans at a resolution of 4 cm^{-1}.

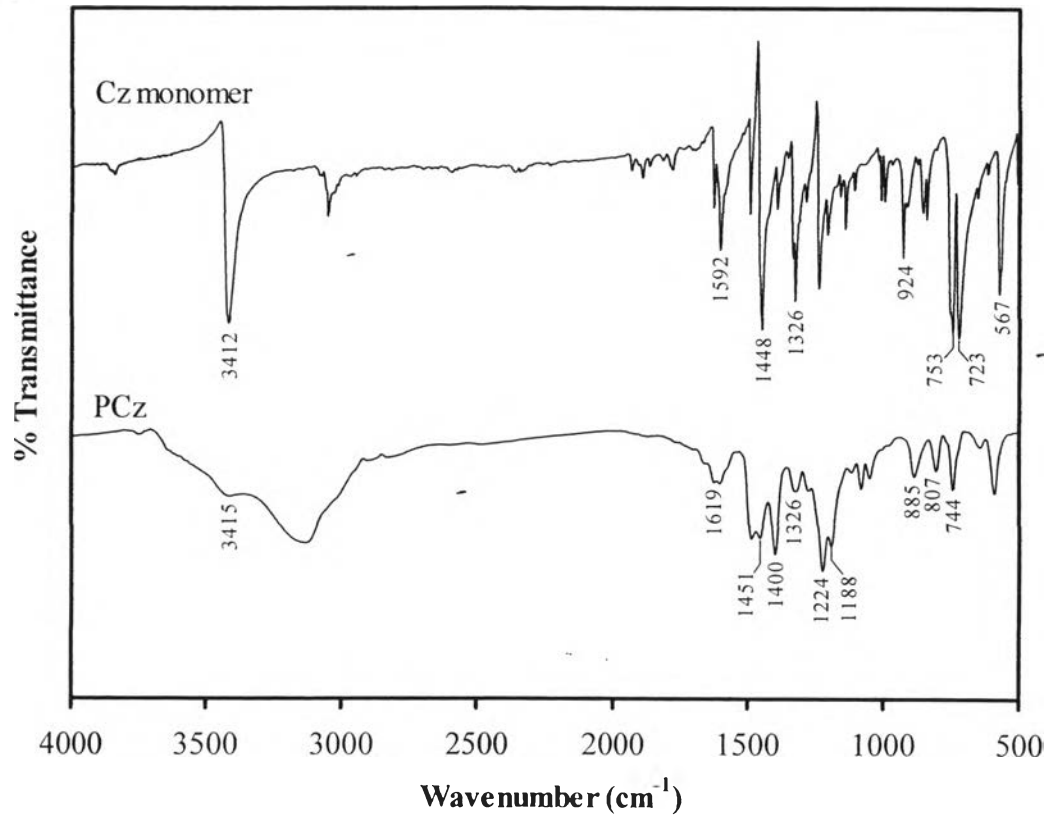

Figure A1 FT-IR spectra of Cz monomer and PCz.

The FT-IR spectrum of PCz shows the N-H stretching of heteroaromatics peak at 3415 cm^{-1} which is broaden than one of Cz monomer, the C=C stretching of the aromatic compound at 1600-1625 cm^{-1}, the C-N-C stretching peak at 1451 cm^{-1}, the C-H out of plan bending at 1326 cm^{-1}, and the 1,2,4-trisubstitution peaks at 806 cm^{-1}, 855 cm^{-1}, and 884 cm^{-1}.

Table A1 The characteristic peaks of PCz

Wavenumber (cm^{-1})	**Assignment**	**Reference**
725 and 745	1,2-disubstitued rings	Taoudi *et al.*, 1997
810 and 1090	Complex salt formation	Taoudi *et al.*, 1998
750	$-CH_2$ rocking vibration	Raj *et al.*, 2010
1328	C-H out of plane bending vibration of aromatic ring	
1404 and 1452	Ring stretching vibration of Carbazole moiety	
1451-1453	C-N-C stretching band for Cz aromatics	Naddaka *et al.*, 2011
2860-2866 and 2929-2934	C_{sp3}-H vibration	
3420	N-H stretching	Taoudi *et al.*, 1997

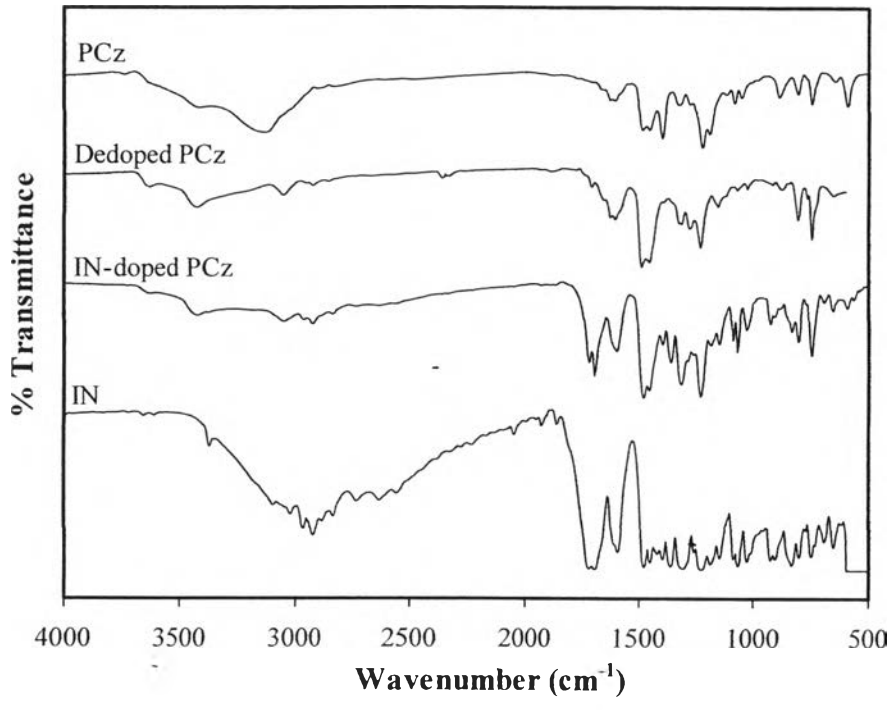

Figure A2 FT-IR spectra of PCz, dedoped PCz, IN-doped PCz, and IN.

The FT-IR spectra shown in Figure A2 present a reduction of N-H stretching peak intensity of dedoped PCz, an appearance of new peaks at 1075-1190 cm^{-1} and 1700-1725 cm^{-1} refer to the C-O stretching, the C=O stretching, respectively.

Table A2 Assignment bands of indomethacin (Dupeyron *et al.*, 2013)

Wavenumber (cm^{-1})	**Assignment**
839, 832, 803, 752, 702 (s-m)	Aromatic ring
926, 905 (s)	γ CH
1086, 1067	γ O-H
1189, 1148, 1028, 1012 (s)	Aromatic ring
1,233, 1,222 (s-m)	ν C-CO-O
1,306, 1,291 (s)	ν C-O
1,372, 1,358 (m-w)	ν C-N
1,428, 1,411, 1,396 (m-w)	ν C-H
1,712, 1,690 (s)	ν C=O
2,967, 2,928 (w)	ν C_{sp3}-H
3,370 (w)	ν O-H

Appendix B Thermal Properties of PCz and Crosslinked DCNR Films

The thermal behavior of PCz and crosslinked DCNR films was determined by the thermogravimetric analyzer (Thermo, TGA Q 50). The sample was weighed in a range 4-5 mg and placed it in a platinum pan, and then weighed sample was heated from 50 to 900 °C under nitrogen flow with the heating rate 10 °C/min.

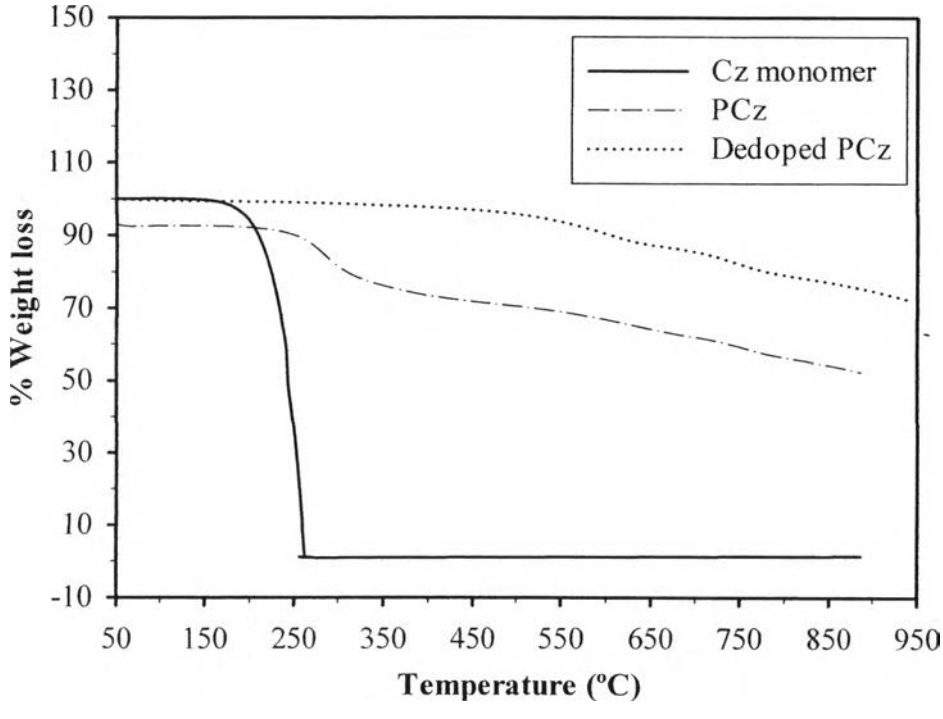

Figure B1 TGA thermograms of Cz monomer, PCz, and dedoped PCz.

The TGA thermogram of PCz shows the first transition at 288.39 °C from a degradation of a dopant followed with the second transition temperature resulted in a separation of PCz backbone at 619.52 °C (Raj *et al.*, 2010). The dedoped PCz thermogram presents the transition temperature at 576.02 °C and 741.41 °C due to a decomposition of a dopant and a polymer backbone, respectively (Abthagir *et al.*, 2004).

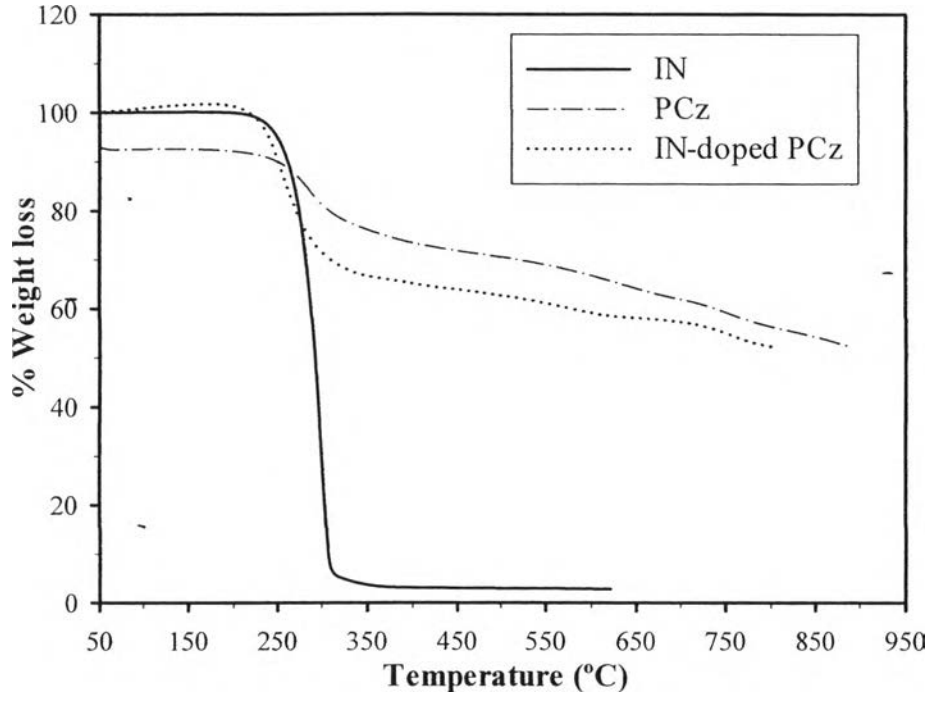

Figure B2 TGA thermograms of IN, PCz, and IN-doped PCz.

The thermal behavior of IN-doped PCz shows three weight loss steps. First, IN cleaves at 256.76 °C which is shifted from 302.05 °C. Second, a residual dopant deforms at 585.60 °C followed by a degradation of a backbone at 753.79 °C.

Table B1 The degradation temperature and weight loss (%) in TGA thermograms of Cz monomer, PCz, dedoped PCz, IN, and IN-doped PCz

Sample	T_d (°C)	Avg	SD	Weight loss (%)	Avg	SD
Cz monomer	243.43 258.91	251.17	10.95	98.27 97.90	98.08	0.26
PCz	291.66 285.12	288.39	4.62	16.77 15.70	16.24	0.76
	623.53 615.52	619.52	5.66	4.01 3.15	3.58	0.61
Dedoped PCz	580.82 571.21	576.02	6.80	4.97 4.30	4.63	0.47
	738.17 744.65	741.41	4.58	3.70 2.67	3.18	0.73
IN	302.05	-	-	93.53	-	-
IN-doped PCz	262.04 251.37 256.87	256.76	5.34	38.97 29.46 33.23	33.89	4.79
	573.45 596.56 586.80	585.60	11.60	2.13 1.40 2.69	2.07	0.64
	759.56 751.83 749.98	753.79	5.08	2.63 2.02 2.81	2.49	0.41

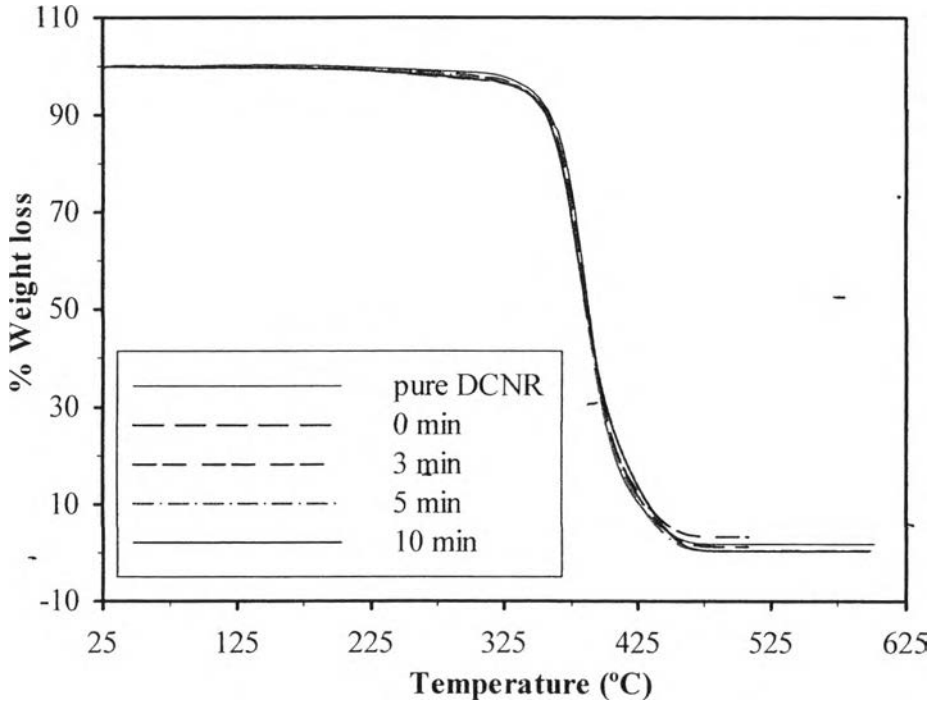

Figure B3 TGA thermograms of pure DCNR film and of crosslinked DCNR at various curing times.

Table B2 The degradation temperature and weight loss (%) of pure DCNR film and of crosslinked DCNR with various curing times

Sample	T_d (°C)	Weight loss (%)
Pure DDNR	385.36	94.89
0 min	380.03	94.12
3 min	384.44	94.48
5 min	386.73	97.38
10 min	382.32	95.82

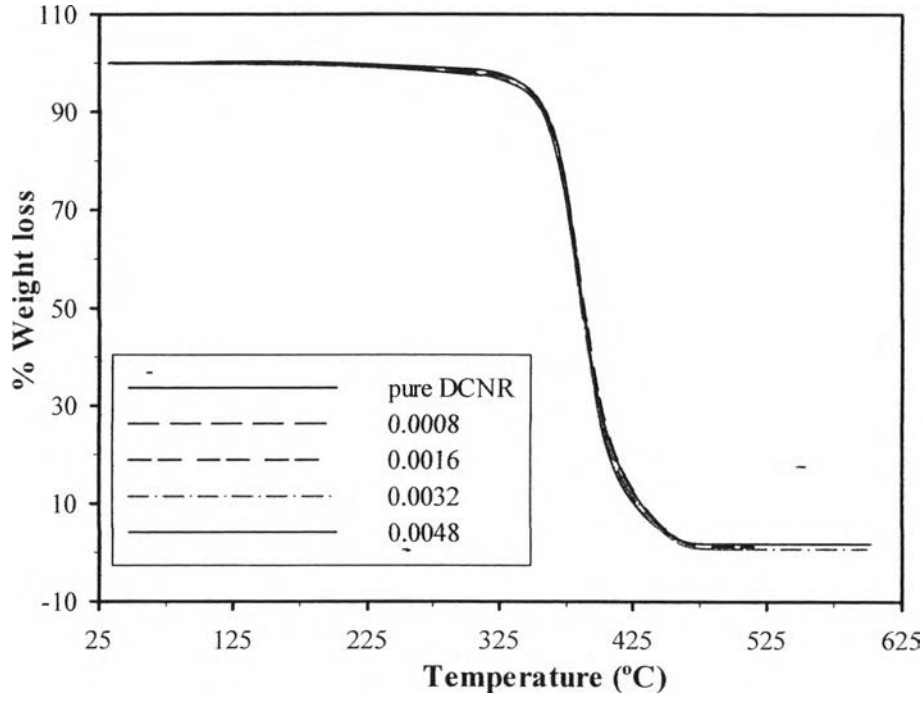

Figure B4 TGA thermograms of pure DCNR film and of crosslinked DCNR with various crosslink ratios.

Table B3 The degradation temperature and weight loss (%) of pure DCNR film and of crosslinked DCNR with various crosslink ratios

Sample	T_d (°C)	Weight loss (%)
Pure DDNR	385.36	94.85
Crosslink ratio = 0.0008	385.46	95.42
Crosslink ratio = 0.0016	385.80	95.42
Crosslink ratio = 0.0032	383.23	96.04
Crosslink ratio = 0.0048	382.34	95.06

There are no significant differences in TGA spectra of crosslinked DCNR films with either various curing times or various crosslink ratios.

Appendix C Determination of Degree of Swelling (%) of LA, MA, and HA Films

The crosslinked NR films were immediately studied the swell in both toluene and water after the crosslinking process and calculated following Eq. (C1) and (C2).

$$\text{degree of swelling (\%)} = \frac{M_s - M_d}{M_d} \times 100 \quad \text{.....(C1)}$$

$$\text{weight loss (\%)} = \frac{M_i - M_d}{M_i} \times 100 \quad \text{.....(C2)}$$

where M_s = the weight after submersion in the buffer solution

M_d = the dried weight after submersion for 72 h

M_i = the initial weight of the sample

The degree of swelling of all crosslinked NR films in toluene decreased with increasing curing time and the equilibrium is observed at 5 min. UV irradiation introduces photoinitiator radicals which react with crosslinking agents resulting in the crosslinking process in NR latex, so the curing time affects the crosslink density which is related to the degree of swelling. On the other hand, the film in water slightly decreases with increasing curing time because NR films are immiscible in water and there is no significant difference from 3 min to 10 min.

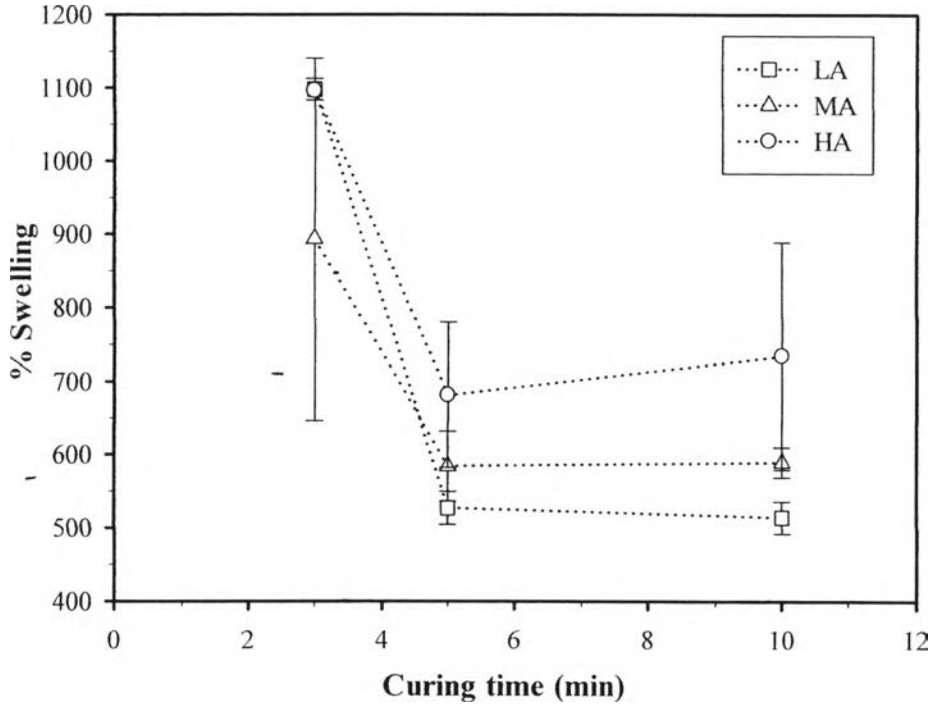

Figure C1 Degree of swelling (%) of different crosslinked NR films including LA film, MA film, and HA film in toluene with various curing times.

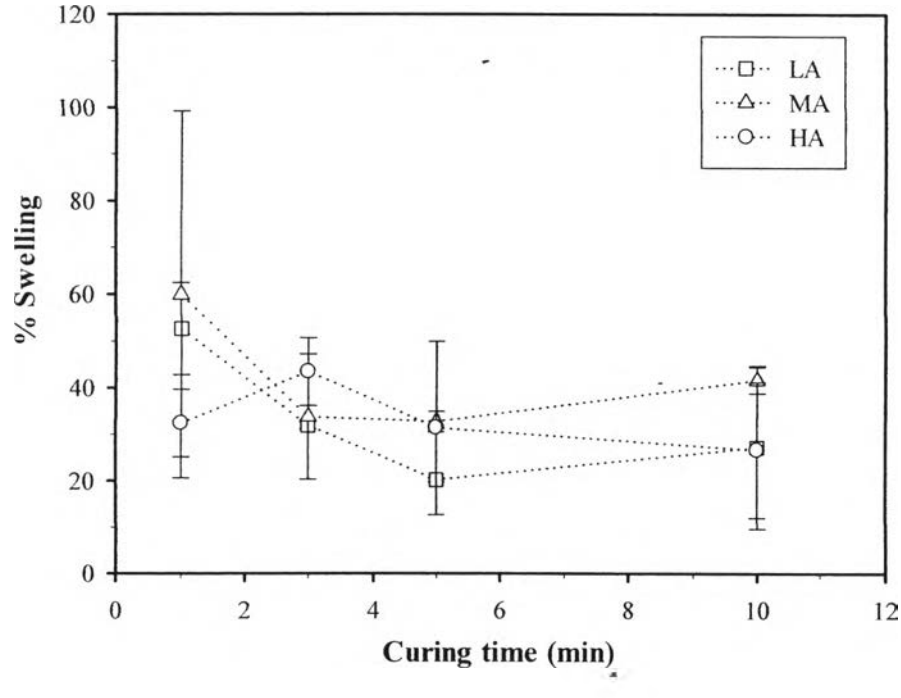

Figure C2 Degree of swelling (%) of different crosslinked NR films including LA film, MA film, and HA film in water with various curing times.

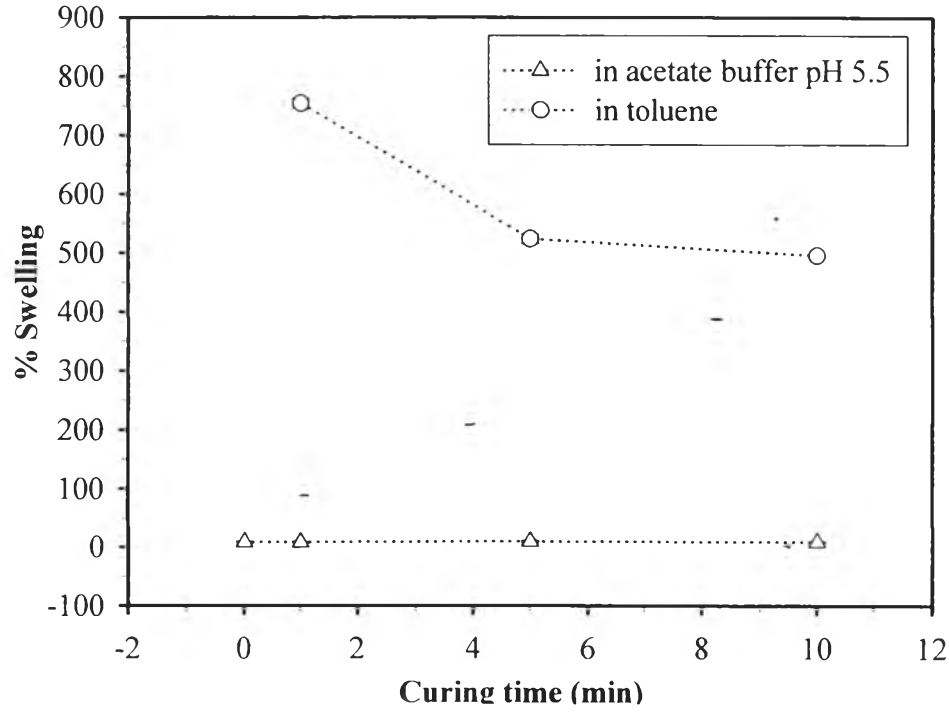

Figure C3 Degree of swelling (%) of crosslinked MA film in toluene and in acetate buffer pH 5.5 with various curing times.

Table C1 The value of degree of swelling (%) of LA, MA, and HA in toluene with various curing times

Curing time (min)	Type of latex	M_d	M_s	Degree of swelling (%)	Avg	SD
1	LA	0.0312 0.0387	- -	- -	-	-
	MA	0.0344 0.0544	- -	- -	-	-
	HA	0.0581 0.0450	- -	- -	-	-
3	LA	0.0433 0.0522	0.5142 0.6308	1088 1108	1098	14.8
	MA	0.0299 0.0601	0.2448 0.7020	719 1068	893	247
	HA	0.0262 0.0423	0.3133 -	1096	1096	-
5	LA	0.0244 0.0308	0.1491 0.1981	511 543	527	22.7
	MA	0.0327 0.0584	0.2127 0.4191	550 618	584	47.5
	HA	0.0380 0.0516	0.2702 0.4393	611 751	681	99.2
10	LA	0.0442 0.0204	0.2783 0.1221	530 499	514	22.0
	MA	0.0623 0.0316	0.4204 0.2224	575 604	589	20.5
	HA	0.0335 0.0531	0.2428 0.5011	625 844	734	155

Table C2 The value of degree of swelling (%) of LA. MA, and HA in water with various curing times

Curing time (min)	Type of latex	M_d	M_s	Degree of swelling (%)	Avg	SD
1	LA	0.0335 0.0354	0.0488 0.0565	45.7 59.6	52.6	9.8
	MA	0.0361 0.0514	0.0477 0.0965	32.1 87.7	59.9	39.3
	HA	0.0627 0.0482	0.0798 0.0663	27.3 37.6	32.4	7.3
3	LA	0.0373 0.0514	0.0494 0.0675	32.4 31.3	31.9	0.8
	MA	0.0335 0.0718	0.0480 0.0892	43.3 24.2	33.8	13.5
	HA	0.0253 0.0457	0.0376 0.0632	48.6 38.3	43.5	7.3
5	LA	0.0423 0.0400	0.0507 0.0482	19.9 20.5	20.2	0.4
	MA	0.0429 0.0675	0.0576 0.0885	34.3 31.1	32.7	2.2
	HA	0.0681 0.0546	0.0805 0.0789	18.2 44.5	31.4	18.6
10	LA	0.0542 0.0250	0.0622 0.0349	14.8 39.6	27.2	17.6
	MA	0.0401 0.0442	0.0560 0.0635	39.7 43.7	41.7	2.8
	HA	0.0325 0.0362	0.0445 0.0421	36.9 16.3	26.6	14.6

Table C3 The value of degree of swelling (%) MA in toluene and in acetate buffer pH 5.5 with various curing times

Solvent	Curing time (min)	M_d	M_s	Degree of swelling (%)
Acetate buffer pH 5.5	0	0.0978	0.1057	8.1
		0.1184	0.1285	8.5
		0.1026	0.1140	11.1
		0.1128	0.1229	8.9
		Avg		9.2
		SD		1.3
	3	0.0977	0.1058	8.3
		0.1069	0.1159	8.4
		0.0911	0.0996	9.3
		0.1069	0.1155	8.0
		Avg		8.5
		SD		0.6
	5	0.0917	0.0993	8.3
		0.0846	0.0921	8.9
		0.0954	0.1045	9.5
		0.1327	0.1460	10.0
		Avg		9.2
		SD		0.8
	10	0.0973	0.1063	9.3
		0.0925	0.0995	7.6
		0.0972	0.1048	7.8
		0.1006	0.1092	8.6
		Avg		8.3
		SD		0.8
Toluene	0	0.1140	-	-
		0.1211	-	-
		Avg		-
		SD		-
	3	0.1249	1.0602	749
		0.1149	0.9884	760
		Avg		755
		SD		8.05
	5	0.1078	0.6666	518
		0.1380	0.8687	529
		Avg		524
		SD		7.87
	10	0.1035	0.6140	493
		0.1088	0.6508	498
		Avg		496
		SD		3.48

Appendix D Properties of Natural Rubber Latex

Lab Name : THAI EASTERN RUBBER CO., LTD.

Date Tested : July 11, 2013

Date Production : July 3-4, 2013

Type of Latex : High ammonia-Double centrifuge (HA-DD)

Table D1 The characteristic of natural rubber latex

Characteristic	Method of test	Test result
Total solid content, (wt %)	ISO 124	60.69
Dry rubber content, (wt %)	ISO 126	60.10
Non-rubber content, (wt %)	-	0.59
Ammonia content (on total weight), (wt %)	ISO 125	0.67
Ammonia content (on water phase), (wt %)	-	1.70
Volatile fatty acid number (VFA number)	ISO 506	0.0173
Mechanical stability time @ 55% TS, seconds	ISO 35	750 (11/07/2013)
Magnesium content on solids, (ppm)	In House	19.90
KOH number	ISO 127	0.20
pH of latex	ISO 976	10.29
Specific gravity, (wt %)	ISO 6057	0.94
Coagulum content, (wt %)	ISO 706	0.005
Viscosity (Spindic No.1, 60 rpm) @ 60% TS, ePs	ISO 1652	910
Color of latex	In House	White

Appendix E Determination of Degree of Swelling (%) and Weight Loss (%) of DCNR Films

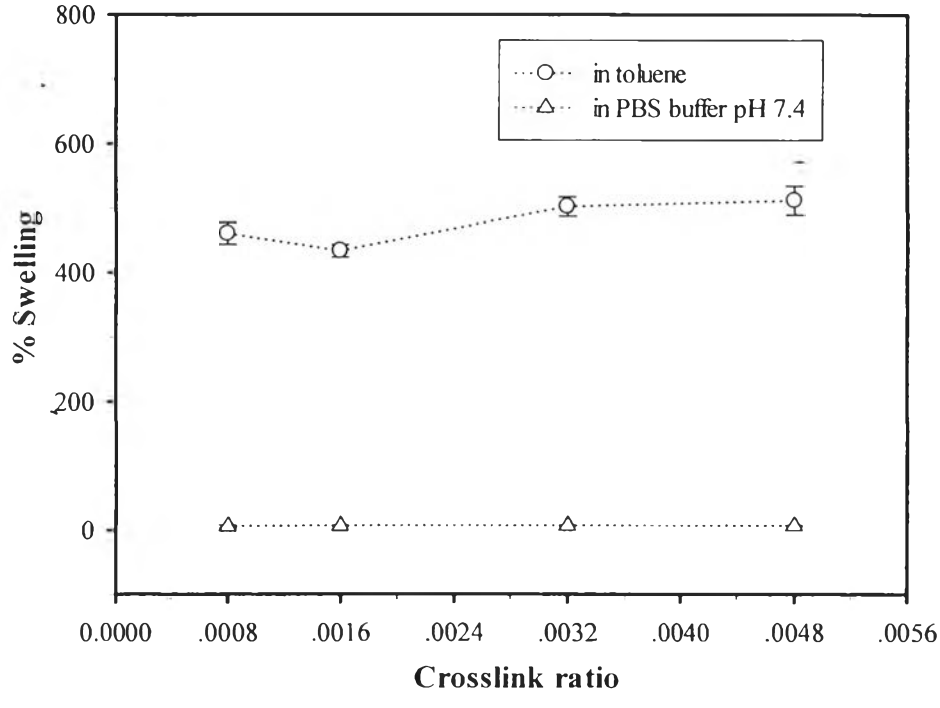

Figure E1 Degree of swelling (%) of crosslinked DCNR films in toluene and in PBS buffer pH 7.4 with various crosslink ratios using 5 min of curing time and 0.45 %v/v photoinitiator.

The ratio of photoinitiator and crosslinking agent in each film was 2:1, 1:1, 1:2, and 1:3. The degree of swelling slightly increases in toluene from the film with 0.0016 crosslink ratio to the one with 0.0032 crosslink ratio and then equilibrium. The concentration of photoinitiator is related to the amount of crosslink radicals in the system that results in a crosslink density, so it exhibits a lower degree of swelling in a higher photoinitiator to crosslinking agent ratio.

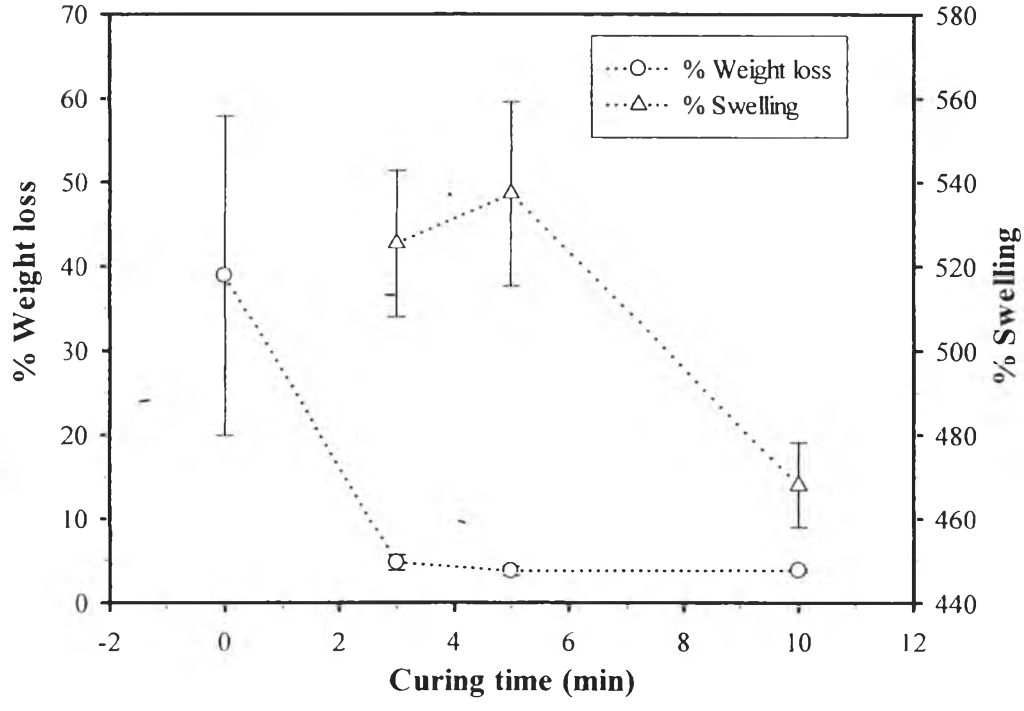

Figure E2 Degree of swelling (%) and weight loss (%) of crosslinked DCNR films in toluene with various curing time using 0.0048 crosslink ratio (Crosslinking agent: photoinitiator = 2: 1 mole ratio).

In equilibrium swelling investigation, the uncured NR film dissolves in a solvent, whereas the others endure in this condition. They exhibit a directly proportion of the curing time and the swelling capacity which can be ranged from 3 min, 5 min, and 10 min of curing time. Degree of weight loss dramatically decreases with increasing curing time until equilibrium is observed at 5 min. Curing time is related to the crosslink density of the polymer which indicates that the crosslinking agent completely reacts with rubber molecules within 5 min of curing time.

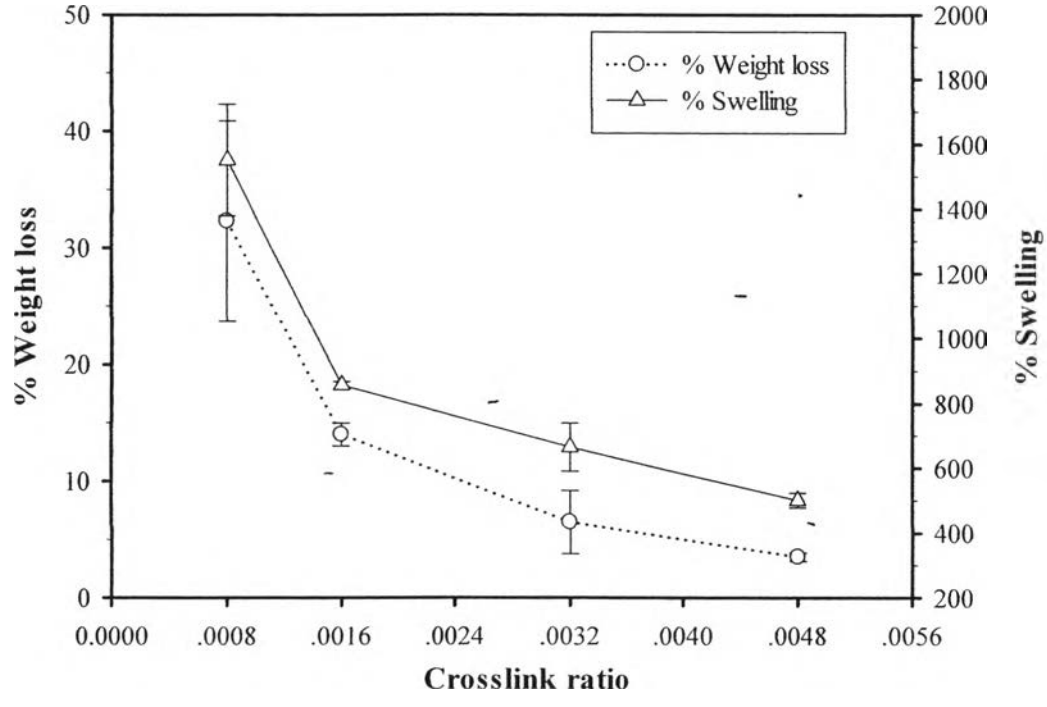

Figure E3 Degree of swelling (%) and weight loss (%) of crosslinked DCNR films in toluene and in PBS buffer pH 7.4 with various crosslinking agents using 5 min of curing time (Crosslinking agent: photoinitiator = 2: 1 mole ratio).

Both degree of weight loss and degree of swelling decreases with increasing amount of crosslinking agents. The rubber chain generally creates higher chain networks with higher crosslink ratio which can reduce the solvent uptake resulting in a decrease of film's swelling. While the NR films with low crosslink ratio has more free rubber chains which can easily dissolve in a solvent and affect to the weight loss of film.

Table E1 The value of degree of swelling (%) of crosslinked DCNR films in toluene with various crosslink ratios using 5 min of curing time and 0.45 %v/v photoinitiator

Crosslink ratio ($mol_{TMPTMP}/mol_{isoprene}$)	M_d	M_s	**Degree of swelling (%)**
0.0008	0.1102	0.6454	486
	0.1003	0.5657	464
	0.0911	0.5020	451
	0.0888	0.4924	455
	0.0819	0.4527	453
	0.0894	0.4828	440
	0.1063	0.6125	476
	0.0762	0.4180	449
	0.1166	0.6812	484
	Avg		452
	SD		16.5
0.0016	0.1066	0.5608	426
	0.0805	0.4223	425
	0.0754	0.3960	425
	0.0995	0.5477	450
	0.0931	0.4971	434
	0.0782	0.4225	440
	0.1047	0.5666	441
	0.0855	0.4665	446
	0.0721	0.3814	429
	Avg		437
	SD		9.6
0.0032	0.0923	0.5698	517
	0.1057	0.5102	383
	0.1064	0.6606	521
	0.1047	0.6114	484
	0.0868	0.6422	640
	0.0981	0.5732	484
	0.1004	0.6085	506
	0.1039	0.6336	510
	0.0945	0.5636	496
	Avg		505
	SD		65.7

Table E1 The value of degree of swelling (%) of crosslinked DCNR films in toluene with various crosslink ratios using 5 min of curing time and 0.45 %v/v photoinitiator (continued)

Crosslink ratio (mol $_{TMPTMP}$/mol $_{isoprene}$)	M_d	M_s	Degree of swelling (%)
0.0048	0.0977	0.6082	523
	0.0924	0.5778	525
	0.0786	0.4907	524
	0.0741	0.4830	552
	0.1128	0.6922	514
	0.0945	0.5674	500
	0.0749	0.4523	504
	0.1005	0.5872	484
	0.0968	0.5630	482
	Avg		512
	SD		22.1

Table E2 The value of degree of swelling (%) of crosslinked DCNR films in PBS buffer pH 7.4 with various crosslink ratios using 5 min of curing time and 0.45 %v/v photoinitiator

Crosslink ratio (mol $_{TMPTMP}$/mol $_{isoprene}$)	M_d	M_s	Degree of swelling (%)
0.0008	0.0835	0.0903	8.1
	0.0947	0.0990	4.5
	0.0856	0.0923	7.8
	0.1077	0.1081	0.4
	0.0982	0.1050	6.9
	0.0853	0.0913	7.0
	0.1031	0.1094	6.1
	0.1076	0.1143	6.2
	0.1087	0.1157	6.4
	Avg		6.0
	SD		2.3

Table E2 The value of degree of swelling (%) of crosslinked DCNR films in PBS buffer pH 7.4 with various crosslink ratios using 5 min of curing time and 0.45 %v/v photoinitiator (continued)

Crosslink ratio ($mol_{TMPTMP}/mol_{isoprene}$)	**M**	**M_s**	**Degree of swelling (%)**
-	0.1022	0.1092	6.9
	0.0987	0.1065	7.9
	0.1095	0.1158	5.8
	0.0737	0.0788	6.9
	0.0917	0.0984	7.3
0.0016	0.0885	0.0943	6.6
	0.0791	0.0850	7.5
	0.0823	0.0876	6.4
	0.1059	0.1131	6.8
	Avg		6.9
	SD		0.6
	0.1166	0.1242	6.5
	0.0800	0.0871	8.9
	0.1166	0.1240	6.4
	0.0948	0.1018	7.4
	0.0921	0.0988	7.3
0.0032	0.1109	0.1177	6.1
	0.0879	0.0947	7.7
	0.0786	0.0849	8.0
	0.0796	0.0865	8.7
	Avg		7.4
	SD		1.0
	0.0734	0.0792	7.9
	0.0776	0.0838	8.0
	0.0894	0.0963	7.7
	0.0929	0.0991	6.7
	0.1142	0.1216	6.5
0.0048	0.1025	0.1100	7.3
	0.0723	0.0775	7.2
	0.0854	0.0912	6.8
	0.1029	0.1094	6.3
	Avg		7.2
	SD		0.6

Table E3 The value of degree of swelling (%) and weight loss (%) of crosslinked DCNR films in toluene with various curing time using 0.0048 crosslink ratio (Crosslinking agent: photoinitiator = 3: 1 %v/v rubber)

Curing time (min)	M_i	M_s	M_d	Degree of swelling (%)	Weight loss (%)
0	0.0709	-	0.0553	-	22.0
	0.0754	-	0.0306	-	59.4
	0.0759	-	0.0491	-	35.3
	Avg			-	38.9
	SD			-	19.0
3	0.0937	0.5698	0.0902	508	3.7
	0.1149	0.7386	0.1087	543	5.4
	0.1147	0.7172	0.1088	525	5.1
	Avg			525	4.8
	SD			17.4	0.9
5	0.0882	0.5500	0.0844	524	4.3
	0.0888	0.5883	0.0855	563	3.7
	0.1001	0.6263	0.0969	526	3.2
	Avg			537	3.7
	SD			21.9	0.6
10	0.0905	0.5244	0.087	479	3.9
	0.0831	0.4692	0.0801	465	3.6
	0.0849	0.4755	0.0815	460	4.0
	Avg			468	3.8
	SD			10.1	0.2

Table E4 The value of degree of swelling (%) and weight loss (%) of crosslinked DCNR films in toluene and in PBS buffer pH 7.4 with various crosslink ratios using 5 min of curing time

Crosslink ratio	M_i	M_s	M_d	Degree of swelling (%)	Weight loss (%)
-	0.1137	2.1076	0.0653	1754	42.6
	0.1014	-	-	-	-
0.0008	0.0952	1.5780	0.0599	1558	37.1
	0.1158	2.0512	0.0767	1671	33.8
	0.0694	0.9843	0.0553	1318	20.3
	0.0958	1.4887	0.0693	1454	27.7
	Avg			1551	32.3
	SD			173	8.6
0.0016	0.1020	0.9725	0.0884	853	13.3
	0.1028	1.0028	0.0885	875	13.9
	0.0995	0.9510	0.0870	856	12.6
	0.0693	0.6668	0.0596	862	14.0
	0.0651	0.6125	0.0553	841	15.1
	0.0730	0.6963	0.0620	854	15.1
	Avg			857	14.0
	SD			11.4	1.0
0.0032	0.0617	0.4174	0.0572	576	7.3
	0.0878	0.6650	0.0819	657	6.7
	0.1066	0.9600	0.0957	801	10.2
	0.0887	0.6520	0.0835	635	5.9
	0.0811	0.6102	0.0796	652	1.9
	0.0890	0.6805	0.0828	665	7.0
	Avg			664	6.5
	SD			73.9	2.7
0.0048	0.0794	0.4957	0.0764	524	3.8
	0.0867	0.5293	0.0834	510	3.8
	0.0892	0.4989	0.0864	459	3.1
	0.0951	0.5780	0.0923	508	2.9
	0.1014	0.6185	0.0977	510	3.7
	0.1077	0.6400	0.1037	494	3.7
	Avg			501	3.5
	SD			23	0.4

Appendix F UV-visible Spectrum of Indomethacin (IN)

IN was determined the maximum wavelength (nm) using UV-visible spectrometer (TECAN, Infinite M200). The drug (0.0045 mg) was dissolved in MeOH followed with an addition of water until a volume was 100.00 mL. The IN solution is observed the characteristic peaks at 266 nm and 324 nm.

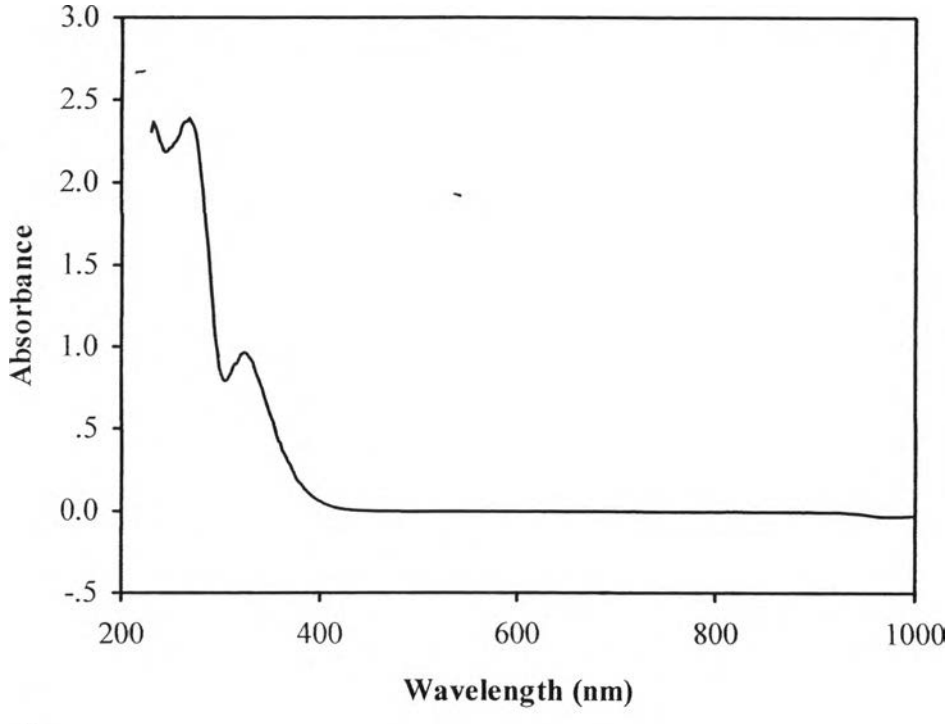

Figure F1 The UV-visible spectrum of IN.

Appendix G Calibration Curve of Indomethacin (IN)

A standard stock solution of IN at 450 ppm was prepared by precisely weighing of 45 mg of drug, dissolving in methanol, and then adjusting the volume to 100 mL with PBS buffer pH 7.4. This standard stock solution was pipetted and diluted with the buffer to produce 50 - 400 ppm of IN. The calibration curve plotted the absorbance at 324 nm versus the concentration of IN (ppm).

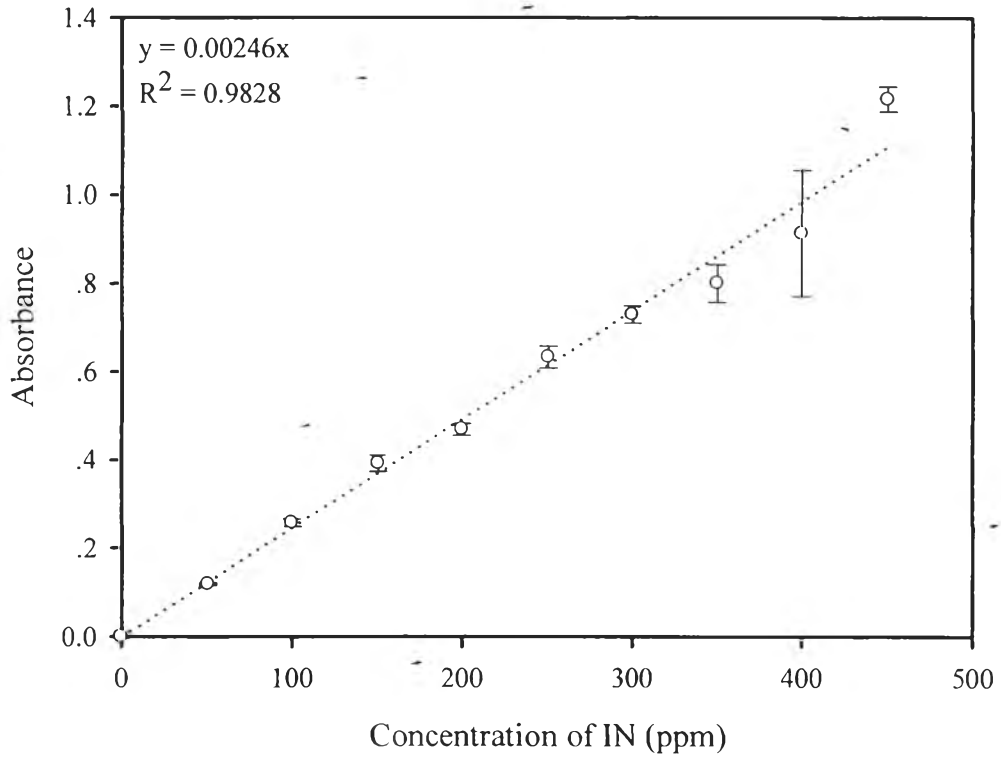

Figure G1 The calibration curve of IN dissolved in MeOH/H_2O at 324 nm.

Table G1 The absorbance of IN with various concentrations at 324 nm

Concentration of IN (ppm)	Absorbance	Avg	SD
0	0.0000 0.0000 0.0000	0.0000	0.0000
50	0.1191 0.1220 0.1167	0.1193	0.0026
100	0.2677 0.2499 0.2547	0.2574	0.0092
150	0.4040 0.3702 0.4011	0.3918	0.0187
200	0.4556 0.4697 0.4821	0.4691	0.0133
250	0.6601 0.6115 0.6286	0.6334	0.0247
300	0.7524 0.7143 0.7236	0.7301	0.0199
350	0.8428 0.7582 0.8008	0.8006	0.0423
400	0.9383 1.0412 0.7607	0.9134	0.1419
450	1.2475 1.2070 1.1925	1.2157	0.0285

Appendix H Photographs of PCz and Crosslinked DCNR Film

PCz was polymerized via interfacial chemical polymerization of Cz monomer and APS dissolved in DCM and 0.5 M HCl, respectively. Dried synthesized PCz obtained from standing the solution for 12 h was a dark green powder. A yield of this product was extremely smaller than a taupe brown one which was produced by stirring the solution for 7 h. In fact, a reaction took place at an interface of organic phase and water phase that could be introduced a higher interface by stirring. PCz was continuously stirred in 0.1 M NH_4OH to dedope the polymer. Finally, a light brown powder was obtained.

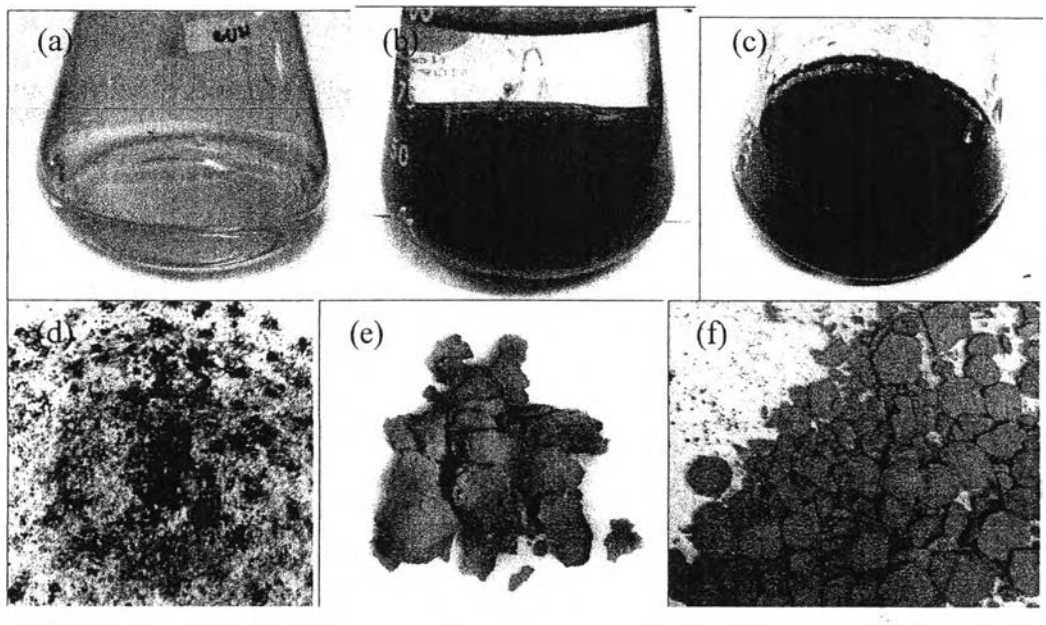

Figure H1 Chemical polymerization of Cz: (a) recently mixing of oxidizing agent and Cz monomers; (b) after stand for l2 h; (c) after stirred for 7 h; (d) dried PCz after stand for 12h; (e) dried PCz after stirred for 7 h; (f) dedoped PCz.

The crosslinked DCNR films were investigated an appropriate curing time from the swelling test according to ASTM D6814-02.

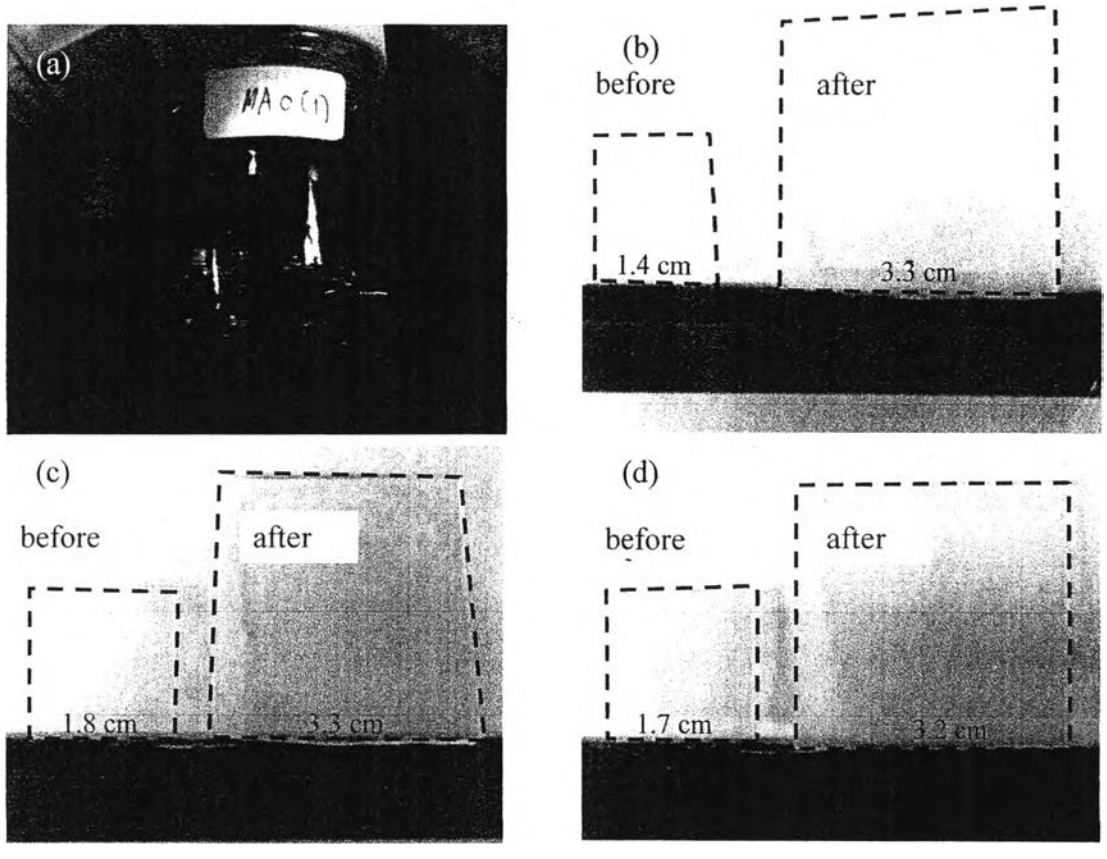

Figure H2 Swelling test of crosslinked NR films with various curing times: (a) 0 min; (b) 3 min; (c) 5min; and (d) 10 min in toluene.

DCNR films were fabricated by UV irradiation using TMPTMP and MMMP as crosslinking agent and photoinitiator, respectively. Different solvents including GLY, Si, and PEG were applied in the system to solve the fracture of the film after insertion of drugs. Finally, IN dissolved in PEG was chosen resulting in dissolution property and it is compatible with DCNR latex.

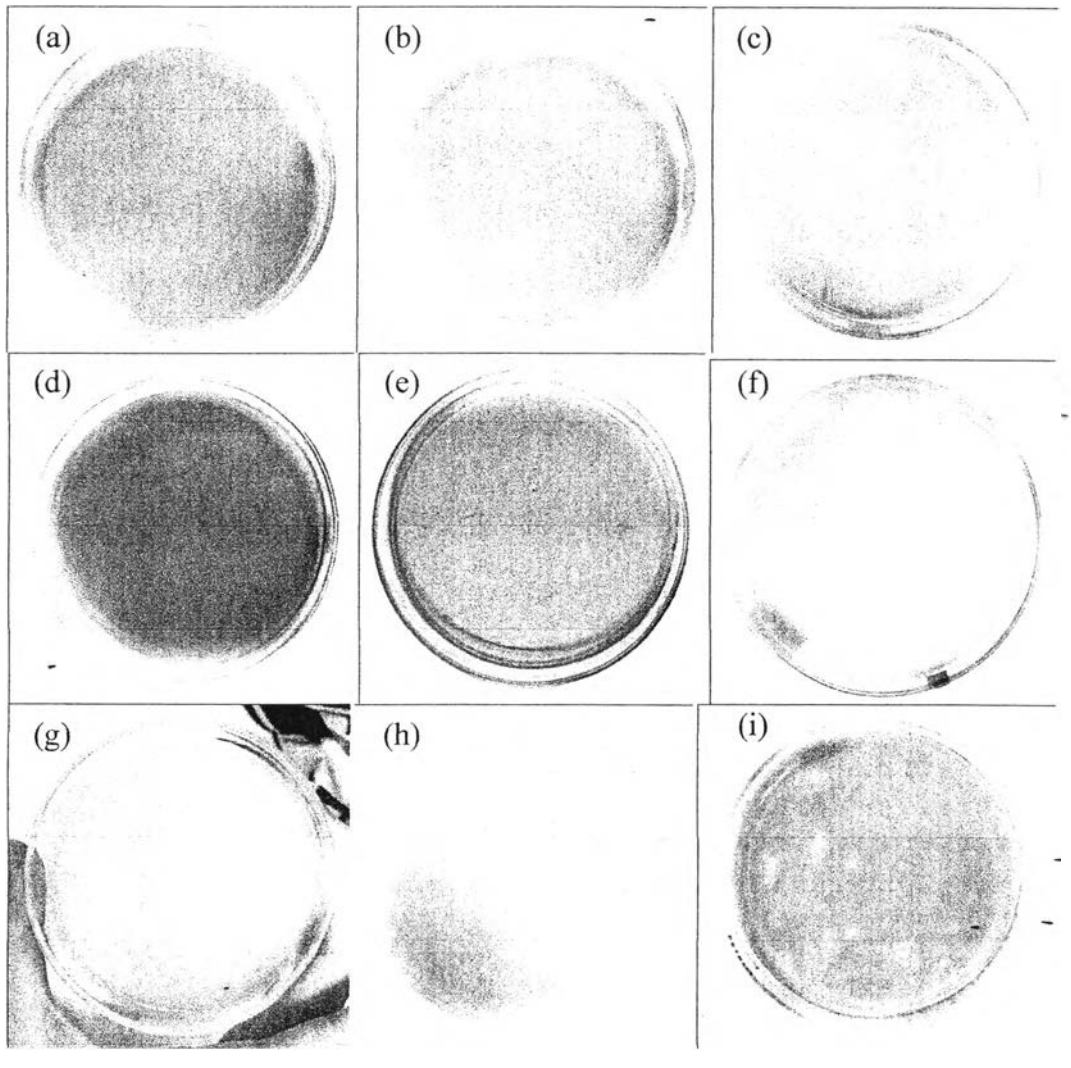

Figure H3 Crosslinked DCNR films with 0.0032 crosslink ratio using curing time at: (a) 0 min; (b) 3 min; (c) 5min; (d) 10 min; 5min containing of (e) loaded IN; (f) of loaded ibuprofen in GLY; (g) loaded ibuprofen in Si; (h) loaded IN in PEG; and (i) loaded ibuprofen in PEG.

Appendix I Scanning Electron Microscope (SEM) Images and Pore Size

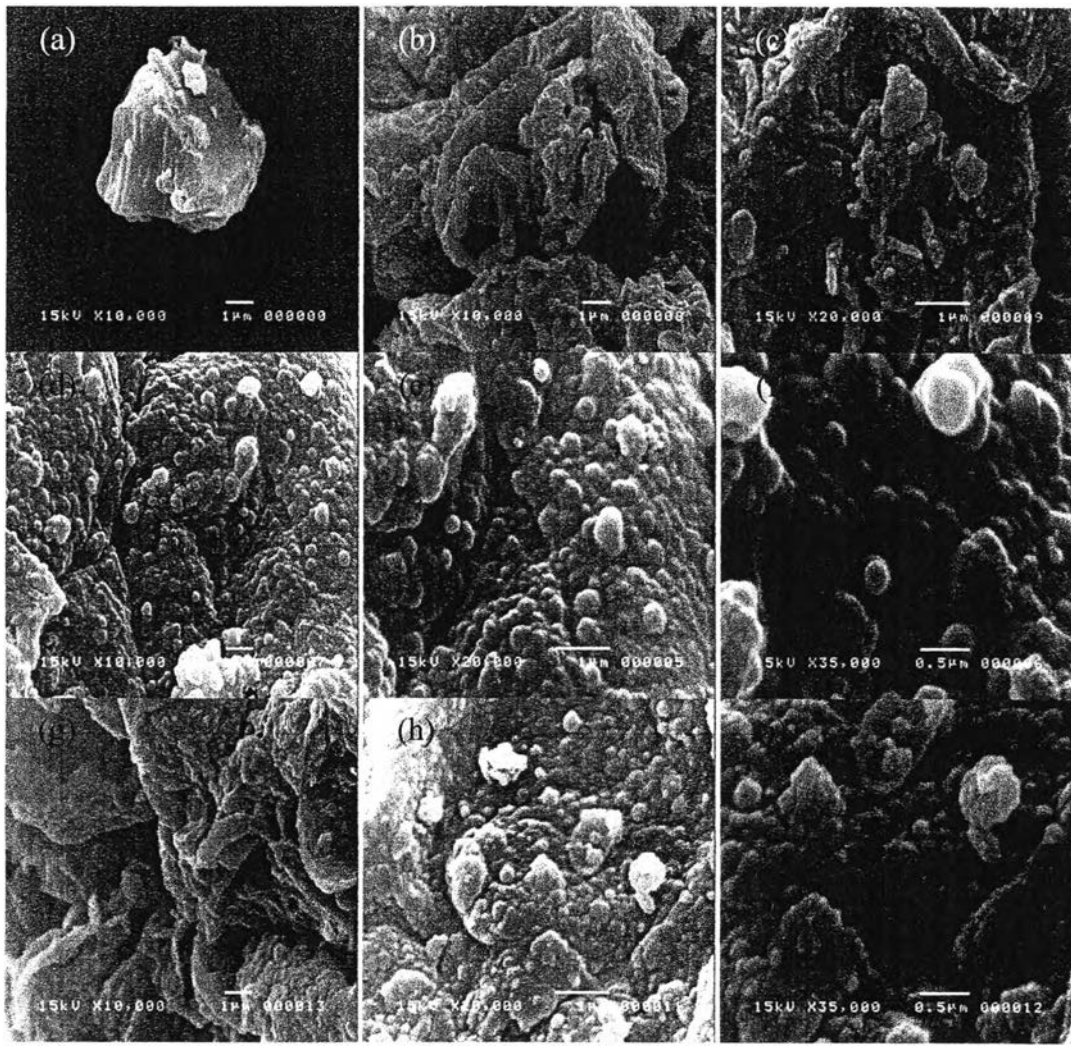

Figure I1 SEM micrographs of: (a) IN; (b) dedoped PCz at 10k; (c) dedoped PCz at 20k; (d) PCz at 10k; (e) PCz at 20k; (f) PCz at 35k; (g) IN-doped PCz at 10k; (h) IN-doped PCz at 20k; and (i) IN-doped PCz at 35k.

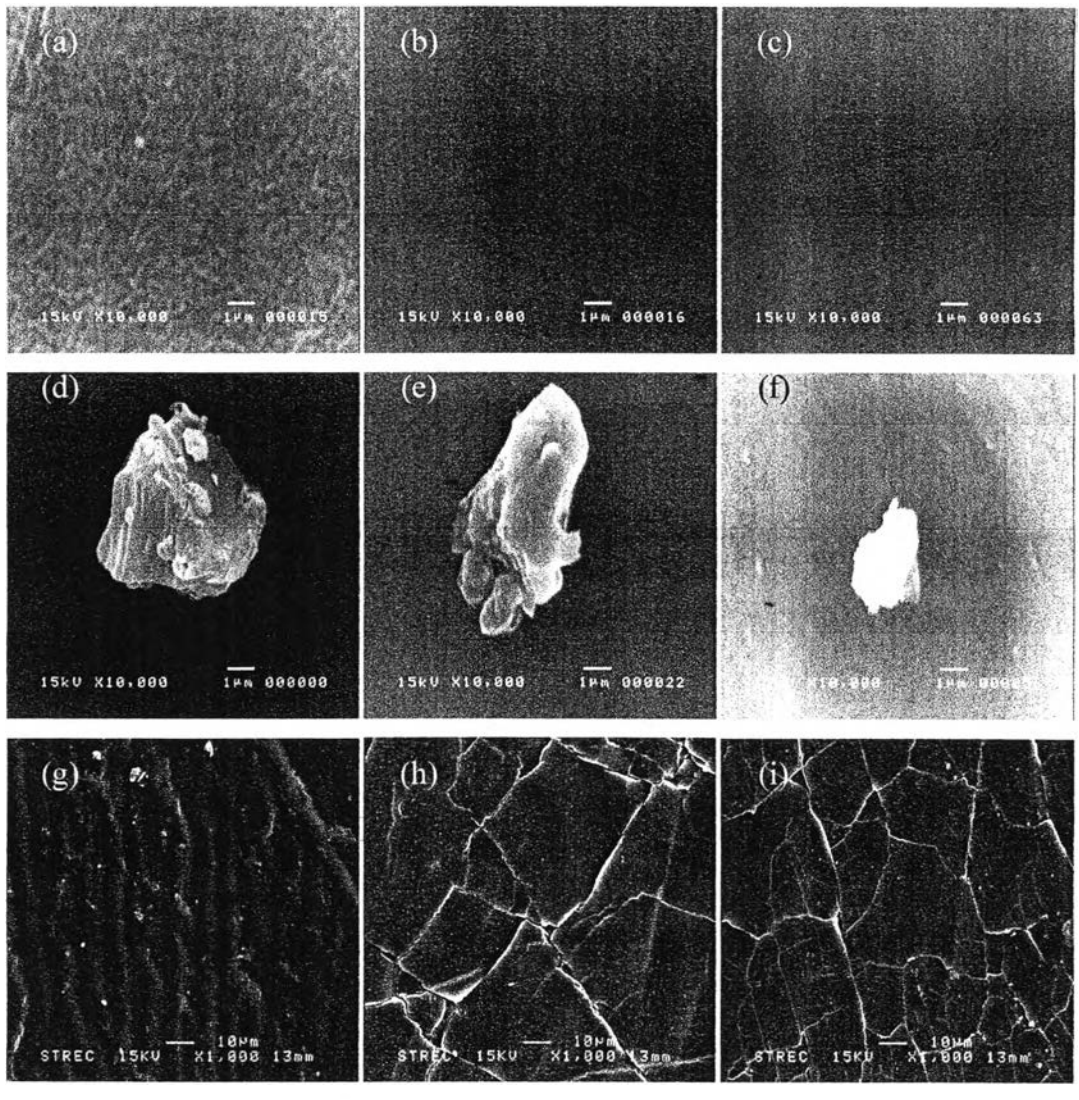

Figure I2 SEM micrographs of: (a) pure DDNR film at 10k; (b) crosslinked DCNR film with 0.0032 crosslink ratio at 10k; (c) cross-section of crosslinked DCNR film with 0.0032 crosslink ratio at 10k; (d) IN; (e) IN-loaded DCNR film with 0.0032 crosslink ratio at 10k; (f) cross-section of IN-loaded DCNR film with 0.0032 crosslink ratio at 10k; (g) crosslinked DCNR film with 0.0032 crosslink ratio after the release study in PBS buffer pH 7.4 at 1k; (h) the crack of IN-loaded DCNR film with 0.0032 crosslink ratio before the release study in PBS buffer pH 7.4 at 1k; and (i) the crack of IN-loaded DCNR film with 0.0032 crosslink ratio after the release study in PBS buffer pH 7.4 at 1k.

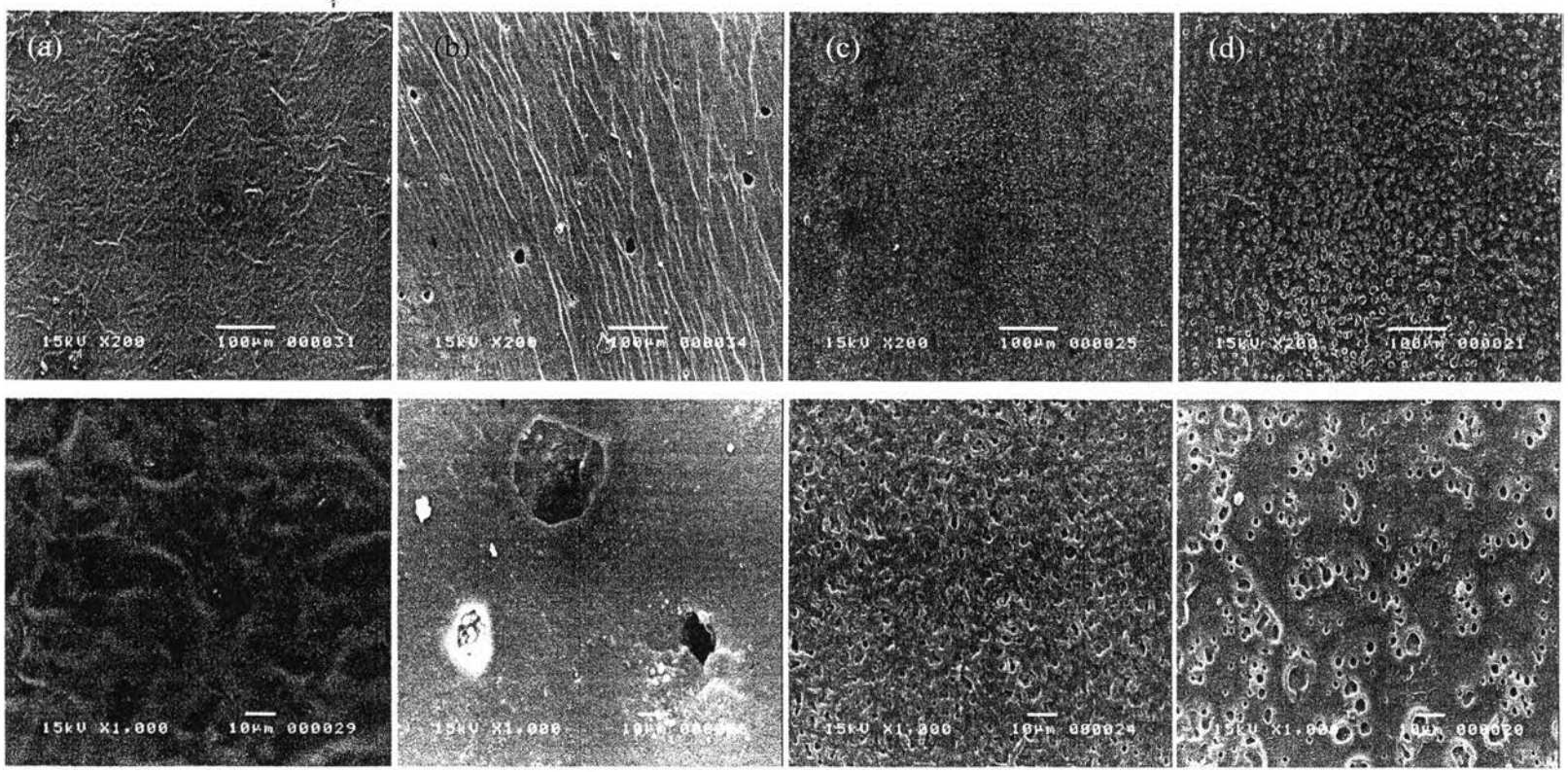

Figure I3 SEM micrographs of crosslinked DCNR film with 0.0032 crosslink ratio: (a) before the permeation study; (b) after the permeation study without electric field; (c) after the permeation study under electric field; and (d) after the release study without electric field in PBS buffer pH 7.4 at 200 and 1k of magnification.

The surface of crosslinked DCNR film after the permeation study without an electric field shows an irregular size and dispersion of holes, whereas the surface of the film after the permeation study with an electric field provides the similar size of holes and the abundant holes dispersed throughout the film. Considering the surface of the film after the release study without an electric field, the hole thoroughly disperses over the film and has a larger size than the hole on the surface of the film after the permeation study applied an electric field.

Table I1 Pore size on a surface of IN-loaded DCNR films and IN-doped PCz/DCNR films after the permeation study

Matrix	Crosslink ratio (mole $_{TMPTMP}$/mole $_{isoprene}$)	Electric field (V)	Pore size (μm)
NR	0.0032	0	19.64 ± 15.95
NR	0.0032	3	1.29 ± 0.37
NR	0.0064	3	14.69 ± 12.80
PCz/NR	0.0032	0	20.78 ± 7.25
PCz/NR	0.0032	1	3.60 ± 1.69
PCz/NR	0.0032	3	2.91 ± 1.34
PCz/NR	0.0032	5	90.71 ± 30.00
PCz/NR	0.0032	7	102.49 ± 66.68

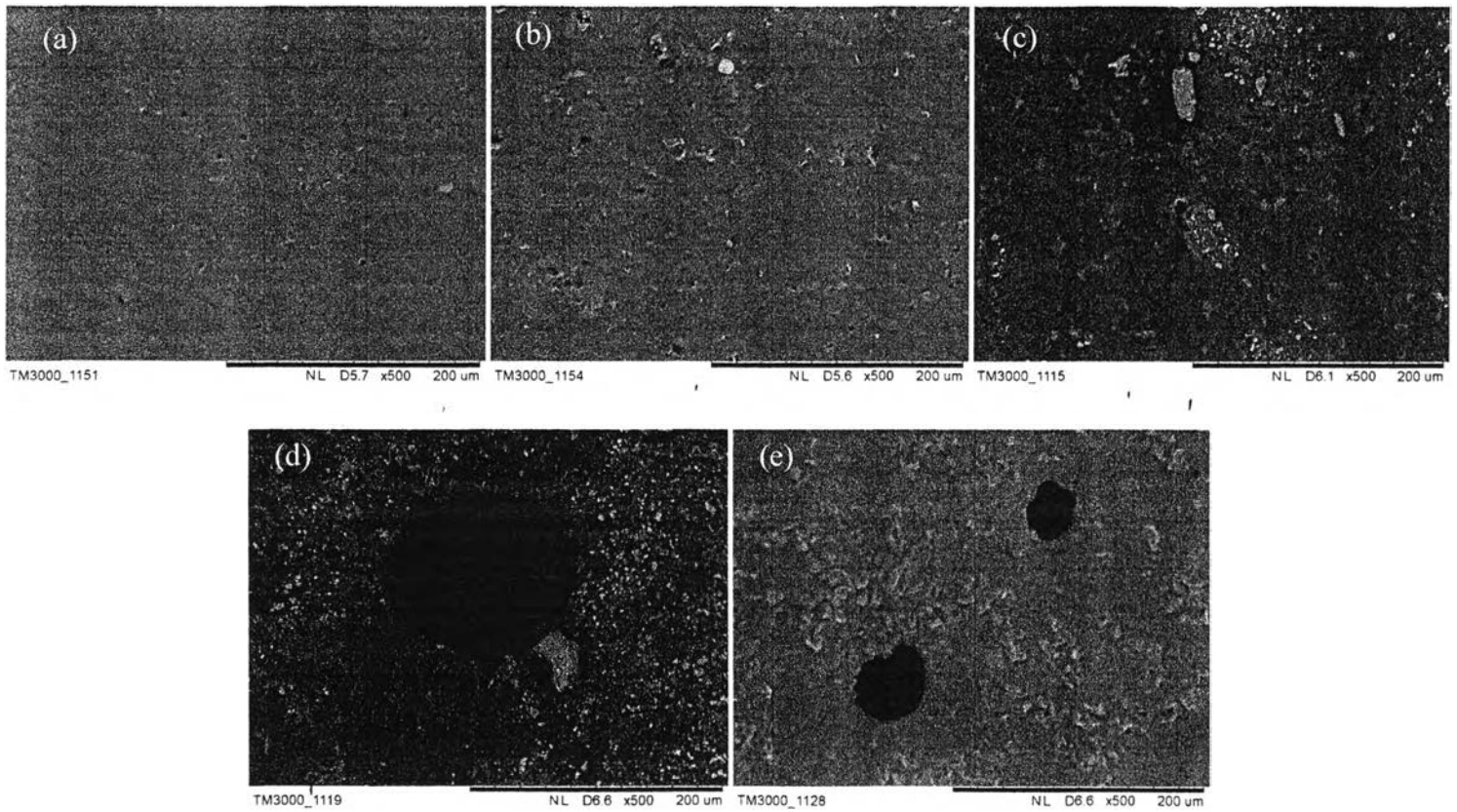

Figure I4 SEM micrographs of PCz/DCNR blend film with 0.0032 crosslink ratio after the permeation study at electric field strength of: (a) 0 V; (b) 1 V; (c) 3 V; (d) 5 V; and (e) 7 V, in PBS buffer pH 7.4, at 500 of magnification.

Appendix J Determination of Electrical Conductivity of IN-doped PCz at Various Doping Levels

IN dissolved in MeOH was reacted with dedoped PCz A 0.002 mole of dedoped PCz was doped again with various moles of IN. IN-doped PCz was determined the electrical conductivity using two-point probe meter.

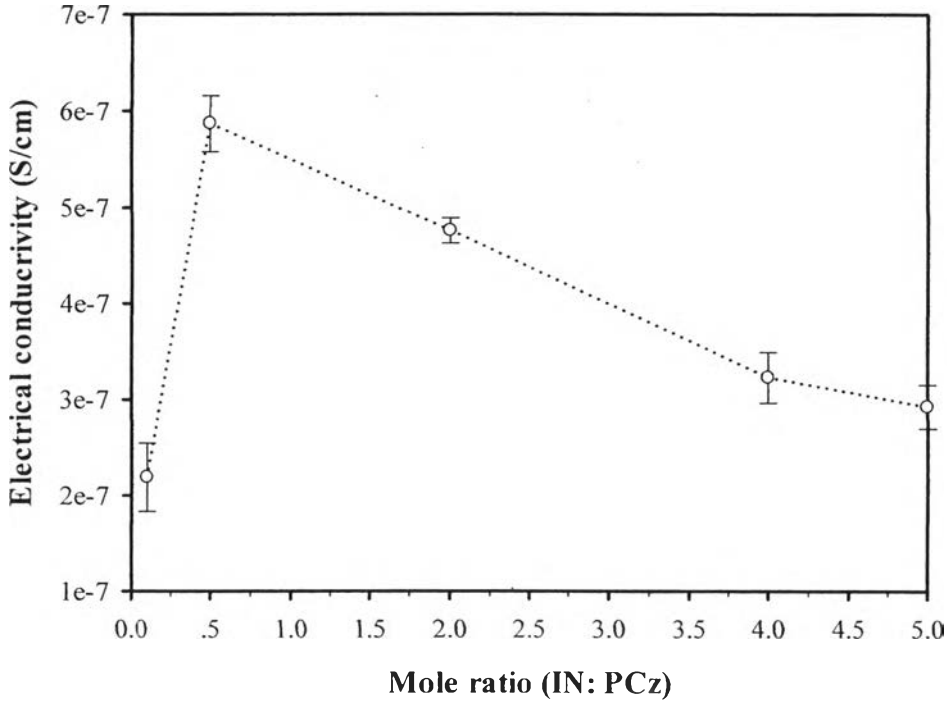

Figure J1 Electrical conductivity of IN-doped PCz at various mole ratios (IN: PCz).

IN: PCz at 0.5: 1 mole ratio provided the highest electrical conductivity and was used for preparation of IN-doped PCz/DCNR films.

Table J1 Electrical conductivity of IN-doped PCz at various mole ratios (IN: PCz)

Mole ratio	σ (S/cm)	Avg (S/cm)	SD
0.1	1.81E-07	2.19E-07	3.54E-08
	2.51E-07		
	2.25E-07		
0.5	5.54E-07	5.87E-07	2.90E-08
	5.99E-07		
	6.09E-07		
2	4.90E-07	4.76E-07	1.33E-08
	4.73E-07		
	4.64E-07		
4	2.96E-07	3.23E-07	2.62E-08
	3.49E-07		
	3.23E-07		
5	2.71E-07	2.92E-07	2.29E-08
	2.89E-07		
	3.17E-07		

Appendix K Release of IN from IN-doped PCz/DCNR Investigation

IN was reacted with dedoped PCz in aqueous hydrogen peroxide (H_2O_2) acted as oxidizing agent. IN-doped PCz was blended with the DCNR to prepare IN-doped PCz/DCNR film. UV-visible spectrometer (TECAN, Infinite M200) was used to investigate the amount of IN released from this film in the release study using modified Franz diffusion cell.

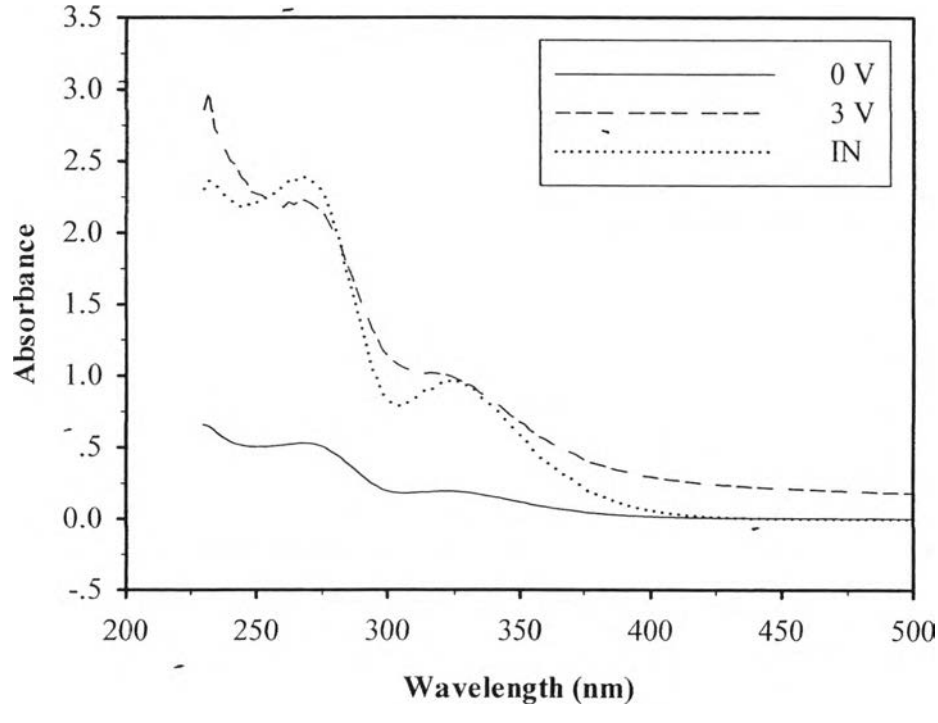

Figure K1 UV-visible spectra of IN and IN released under E = 0 V and E = 3 V.

Appendix L Determination of the Crosslink Density of Crosslinked DCNR Films

The crosslink density of films was calculated following a procedure of ATSM6814-02. The films (1 cm^2) were weighed in air and MeOH before and after leaving them to get the equilibrium swelling state in toluene for 5 days. A crosslink density was calculated using Eq. (L1) (Flory-Rehner equation)

$$\nu_e = \frac{-[\ln(1-V_r)+V_r+\chi_1 V_r^2]}{[V_1(V_r^{1/3}-V_r)/2]} \quad \text{..... (L1)}$$

where: ν_e = the number of chains in a real network per unit volume,

V_1 = the molar volume of tolune (106.29 mL/mol),

V_r = the crosslinked DCNR volume fraction in swollen state,

χ = the Flory interaction parameter of cis-1,4-polyisoprene in toluene (0.391).

V_r can be calculated following Eq. (L2);

$$V_r = \frac{\text{Weightof dry rubber / Density of dry rubber}}{\left(\frac{\text{Weight of dry rubber}}{\text{Density of dry rubber}}\right)+\left(\frac{\text{Weight of toluene absorbed by sample}}{\text{Density of toluene}}\right)} \quad \text{..... (L2)}$$

in which the density of the dry rubber can be computed by using the Eq. (L3)

$$\text{Density at } 23 \pm 2\ ^\circ\text{C (g/mL)} = 0.7913 \times \frac{A}{A-B} \quad \text{.....(L3)}$$

where: A = the weight of dried film measured in air (g),

B = the weight of dried film measured in MeOH (g),

0.7913 = the density of MeOH at 23 ± 2 °C (g/mL).

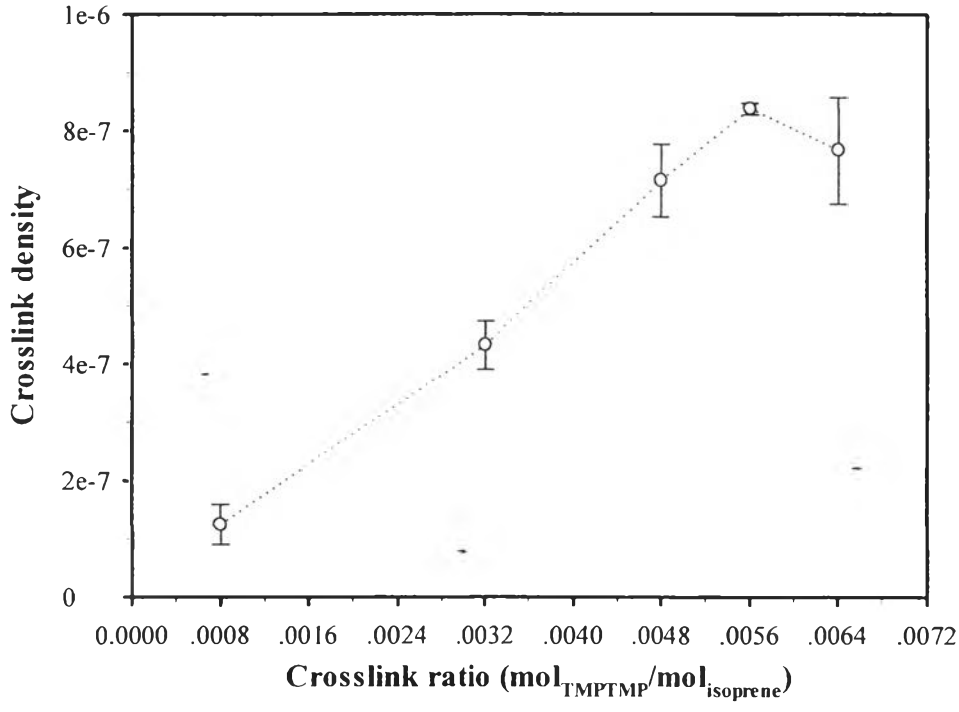

Figure L1 The crosslink density of the crosslinked DCNR film with various crosslink ratios.

Table L1 The crosslink density of the crosslinked DCNR film with various crosslink ratios after immersion in toluene for 5 days

Sample	W_i (g)		W_s (g)		W_d (g)		Crosslink density
	air	MeOH	air	MeOH	air	MeOH	
NR 0.22_1	0.0396	0.0380	0.4845	0.4203	0.0272	0.0253	1.10E-07
NR 0.22_2	0.0377	0.0362	0.4570	0.3956	0.0248	0.0239	1.02E-07
NR 0.22_3	0.0373	0.0357	0.3909	0.4592	0.0258	0.0223	1.64E-07
Avg							1.25E-07
SD							3.40E-08
NR 0.88_1	0.0570	0.0551	0.3344	0.3087	0.0442	0.0427	4.02E-07
NR 0.88_2	0.0523	0.0504	0.3044	0.2812	0.0409	0.0367	4.80E-07
NR 0.88_3	0.0474	0.0459	0.2636	0.2460	0.0371	0.0341	4.18E-07
Avg							4.33E-07
SD							4.12E-08
NR 1.32_1	0.0461	0.0442	0.2334	0.2125	0.0356	0.0340	7.79E-07
NR 1.32_2	0.0501	0.0483	0.2535	0.2316	0.0401	0.0377	6.56E-07
NR 1.32_3	0.0545	0.0524	0.2758	0.2489	0.0427	0.0410	7.12E-07
Avg							7.16E-07
SD							6.15E-08
NR 1.56_1	0.0406	0.0388	0.2317	0.2063	0.0355	0.0337	8.48E-07
NR 1.56_2	0.0451	0.0434	0.1962	0.1784	0.0328	0.0307	8.39E-07
NR 1.56_3	0.0510	0.0487	0.2664	0.2430	0.0388	0.0380	8.29E-07
Avg							8.39E-07
SD							9.85E-09
NR 1.76_1	0.0374	0.0360	0.1747	0.1581	0.0294	0.0283	8.10E-07
NR 1.76_2	0.0584	0.0561	0.3048	0.2759	0.0446	0.0437	6.63E-07
NR 1.76_3	0.0536	0.0512	0.2812	0.2538	0.0413	0.0394	8.29E-07
Avg							7.67E-07
SD							9.08E-08

Appendix M Determination of Actual Drug Content

The actual amounts of drug in the IN-loaded DCNR film and IN-doped PCz/DCNR film, a piece of film with area of 3.14 cm^2, were measured by immersing the samples in 100 mL of hexane. The amounts of drugs in 0.3 mL of solution were quantified by using the UV-visible spectrophotometer at a wavelength of 324 nm. The initial drug concentration in the film, C_0, was calculated from an actual amount of IN in the film (g) divided by a volume of the film (cm^3).

Table M1 The raw data of the determination of actual amount of IN in the IN-loaded DCNR films at various crosslink ratios ($mol_{TMPTMP}/mol_{isoprene}$) and IN-doped PCz/DCNR films

Sample	Actual amount of IN in the film area 3.14 cm^2		Volume (πr^2h*, cm^3)	C_0 (mg/cm^3)
	ppm	mg		
DCNR 0.0008 1	5.31	0.53		0.79
DCNR 0.0008 2	13.34	1.33		1.98
DCNR 0.0008 3	11.77	1.18		1.76
DCNR 0.0008 4	1.12	0.11		0.16
Avg	**7.88**	**0.79**		**1.17**
SD	**5.69**	**0.57**		**0.85**
DCNR 0.0032 1	5.06	0.51		0.76
DCNR 0.0032 2	8.21	0.82		1.22
DCNR 0.0032 3	8.00	0.80		1.19
DCNR 0.0032 4	7.50	0.75		1.12
Avg	**7.19**	**0.72**		**1.07**
SD	**1.45**	**0.15**	0.672	**0.21**
DCNR 0.0064 1	11.36	1.14		1.70
DCNR 0.0064 2	1.51	0.15		0.22
DCNR 0.0064 3	12.94	1.29		1.92
DCNR 0.0064 4	8.14	0.81		1.20
Avg	**8.49**	**0.85**		**1.26**
SD	**5.06**	**0.11**		**0.75**
IN-doped PCz/DCNR 1	7.16	0.71		1.06
IN-doped PCz/DCNR 2	6.83	0.68		1.01
IN-doped PCz/DCNR 3	7.29	0.72		1.07
Avg	**7.06**	**0.71**		**1.05**
SD	**0.20**	**0.02**		**0.03**

*h = the thickness of the film (0.214 cm)

Appendix N Determination of Amounts and Diffusion Coefficient of IN Permeated from Crosslinked DCNR Film at Various Crosslink Ratios in an Absence of Electric Field

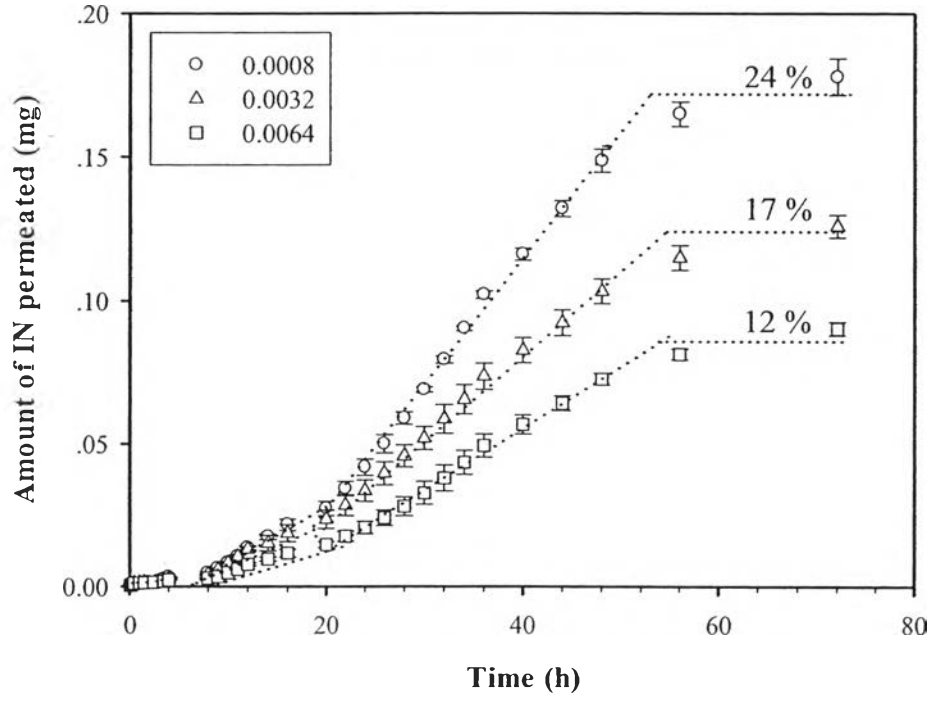

Figure N1 Amount of IN permeated from crosslinked DCNR film with various crosslink ratios ($mol_{TMPTMP}/mol_{isoprene}$) versus time t under an absence of electric field, pH 7.4, 37 °C.

The total amounts of IN permeated from 3.14 cm^2 of film with 0.0008, 0.0032, and 0.0064 crosslink ratios are 0.170 (24 %), 0.123 (17 %), and 0.085 (12 %) mg, respectively. The amount of permeant is inverslyly proportional to crosslink ratio as the drug mobility is reduced with an increase of crosslinking agent.

Table N1 The absorbance intensity and amount of IN permeated from crosslinked DCNR at 0.0008 crosslink ratio without electric field

Time	Absorbance			Amount of drug permeated (mg)				
(h)	1	2	3	1	2	3	Avg	SD
0.083	0.0082	0.0050	0.0081	0.0003	0.0002	0.0002	0.0002	0.0001
0.167	0.0120	0.0102	0.0085	0.0006	0.0005	0.0005	0.0005	0.0001
0.250	0.0046	0.0071	0.0033	0.0008	0.0007	0.0006	0.0007	0.0001
0.333	0.0029	0.0024	0.0030	0.0008	0.0008	0.0007	0.0008	0.0001
0.417	0.0028	0.0030	0.0026	0.0009	0.0008	0.0008	0.0009	0.0001
1.5	0.0108	0.0134	0.0160	0.0013	0.0013	0.0013	0.0013	0.0000
2.0	0.0065	0.0102	0.0073	0.0015	0.0016	0.0015	0.0015	0.0001
3.0	0.0130	0.0167	0.0149	0.0019	0.0021	0.0019	0.0020	0.0001
3.5	0.0260	0.0193	0.0212	0.0027	0.0027	0.0026	0.0026	0.0000
4.0	0.0277	0.0205	0.0223	0.0035	0.0033	0.0033	0.0034	0.0001
8.0	0.0366	0.0699	0.0321	0.0046	0.0054	0.0042	0.0048	0.0006
9.0	0.0563	0.0537	0.0527	0.0063	0.0071	0.0059	0.0064	0.0006
10.0	0.0657	0.0623	0.0640	0.0083	0.0090	0.0078	0.0084	0.0006
11.0	0.0697	0.0747	0.0693	0.0105	0.0112	0.0099	0.0105	0.0007
12.0	0.1123	0.0970	0.0947	0.0139	0.0142	0.0128	0.0136	0.0007
14.0	0.1510	0.0957	0.1240	0.0185	0.0171	0.0166	0.0174	0.0010
16.0	0.1737	0.1363	0.1053	0.0238	0.0213	0.0198	0.0216	0.0020
20.0	0.2083	0.1730	0.1767	0.0301	0.0265	0.0252	0.0273	0.0026
22.0	0.2237	0.2467	0.2187	0.0369	0.0341	0.0319	0.0343	0.0026
24.0	0.2553	0.2487	0.2337	0.0447	0.0416	0.0390	0.0418	0.0029
26.0	0.2687	0.2903	0.2503	0.0529	0.0505	0.0466	0.0500	0.0032
28.0	0.2620	0.2940	0.3287	0.0609	0.0595	0.0566	0.0590	0.0022
30.0	0.2737	0.3400	0.3727	0.0693	0.0698	0.0680	0.0690	0.0009
32.0	0.3727	0.3327	0.3327	0.0806	0.0800	0.0781	0.0796	0.0013
34.0	0.3340	0.3627	0.3727	0.0908	0.0910	0.0895	0.0904	0.0008
36.0	0.4033	0.3860	0.3657	0.1031	0.1028	0.1006	0.1022	0.0013
40.0	0.4810	0.4700	0.4307	0.1178	0.1171	0.1138	0.1162	0.0021
44.0	0.5370	0.5280	0.4947	0.1341	0.1332	0.1289	0.1321	0.0028
48.0	0.5880	0.5423	0.5033	0.1521	0.1497	0.1442	0.1487	0.0040
56.0	0.5527	0.5120	0.5323	0.1689	0.1654	0.1604	0.1649	0.0043
72.0	0.5387	0.5213	0.5507	0.1831	0.1798	0.1708	0.1779	0.0064

Table N2 The absorbance intensity and amount of IN permeated from crosslinked DCNR at 0.0032 crosslink ratio without electric field

Time	Absorbance			Amount of drug permeated (mg)				
(h)	1	2	3	1	2	3	Avg	SD
0.083	0.0000	0.0000	0.0000	0.0003	0.0001	0.0004	0.0003	0.0001
0.167	0.0094	0.0032	0.0127	0.0005	0.0003	0.0007	0.0005	0.0002
0.250	0.0063	0.0069	0.0087	0.0008	0.0004	0.0009	0.0007	0.0002
0.333	0.0092	0.0040	0.0078	0.0009	0.0005	0.0010	0.0008	0.0002
0.417	0.0033	0.0039	0.0033	0.0011	0.0008	0.0013	0.0011	0.0002
0.5	0.0091	0.0088	0.0094	0.0024	0.0019	0.0025	0.0023	0.0003
1.0	0.0085	0.0053	0.0065	0.0028	0.0024	0.0029	0.0027	0.0002
1.5	0.0065	0.0048	0.0054	0.0042	0.0045	0.0038	0.0042	0.0004
3.5	0.0276	0.0266	0.0278	0.0054	0.0066	0.0054	0.0058	0.0007
4.0	0.0125	0.0169	0.0127	0.0078	0.0089	0.0079	0.0082	0.0006
8.0	0.0457	0.0687	0.0308	0.0099	0.0113	0.0104	0.0105	0.0007
9.0	0.0387	0.0680	0.0523	0.0137	0.0134	0.0122	0.0131	0.0008
10.0	0.0803	0.0747	0.0811	0.0160	0.0175	0.0122	0.0152	0.0027
11.0	0.0690	0.0787	0.0815	0.0198	0.0209	0.0154	0.0187	0.0029
12.0	0.1230	0.0707	0.0597	0.0250	0.0257	0.0199	0.0235	0.0032
14.0	0.0743	0.1330	0.0943	0.0292	0.0317	0.0245	0.0285	0.0036
16.0	0.1267	0.1123	0.1050	0.0335	0.0373	0.0298	0.0335	0.0037
20.0	0.1697	0.1560	0.1467	0.0394	0.0439	0.0358	0.0397	0.0040
22.0	0.1377	0.1967	0.1520	0.0451	0.0499	0.0422	0.0457	0.0039
24.0	0.1407	0.1850	0.1750	0.0510	0.0565	0.0485	0.0520	0.0041
26.0	0.1943	0.2150	0.1967	0.0578	0.0641	0.0541	0.0587	0.0051
28.0	0.1863	0.1987	0.2103	0.0651	0.0710	0.0609	0.0656	0.0051
30.0	0.1940	0.2143	0.2047	0.0737	0.0783	0.0692	0.0737	0.0046
32.0	0.2247	0.2517	0.1857	0.0833	0.0870	0.0783	0.0829	0.0044
34.0	0.2363	0.2253	0.2208	0.0920	0.0971	0.0881	0.0924	0.0045
36.0	0.2833	0.2403	0.2720	0.1036	0.1076	0.0990	0.1034	0.0043
40.0	0.3157	0.2840	0.2993	0.1160	0.1187	0.1103	0.1150	0.0043
44.0	0.2853	0.3310	0.3220	0.1272	0.1292	0.1216	0.1260	0.0039
48.0	0.3793	0.3443	0.3570	0.0024	0.0019	0.0025	0.0023	0.0003
56.0	0.4067	0.3660	0.3720	0.0028	0.0024	0.0029	0.0027	0.0002
72.0	0.3667	0.3433	0.3693	0.0042	0.0045	0.0038	0.0042	0.0004

Table N3 The absorbance intensity and amount of IN permeated from crosslinked DCNR at 0.0064 crosslink ratio without electric field

Time	Absorbance			Amount of drug permeated (mg)				
(h)	1	2	3	1	2	3	Avg	SD
0.083	0.0106	0.0113	0.0092	0.0003	0.0003	0.0003	0.0003	0.0000
0.167	0.0114	0.0111	0.0105	0.0007	0.0007	0.0006	0.0007	0.0000
0.250	0.0031	0.0054	0.0044	0.0008	0.0008	0.0007	0.0008	0.0001
0.333	0.0053	0.0083	0.0047	0.0009	0.0011	0.0009	0.0010	0.0001
0.417	0.0033	0.0042	0.0038	0.0010	0.0012	0.0010	0.0011	0.0001
1.0	0.0044	0.0043	0.0044	0.0012	0.0014	0.0011	0.0012	0.0001
1.5	0.0041	0.0042	0.0038	0.0013	0.0015	0.0012	0.0013	0.0001
2.5	0.0045	0.0044	0.0044	0.0014	0.0016	0.0014	0.0015	0.0001
3.5	0.0121	0.0094	0.0136	0.0018	0.0019	0.0018	0.0018	0.0001
4.0	0.0145	0.0153	0.0171	0.0022	0.0024	0.0023	0.0023	0.0001
8.0	0.0231	0.0244	0.0222	0.0029	0.0031	0.0030	0.0030	0.0001
9.0	0.0154	0.0147	0.0212	0.0034	0.0036	0.0036	0.0035	0.0001
10.0	0.0397	0.0430	0.0450	0.0046	0.0049	0.0050	0.0048	0.0002
11.0	0.0397	0.0410	0.0393	0.0058	0.0061	0.0062	0.0061	0.0002
12.0	0.0553	0.0462	0.0717	0.0075	0.0075	0.0084	0.0078	0.0005
14.0	0.0427	0.0723	0.0617	0.0088	0.0097	0.0103	0.0096	0.0007
16.0	0.0677	0.0413	0.0993	0.0109	0.0110	0.0133	0.0117	0.0014
20.0	0.1030	0.0987	0.0850	0.0140	0.0140	0.0159	0.0146	0.0011
22.0	0.0730	0.0970	0.1200	0.0162	0.0170	0.0195	0.0176	0.0017
24.0	0.0873	0.0997	0.1170	0.0189	0.0200	0.0231	0.0207	0.0022
26.0	0.0807	0.1303	0.1223	0.0214	0.0240	0.0268	0.0241	0.0027
28.0	0.1293	0.1093	0.1597	0.0253	0.0273	0.0317	0.0281	0.0033
30.0	0.1497	0.1207	0.1877	0.0299	0.0310	0.0374	0.0328	0.0041
32.0	0.1697	0.1520	0.1930	0.0350	0.0356	0.0433	0.0380	0.0046
34.0	0.1730	0.2020	0.1637	0.0403	0.0418	0.0483	0.0435	0.0043
36.0	0.2067	0.1843	0.1867	0.0466	0.0474	0.0540	0.0493	0.0041
40.0	0.2503	0.2627	0.2193	0.0543	0.0554	0.0607	0.0568	0.0034
44.0	0.2643	0.2540	0.2150	0.0623	0.0632	0.0672	0.0642	0.0026
48.0	0.2763	0.3097	0.2503	0.0707	0.0726	0.0749	0.0727	0.0021
56.0	0.2893	0.2947	0.2787	0.0796	0.0816	0.0834	0.0815	0.0019
72.0	0.2707	0.3060	0.2967	0.0878	0.0909	0.0924	0.0904	0.0023

Release Kinetics of Model Drug from IN-loaded Crosslinked DCNR Films

The appearance of two steps of IN permeation from all crosslinked DCNR films in figure N1 was investigated for a transport behavior using the Korsmeyer-Peppas equation:

$$\frac{M_t}{M_\infty} = kt^n \quad \text{(N1)}$$

where M_t and M_∞ = the amount of drug released from DCNR film at time t and the total amount of drug release, respectively (mg),

k = the kinetic constant (h^{-n}),

t = time (h),

n = the diffusion scaling exponent.

Then, the log value of M_t/M_∞ was plotted against log time to calculate the release exponent, n according to Eq. (N2)

$$\log\left(\frac{M_t}{M_\infty}\right) = \log k + n \log t \quad \text{(N2)}$$

The diffusional exponent, n, from each batch shows two diffusion stages (n_1 and n_2). For the first stage, n_1 is equal to 0.519, 0.569, and 0.322 in 0.0008, 0.0032, and 0.0064 crosslink ratios, respectively. For the second stage, n_2 is equal to 1.772, 1.705, and 1.755 in 0.0008, 0.0032, and 0.0064 crosslink ratio, respectively. The result indicates that the drug transport behavior in the first stage of all systems is considered as Fickian which occurs from a diffusion of IN through the matrix. In the second stage, the transport behavior is considered as Super Case II transport. This transport mechanism results from a relaxation of polymer and an erosion mechanism (Sriamornsak *et al.*, 2007).

The release mechanisms are force-fitted to the Higuchi equation (n = 0.5) and then the diffusion coefficient of IN from a crosslinked DCNR film was calculated by Eq. (N3), Eq. (N4), and Eq. (N5):

$$\frac{M_t}{M_\infty} = kt^{1/2} \quad \text{(N3)}$$

$$Q = \frac{M_t}{A} = 2C_0\left(\frac{Dt}{\pi}\right)^{1/2} \quad \text{(N4)}$$

$$M_t = k_H M_\infty t^{1/2} = 2C_0 \left(\frac{D^{1/2}}{\pi^{1/2}}\right) A\, t^{1/2} \quad \text{(N5)}$$

where M_t/M_∞ = the fractional drug release

k_H = a kinetic constant (with the unit of t^{-n})

t = the release time

Q = the amount of material flowing through a unit cross section of barrier (g/cm^2) in unit time, t (s)

C_0 = the initial drug concentration in the film (g/cm^3)

D = the diffusion coefficient of a drug (cm^2/s)

The diffusion coefficient was calculated from the slope of the plot of the amounts of IN permeated from IN-loaded DCNR at time t versus square root of time.

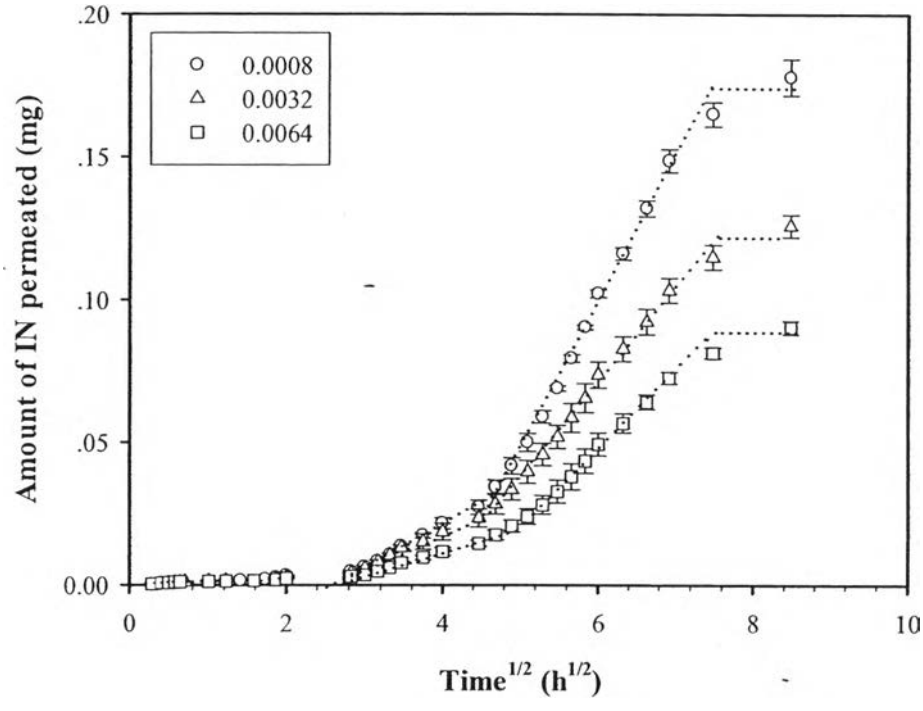

Figure N2 Amounts of IN permeated from IN-loaded DCNR film versus time$^{1/2}$ with various crosslink ratios ($mol_{TMPTMP}/mol_{isoprene}$) under absence of electric field, pH 7.4, 37 °C.

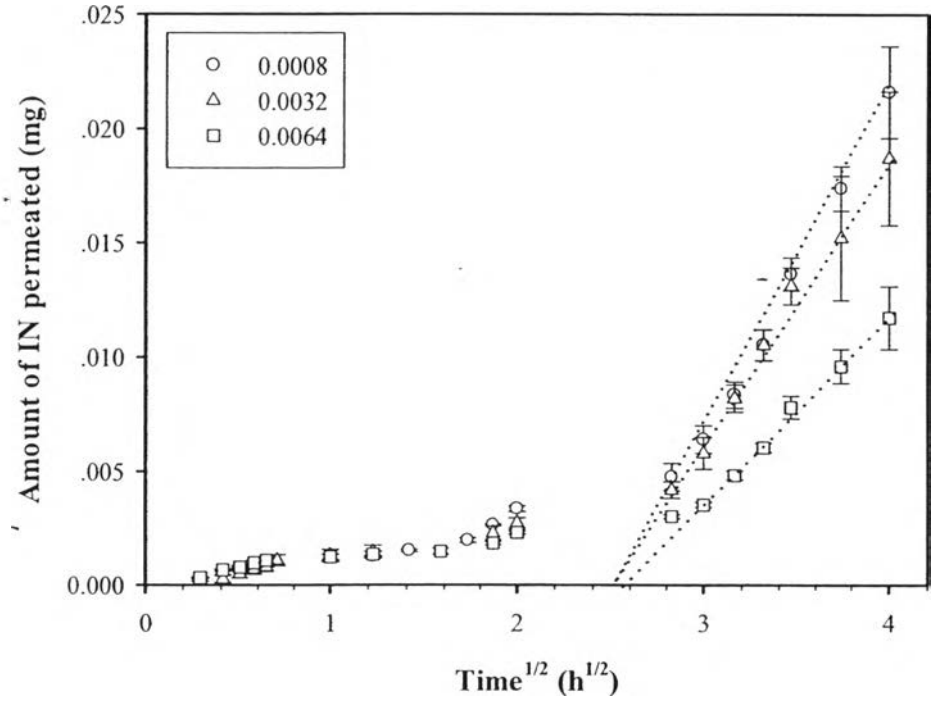

Figure N3 Amounts of IN permeated from IN-loaded DCNR film versus time$^{1/2}$ with various crosslink ratios ($mol_{TMPTMP}/mol_{isoprene}$) in the first region under absence of electric field.

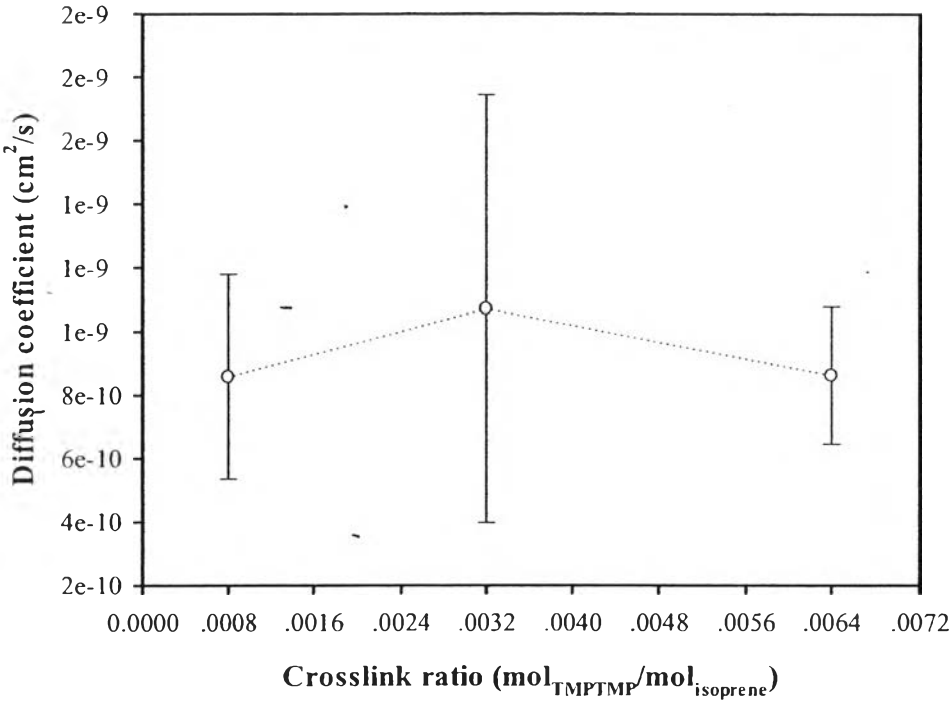

Figure N4 Diffusion coefficients (D_1) of IN from IN-loaded DCNR films versus crosslink ratio ($mol_{TMPTMP}/mol_{isoprene}$) under absence of electric field, pH 7.4, 37 °C.

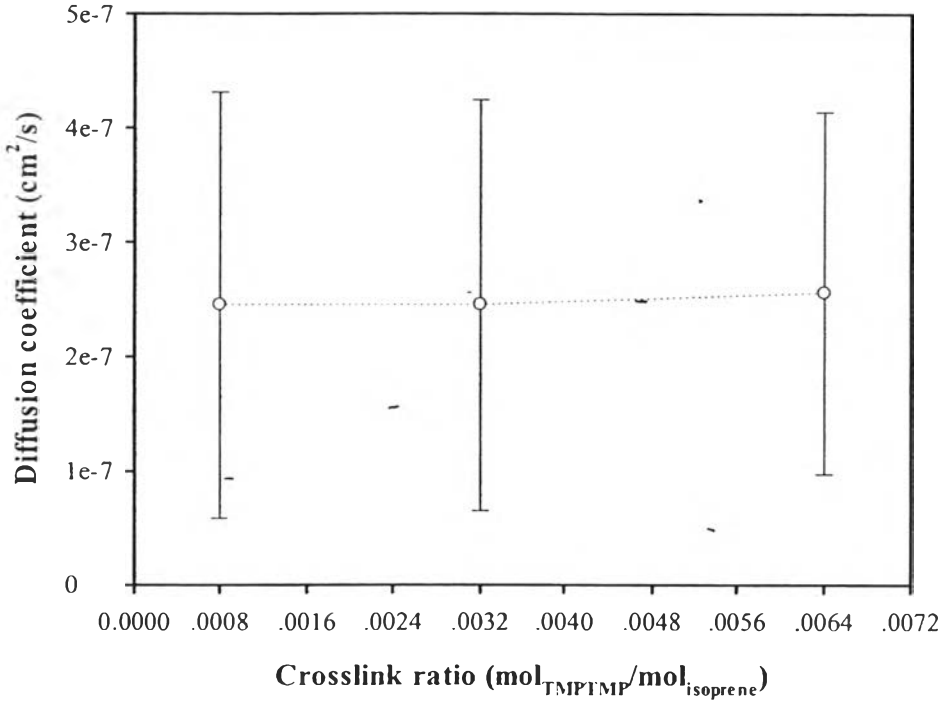

Figure N5 Diffusion coefficients (D_2) of IN from IN-loaded DCNR films versus crosslink ratio ($mol_{TMPTMP}/mol_{isoprene}$) under absence of electric field, pH 7.4, 37 °C.

Table N4 The diffusion coefficients (D_1) of IN permeated from various crosslinked DCNR films, pH 7.4 at 37 °C, E = 0 V

Crosslink ratio ($mol_{TMPTMP}/mol_{isoprene}$)	**Slope**	**Diffusion coefficient** (cm^2/h)	**Diffusion coefficient** (cm^2/s)	**Average** (cm^2/s)	**SD**
0.0008	0.0023	3.01E-06	8.36E-10	8.36E-10	0.00E+00
	0.0023	3.01E-06	8.36E-10		
	0.0023	3.01E-06	8.36E-10		
0.0032	0.0025	4.28E-06	1.19E-09	1.37E-09	3.99E-10
	0.0031	6.58E-06	1.83E-09		
	0.0024	3.94E-06	1.09E-09		
0.0064	0.0020	1.97E-06	5.47E-10	5.85E-06	6.57E-11
	0.0020	1.97E-06	5.47E-10		
	0.0022	2.38E-06	6.61E-10		

Table N5 The diffusion coefficients (D_2) of IN permeated from various crosslinked DCNR films, pH 7.4 at 37 °C, E = 0 V

Crosslink ratio ($mol_{TMPTMP}/mol_{isoprene}$)	**Slope**	**Diffusion coefficient (cm^2/h)**	**Diffusion coefficient (cm^2/s)**	**Average (cm^2/s)**	**SD**
0.0008	0.0535	1.63E-03	4.52E-07	4.39E-07	1.73E-08
	0.0531	1.60E-03	4.44E-07		
	0.0515	1.51E-03	4.19E-07		
0.0032	0.0318	6.92E-04	1.92E-07	2.11E-07	2.95E-08
	0.0321	7.06E-04	1.96E-07		
	0.0359	8.83E-04	2.45E-07		
0.0064	0.0258	3.27E-04	9.08E-08	9.61E-08	5.91E-09
	0.0264	3.42E-04	9.50E-08		
	0.0274	3.69E-04	1.03E-07		

Appendix O Determination of Amounts and Diffusion Coefficient of IN Permeated from IN-loaded DCNR Films at Crosslink Ratio = 0.0032 and at various Electric Field Strengths under Cathode

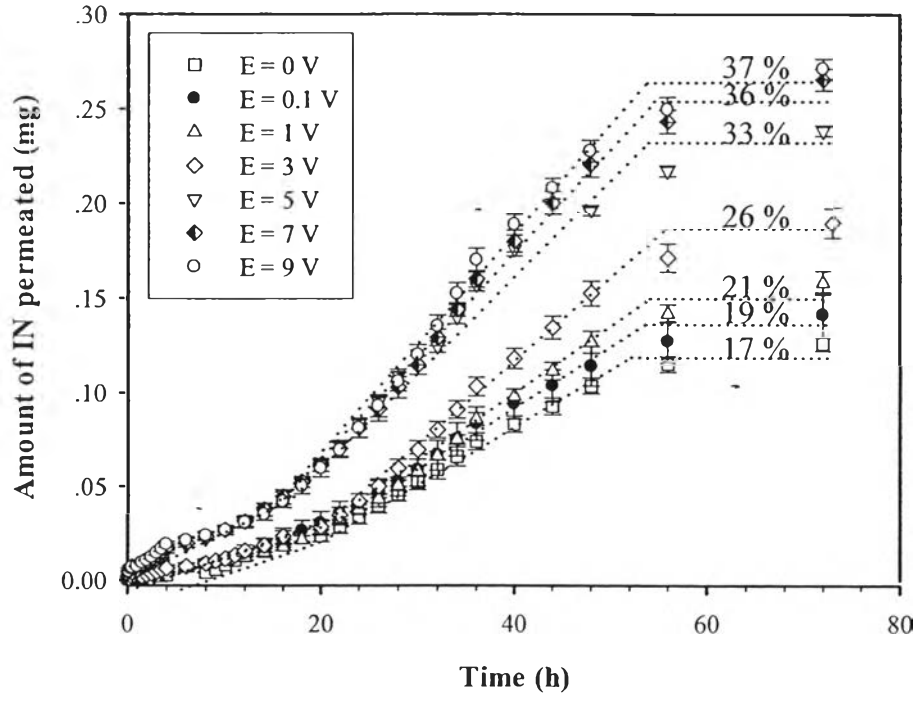

Figure O1 Amount of IN permeated from crosslinked DCNR film with various electric field strengths at 0.0032 crosslink ratio, pH 7.4, 37 °C.

The total amounts of IN permeated from 3.14 cm^2 of DCNR films with 0.0032 crosslink ratio at E = 0, 0.1, 1, 3, 5, 7, and 9 V are 0.118 (17 %), 0.136 (19 %), 0.150 (21 %), 0.186 (26 %), 0.232 (33 %), 0.254 (36 %), and 0.264 (37 %) mg, respectively. The amount of IN is directly proportional to electric field strength. The electrorepulsive force generated by repulsion between a negative charge of anionic drug and positive charge of cathode is the driving force for the drug transportation. Thus, the enhancement of electric field strength influences in increasing the driving force which promotes a diffusion of IN from the DCNR film.

Table O1 The absorbance intensity and amount of IN permeated from crosslinked DCNR at 0.0032 crosslink ratio under an absence of electric field (E = 0 V)

Time	Absorbance			Amount of drug permeated (mg)				
(h)	1	2	3	1	2	3	Avg	SD
0.083	0.0000	0.0000	0.0000	0.0000	0.0000	0.0000	0.0000	0.0000
0.167	0.0094	0.0032	0.0127	0.0003	0.0001	0.0004	0.0003	0.0001
0.250	0.0063	0.0069	0.0087	0.0005	0.0003	0.0007	0.0005	0.0002
0.333	0.0092	0.0040	0.0078	0.0008	0.0004	0.0009	0.0007	0.0002
0.417	0.0033	0.0039	0.0033	0.0009	0.0005	0.0010	0.0008	0.0002
0.5	0.0091	0.0088	0.0094	0.0011	0.0008	0.0013	0.0011	0.0002
1.0	0.0085	0.0053	0.0065	0.0014	0.0010	0.0015	0.0013	0.0003
1.5	0.0065	0.0048	0.0054	0.0016	0.0011	0.0016	0.0015	0.0003
3.5	0.0276	0.0266	0.0278	0.0024	0.0019	0.0025	0.0023	0.0003
4.0	0.0125	0.0169	0.0127	0.0028	0.0024	0.0029	0.0027	0.0002
8.0	0.0457	0.0687	0.0308	0.0042	0.0045	0.0038	0.0042	0.0004
9.0	0.0387	0.0680	0.0523	0.0054	0.0066	0.0054	0.0058	0.0007
10.0	0.0803	0.0747	0.0811	0.0078	0.0089	0.0079	0.0082	0.0006
11.0	0.0690	0.0787	0.0815	0.0099	0.0113	0.0104	0.0105	0.0007
12.0	0.1230	0.0707	0.0597	0.0137	0.0134	0.0122	0.0131	0.0008
14.0	0.0743	0.1330	0.0943	0.0160	0.0175	0.0122	0.0152	0.0027
16.0	0.1267	0.1123	0.1050	0.0198	0.0209	0.0154	0.0187	0.0029
20.0	0.1697	0.1560	0.1467	0.0250	0.0257	0.0199	0.0235	0.0032
22.0	0.1377	0.1967	0.1520	0.0292	0.0317	0.0245	0.0285	0.0036
24.0	0.1407	0.1850	0.1750	0.0335	0.0373	0.0298	0.0335	0.0037
26.0	0.1943	0.2150	0.1967	0.0394	0.0439	0.0358	0.0397	0.0040
28.0	0.1863	0.1987	0.2103	0.0451	0.0499	0.0422	0.0457	0.0039
30.0	0.1940	0.2143	0.2047	0.0510	0.0565	0.0485	0.0520	0.0041
32.0	0.2247	0.2517	0.1857	0.0578	0.0641	0.0541	0.0587	0.0051
34.0	0.2363	0.2253	0.2208	0.0651	0.0710	0.0609	0.0656	0.0051
36.0	0.2833	0.2403	0.2720	0.0737	0.0783	0.0692	0.0737	0.0046
40.0	0.3157	0.2840	0.2993	0.0833	0.0870	0.0783	0.0829	0.0044
44.0	0.2853	0.3310	0.3220	0.0920	0.0971	0.0881	0.0924	0.0045
48.0	0.3793	0.3443	0.3570	0.1036	0.1076	0.0990	0.1034	0.0043
56.0	0.4067	0.3660	0.3720	0.1160	0.1187	0.1103	0.1150	0.0043
72.0	0.3667	0.3433	0.3693	0.1272	0.1292	0.1216	0.1260	0.0039

Table O2 The absorbance intensity and amount of IN permeated from crosslinked DCNR at 0.0032 crosslink ratio under an electric field (E = 0.1 V)

Time	Absorbance			Amount of drug permeated (mg)				
(h)	1	2	3	1	2	3	Avg	SD
0.083	0.0263	0.0473	0.0640	0.0008	0.0014	0.0020	0.0014	0.0006
0.167	0.0220	0.0021	0.0137	0.0015	0.0015	0.0024	0.0018	0.0005
0.250	0.0086	0.0012	0.0125	0.0017	0.0015	0.0028	0.0020	0.0007
0.333	0.0216	0.0036	0.0110	0.0024	0.0017	0.0031	0.0024	0.0007
0.417	0.0068	0.0105	0.0040	0.0026	0.0020	0.0032	0.0026	0.0006
0.5	0.0068	0.0011	0.0035	0.0028	0.0020	0.0033	0.0027	0.0007
1.0	0.0357	0.0211	0.0383	0.0029	0.0027	0.0034	0.0030	0.0004
1.5	0.0119	0.0143	0.0082	0.0033	0.0031	0.0037	0.0034	0.0003
2.0	0.0008	0.0302	0.0121	0.0033	0.0040	0.0041	0.0038	0.0004
2.5	0.0001	0.0259	0.0036	0.0033	0.0048	0.0042	0.0041	0.0007
3.0	0.0194	0.0613	0.0256	0.0039	0.0057	0.0049	0.0048	0.0009
3.5	0.0120	0.0463	0.0010	0.0043	0.0071	0.0050	0.0054	0.0015
4.0	0.0062	0.0477	0.0135	0.0045	0.0082	0.0054	0.0060	0.0020
8.0	0.0196	0.0563	0.0069	0.0051	0.0094	0.0056	0.0067	0.0024
9.0	0.0363	0.0800	0.0840	0.0072	0.0115	0.0076	0.0088	0.0024
10.0	0.0893	0.0473	0.0563	0.0093	0.0136	0.0094	0.0108	0.0025
11.0	0.0767	0.1180	0.0887	0.0116	0.0172	0.0121	0.0136	0.0031
12.0	0.2113	0.1547	0.0977	0.0181	0.0219	0.0150	0.0183	0.0034
14.0	0.0513	0.1663	0.1340	0.0196	0.0270	0.0191	0.0219	0.0044
16.0	0.1783	0.1730	0.0683	0.0251	0.0323	0.0212	0.0262	0.0056
20.0	0.0853	0.1697	0.1390	0.0277	0.0374	0.0255	0.0302	0.0064
22.0	0.1157	0.1717	0.2380	0.0312	0.0427	0.0327	0.0355	0.0062
24.0	0.0600	0.2250	0.1863	0.0361	0.0465	0.0384	0.0403	0.0055
26.0	0.1137	0.2250	0.2077	0.0395	0.0533	0.0447	0.0459	0.0070
28.0	0.2487	0.2483	0.1290	0.0471	0.0609	0.0487	0.0522	0.0076
30.0	0.1977	0.2417	0.1733	0.0532	0.0683	0.0539	0.0585	0.0085
32.0	0.2817	0.2393	0.2540	0.0617	0.0756	0.0617	0.0663	0.0080
34.0	0.2947	0.3040	0.2273	0.0707	0.0848	0.0686	0.0747	0.0088
36.0	0.3233	0.2710	0.2397	0.0806	0.0931	0.0759	0.0832	0.0089
40.0	0.3067	0.3150	0.3910	0.0899	0.1027	0.0878	0.0935	0.0080
44.0	0.3123	0.3437	0.3103	0.0995	0.1132	0.0973	0.1033	0.0086
48.0	0.3093	0.4130	0.3083	0.1089	0.1258	0.1067	0.1138	0.0104
56.0	0.4520	0.4477	0.4177	0.1227	0.1394	0.1194	0.1272	0.0107
72.0	0.4547	0.5043	0.4280	0.1365	0.1548	0.1325	0.1413	0.0119

Table O3 The absorbance intensity and amount of IN permeated from crosslinked DCNR at 0.0032 crosslink ratio under an electric field (E = 1 V)

Time	Absorbance			Amount of drug permeated (mg)				
(h)	1	2	3	1	2	3	Avg	SD
0.083	0.0252	0.0037	0.0137	0.0008	0.0001	0.0004	0.0004	0.0003
0.167	0.0091	0.0070	0.0071	0.0010	0.0003	0.0006	0.0007	0.0004
0.250	0.0076	0.0048	0.0017	0.0013	0.0005	0.0007	0.0008	0.0004
0.333	0.0052	0.0054	0.0150	0.0014	0.0006	0.0011	0.0011	0.0004
0.417	0.0148	0.0085	0.0034	0.0019	0.0009	0.0012	0.0013	0.0005
0.5	0.0167	0.0102	0.0313	0.0024	0.0012	0.0022	0.0019	0.0006
1.0	0.0095	0.0068	0.0054	0.0027	0.0014	0.0024	0.0022	0.0007
1.5	0.0100	0.0099	0.0159	0.0030	0.0017	0.0029	0.0025	0.0007
2.0	0.0069	0.0149	0.0156	0.0032	0.0022	0.0033	0.0029	0.0006
2.5	0.0162	0.0100	0.0221	0.0037	0.0025	0.0040	0.0034	0.0008
3.0	0.0293	0.0207	0.0333	0.0046	0.0031	0.0050	0.0042	0.0010
3.5	0.0230	0.0270	0.0327	0.0053	0.0039	0.0060	0.0051	0.0011
4.0	0.0280	0.0267	0.0703	0.0061	0.0047	0.0082	0.0063	0.0017
8.0	0.0410	0.0233	0.0257	0.0074	0.0055	0.0089	0.0073	0.0017
9.0	0.0310	0.0607	0.0527	0.0083	0.0073	0.0105	0.0087	0.0017
10.0	0.0567	0.0453	0.0343	0.0101	0.0087	0.0116	0.0101	0.0015
11.0	0.0707	0.0513	0.0847	0.0122	0.0103	0.0142	0.0122	0.0020
12.0	0.0930	0.0857	0.0847	0.0150	0.0129	0.0168	0.0149	0.0020
14.0	0.0950	0.0947	0.0893	0.0179	0.0157	0.0195	0.0177	0.0019
16.0	0.1107	0.1320	0.1373	0.0213	0.0198	0.0237	0.0216	0.0020
20.0	0.1437	0.1500	0.1713	0.0257	0.0243	0.0289	0.0263	0.0023
22.0	0.1393	0.2010	0.1833	0.0299	0.0305	0.0345	0.0316	0.0025
24.0	0.2147	0.1657	0.1993	0.0365	0.0355	0.0406	0.0375	0.0027
26.0	0.1720	0.2070	0.1713	0.0417	0.0418	0.0458	0.0431	0.0023
28.0	0.2267	0.2170	0.2470	0.0486	0.0485	0.0533	0.0501	0.0027
30.0	0.2977	0.2127	0.2350	0.0577	0.0549	0.0605	0.0577	0.0028
32.0	0.2853	0.2833	0.2533	0.0664	0.0636	0.0682	0.0661	0.0023
34.0	0.2697	0.2833	0.2963	0.0746	0.0722	0.0772	0.0747	0.0025
36.0	0.3470	0.3350	0.3867	0.0852	0.0824	0.0890	0.0856	0.0033
40.0	0.4187	0.3737	0.4167	0.0980	0.0938	0.1017	0.0978	0.0040
44.0	0.4013	0.4403	0.4817	0.1102	0.1072	0.1164	0.1113	0.0047
48.0	0.5260	0.4443	0.5260	0.1263	0.1208	0.1324	0.1265	0.0058
56.0	0.5233	0.5330	0.4677	0.1422	0.1370	0.1467	0.1420	0.0048
72.0	0.5107	0.4943	0.5833	0.1578	0.1521	0.1645	0.1581	0.0062

Table O4 The absorbance intensity and amount of IN permeated from crosslinked DCNR at 0.0032 crosslink ratio under an electric field (E = 3 V)

Time	Absorbance			Amount of drug permeated (mg)				
(h)	1	2	3	1	2	3	Avg	SD
0.083	0.0123	0.0147	0.0216	0.0004	0.0004	0.0007	0.0005	0.0001
0.167	0.0005	0.0033	0.0000	0.0009	0.0008	0.0009	0.0009	0.0001
0.333	0.0108	0.0226	0.0073	0.0012	0.0015	0.0011	0.0013	0.0002
0.417	0.0084	0.0137	0.0057	0.0015	0.0019	0.0013	0.0015	0.0003
0.5	0.0071	0.0128	0.0115	0.0017	0.0023	0.0017	0.0019	0.0003
1.5	0.0107	0.0054	0.0071	0.0020	0.0024	0.0019	0.0021	0.0003
2.0	0.0278	0.0240	0.0333	0.0029	0.0032	0.0029	0.0030	0.0002
2.5	0.0253	0.0231	0.0258	0.0036	0.0039	0.0037	0.0037	0.0001
3.0	0.0298	0.0238	0.0286	0.0045	0.0046	0.0045	0.0046	0.0000
3.5	0.0433	0.0219	0.0310	0.0059	0.0053	0.0055	0.0055	0.0003
4.0	0.0289	0.0287	0.0248	0.0067	0.0061	0.0062	0.0064	0.0003
6.0	0.0319	0.0353	0.0347	0.0077	0.0072	0.0073	0.0074	0.0003
8.0	0.0627	0.0630	0.0267	0.0096	0.0091	0.0081	0.0090	0.0008
9.0	0.0279	0.0770	0.0243	0.0105	0.0115	0.0089	0.0103	0.0013
10.0	0.0300	0.0457	0.0427	0.0114	0.0129	0.0102	0.0115	0.0014
11.0	0.0202	0.0837	0.0640	0.0120	0.0154	0.0121	0.0132	0.0019
12.0	0.0710	0.1243	0.0477	0.0142	0.0192	0.0136	0.0157	0.0031
14.0	0.0827	0.1210	0.0893	0.0167	0.0229	0.0163	0.0186	0.0037
16.0	0.1313	0.1790	0.1493	0.0207	0.0284	0.0208	0.0233	0.0044
20.0	0.1540	0.1373	0.2060	0.0254	0.0326	0.0271	0.0284	0.0037
22.0	0.2107	0.2263	0.1823	0.0318	0.0395	0.0327	0.0346	0.0042
24.0	0.2353	0.2217	0.2647	0.0390	0.0462	0.0408	0.0420	0.0038
26.0	0.2580	0.2710	0.2503	0.0468	0.0545	0.0484	0.0499	0.0040
28.0	0.3077	0.3430	0.2810	0.0562	0.0649	0.0569	0.0594	0.0048
30.0	0.2883	0.3183	0.3580	0.0650	0.0746	0.0679	0.0692	0.0049
32.0	0.3603	0.3280	0.3680	0.0760	0.0846	0.0791	0.0799	0.0044
34.0	0.3203	0.3430	0.3970	0.0858	0.0951	0.0912	0.0907	0.0047
36.0	0.4070	0.4240	0.3777	0.0982	0.1080	0.1027	0.1030	0.0049
40.0	0.4800	0.5060	0.4790	0.1128	0.1234	0.1173	0.1179	0.0053
44.0	0.5167	0.5637	0.5323	0.1286	0.1406	0.1335	0.1342	0.0061
48.0	0.5733	0.6017	0.6000	0.1460	0.1590	0.1518	0.1523	0.0065
56.0	0.5810	0.6487	0.6440	0.1638	0.1788	0.1715	0.1713	0.0075
72.0	0.5750	0.5970	0.6523	0.1813	0.1970	0.1913	0.1899	0.0079

Table O5 The absorbance intensity and amount of IN permeated from crosslinked DCNR at 0.0032 crosslink ratio under an electric field (E = 5 V)

Time	Absorbance			Amount of drug permeated (mg)				
(h)	1	2	3	1	2	3	Avg	SD
0.167	0.0224	0.0224	0.0181	0.0007	0.0007	0.0006	0.0006	0.0001
0.333	0.0417	0.0417	0.0483	0.0020	0.0020	0.0020	0.0020	0.0000
0.5	0.0613	0.0613	0.0530	0.0038	0.0038	0.0036	0.0038	0.0001
1.0	0.0443	0.0443	0.0333	0.0052	0.0052	0.0047	0.0050	0.0003
1.5	0.0710	0.0710	0.0363	0.0073	0.0073	0.0058	0.0068	0.0009
2.0	0.0443	0.0443	0.0570	0.0087	0.0087	0.0075	0.0083	0.0007
2.5	0.0333	0.0333	0.0897	0.0097	0.0097	0.0102	0.0099	0.0003
3.0	0.0467	0.0347	0.0670	0.0111	0.0108	0.0123	0.0114	0.0008
3.5	0.0727	0.0393	0.0650	0.0133	0.0120	0.0143	0.0132	0.0012
4.0	0.0763	0.0763	0.0803	0.0157	0.0143	0.0167	0.0156	0.0012
6.0	0.1037	0.1037	0.0827	0.0188	0.0175	0.0192	0.0185	0.0009
8.0	0.1167	0.1137	0.1200	0.0224	0.0209	0.0229	0.0221	0.0010
10.0	0.1547	0.1420	0.1597	0.0271	0.0252	0.0278	0.0267	0.0013
12.0	0.1623	0.2220	0.1703	0.0321	0.0320	0.0330	0.0323	0.0005
14.0	0.1967	0.2300	0.1693	0.0381	0.0390	0.0381	0.0384	0.0005
16.0	0.2710	0.2377	0.2043	0.0463	0.0463	0.0443	0.0456	0.0011
18.0	0.2267	0.2600	0.2210	0.0532	0.0542	0.0511	0.0528	0.0016
20.0	0.2850	0.2517	0.3050	0.0619	0.0619	0.0604	0.0614	0.0009
22.0	0.3527	0.3527	0.2977	0.0727	0.0726	0.0695	0.0716	0.0018
24.0	0.3913	0.3913	0.3373	0.0846	0.0846	0.0797	0.0830	0.0028
26.0	0.3947	0.4193	0.3460	0.0966	0.0973	0.0903	0.0948	0.0039
28.0	0.4353	0.4587	0.4863	0.1099	0.1113	0.1051	0.1088	0.0033
32.0	0.4993	0.4993	0.5047	0.1251	0.1265	0.1205	0.1241	0.0032
34.0	0.5010	0.5343	0.5057	0.1404	0.1428	0.1359	0.1397	0.0035
36.0	0.5233	0.5667	0.5747	0.1564	0.1601	0.1534	0.1566	0.0033
40.0	0.5670	0.6337	0.6433	0.1736	0.1794	0.1731	0.1754	0.0035
48.0	0.6683	0.6683	0.7143	0.1940	0.1998	0.1948	0.1962	0.0031
56.0	0.6913	0.6783	0.7117	0.2151	0.2205	0.2165	0.2174	0.0028
72.0	0.7187	0.6980	0.6673	0.2370	0.2418	0.2369	0.2385	0.0028

Table O6 The absorbance intensity and amount of IN permeated from crosslinked DCNR at 0.0032 crosslink ratio under an electric field (E = 7 V)

Time	Absorbance			Amount of drug permeated (mg)				
(h)	1	2	3	1	2	3	Avg	SD
0.167	0.0957	0.1940	0.1777	0.0029	0.0059	0.0054	0.0047	0.0016
0.333	0.0503	0.0517	0.0417	0.0045	0.0075	0.0067	0.0062	0.0016
0.5	0.0487	0.0238	0.0282	0.0059	0.0082	0.0075	0.0072	0.0012
1.0	0.0142	0.0245	0.0000	0.0064	0.0090	0.0080	0.0078	0.0013
1.5	0.0460	0.0193	0.0151	0.0078	0.0095	0.0085	0.0086	0.0009
2.0	0.0637	0.0333	0.0235	0.0097	0.0106	0.0092	0.0098	0.0007
2.5	0.0877	0.0261	0.0580	0.0124	0.0114	0.0110	0.0116	0.0007
3.0	0.0700	0.0473	0.0443	0.0145	0.0128	0.0123	0.0132	0.0011
3.5	0.0460	0.0797	0.0433	0.0159	0.0152	0.0137	0.0149	0.0012
4.0	0.1093	0.0770	0.0643	0.0193	0.0176	0.0156	0.0175	0.0018
6.0	0.1057	0.0377	0.0833	0.0225	0.0187	0.0182	0.0198	0.0023
8.0	0.0953	0.1257	0.1017	0.0254	0.0226	0.0213	0.0231	0.0021
10.0	0.1333	0.1147	0.1077	0.0294	0.0261	0.0245	0.0267	0.0025
12.0	0.1390	0.1750	0.1260	0.0337	0.0314	0.0284	0.0312	0.0027
14.0	0.2297	0.2153	0.1800	0.0407	0.0380	0.0339	0.0375	0.0034
16.0	0.2023	0.2680	0.1973	0.0469	0.0461	0.0399	0.0443	0.0038
18.0	0.2567	0.2280	0.2947	0.0547	0.0531	0.0489	0.0522	0.0030
20.0	0.3107	0.2997	0.2760	0.0642	0.0622	0.0573	0.0612	0.0035
22.0	0.2830	0.3347	0.2520	0.0728	0.0724	0.0650	0.0701	0.0044
24.0	0.3463	0.3937	0.3227	0.0833	0.0844	0.0748	0.0809	0.0053
26.0	0.3697	0.3420	0.2820	0.0946	0.0948	0.0834	0.0910	0.0065
28.0	0.3037	0.4110	0.4183	0.1039	0.1074	0.0962	0.1025	0.0057
30.0	0.3677	0.3743	0.4170	0.1151	0.1188	0.1089	0.1142	0.0050
32.0	0.4660	0.4630	0.5023	0.1293	0.1329	0.1242	0.1288	0.0044
34.0	0.4993	0.4537	0.5143	0.1445	0.1467	0.1399	0.1437	0.0035
36.0	0.5167	0.5607	0.5003	0.1603	0.1638	0.1551	0.1597	0.0044
40.0	0.6980	0.6683	0.5917	0.1815	0.1842	0.1732	0.1796	0.0058
44.0	0.6667	0.6870	0.6557	0.2019	0.2052	0.1932	0.2001	0.0062
48.0	0.6693	0.7053	0.6743	0.2223	0.2267	0.2137	0.2209	0.0066
56.0	0.7083	0.7417	0.7613	0.2439	0.2493	0.2369	0.2434	0.0062
72.0	0.7513	0.6883	0.7277	0.2668	0.2703	0.2591	0.2654	0.0057

Table O7 The absorbance intensity and amount of IN permeated from crosslinked DCNR at 0.0032 crosslink ratio under an electric field (E = 9 V)

Time	Absorbance			Amount of drug permeated (mg)				
(h)	1	2	3	1	2	3	Avg	SD
0.167	0.1350	0.1603	0.1673	0.0041	0.0049	0.0051	0.0047	0.0005
0.333	0.0350	0.0607	0.0337	0.0052	0.0067	0.0061	0.0060	0.0008
0.5	0.0268	0.0120	0.0291	0.0060	0.0071	0.0070	0.0067	0.0006
1.0	0.0329	0.0092	0.0152	0.0070	0.0074	0.0075	0.0073	0.0003
1.5	0.0607	0.0690	0.0597	0.0089	0.0095	0.0093	0.0092	0.0003
2.0	0.0450	0.0347	0.0527	0.0102	0.0105	0.0109	0.0106	0.0003
2.5	0.0380	0.0793	0.0380	0.0114	0.0130	0.0121	0.0121	0.0008
3.0	0.0627	0.0857	0.0747	0.0133	0.0156	0.0143	0.0144	0.0011
3.5	0.0577	0.0737	0.0873	0.0151	0.0178	0.0170	0.0166	0.0014
4.0	0.0857	0.0917	0.0563	0.0177	0.0206	0.0187	0.0190	0.0015
6.0	0.0533	0.0880	0.0707	0.0193	0.0233	0.0209	0.0212	0.0020
8.0	0.0847	0.0893	0.0777	0.0219	0.0260	0.0232	0.0237	0.0021
10.0	0.0733	0.0967	0.1043	0.0241	0.0290	0.0264	0.0265	0.0024
12.0	0.1443	0.1620	0.0967	0.0285	0.0339	0.0294	0.0306	0.0029
14.0	0.1547	0.1477	0.1163	0.0332	0.0384	0.0329	0.0348	0.0031
16.0	0.2003	0.2237	0.2480	0.0393	0.0452	0.0405	0.0417	0.0031
18.0	0.2407	0.2913	0.2680	0.0467	0.0541	0.0486	0.0498	0.0039
20.0	0.3200	0.3350	0.2780	0.0564	0.0643	0.0571	0.0593	0.0044
22.0	0.3267	0.3047	0.3247	0.0664	0.0736	0.0670	0.0690	0.0040
24.0	0.3683	0.4103	0.3673	0.0776	0.0861	0.0782	0.0807	0.0048
26.0	0.3907	0.4247	0.3427	0.0895	0.0991	0.0887	0.0924	0.0058
28.0	0.4533	0.3963	0.4340	0.1033	0.1112	0.1019	0.1055	0.0050
30.0	0.4713	0.4780	0.4517	0.1177	0.1257	0.1157	0.1197	0.0053
32.0	0.5020	0.5180	0.4763	0.1330	0.1415	0.1302	0.1349	0.0059
34.0	0.5683	0.5530	0.5613	0.1503	0.1584	0.1473	0.1520	0.0057
36.0	0.5753	0.5970	0.5600	0.1679	0.1766	0.1644	0.1696	0.0063
40.0	0.6180	0.5890	0.6403	0.1867	0.1945	0.1839	0.1884	0.0055
44.0	0.6057	0.6367	0.6600	0.2052	0.2140	0.2040	0.2077	0.0054
48.0	0.6657	0.6700	0.6450	0.2255	0.2344	0.2237	0.2279	0.0057
56.0	0.7173	0.7410	0.6817	0.2474	0.2570	0.2445	0.2496	0.0065
72.0	0.7470	0.6483	0.7177	0.2701	0.2767	0.2663	0.2711	0.0053

Release Kinetics of Model Drug from IN-loaded Crosslinked DCNR Films

The appearance of two steps of IN permeation from all crosslinked DCNR films in figure O1, was investigated for a transport behavior using the Korsmeyer-Peppas equation:

$$\frac{M_t}{M_\infty} = kt^n \quad \text{(O1)}$$

where M_t and M_∞ = the amount of drug released from DCNR film at time t and the total amount of drug release, respectively (mg),

k = the kinetic constant (h^{-n}),

t = time (h),

n = the diffusion scaling exponent.

Then, the log value of M_t/M_∞ was plotted against log time to calculate the release exponent, n according to Eq. (O2)

$$\log\left(\frac{M_t}{M_\infty}\right) = \log k + n \log t \quad \text{(O2)}$$

The first diffusional exponents, n_1, from each batch are equal to 0.569, 0.354, 0.608, 0.626, 0.748, 0.423, and 0.463 at E = 0, 0.1, 1, 3, 5, 7, and 9 V, respectively. The result indicates that the drug transport behavior in this region can be considered as the Fickian diffusion. For the second diffusional exponent, n_2, the values are 1.705, 1.476, 1.216, 1.644, 1.407, 1.438, and 1.615 at E = 0, 0.1, 1, 3, 5, 7, and 9 V, respectively. This transport mechanism is considered as Super Case II transport which results from a relaxation of polymer and an erosion mechanism (Sriamornsak *et al.*, 2007).

The release mechanism is force-fitted to Higuchi equation (n = 0.5) and then the diffusion coefficient of IN from a crosslinked DCNR film can be calculated by Eq. (O3), Eq. (O4), and Eq. (O5):

$$\frac{M_t}{M_\infty} = kt^{1/2} \quad \text{(O3)}$$

$$Q = \frac{M_t}{A} = 2C_0\left(\frac{Dt}{\pi}\right)^{1/2} \quad \text{(O4)}$$

$$M_t = k_H M_\infty t^{1/2} = 2C_0 \left(\frac{D^{1/2}}{\pi^{1/2}}\right) A\, t^{1/2} \quad \text{(O5)}$$

where M_t/M_∞ = the fractional drug release

k_H = a kinetic constant (with the unit of t^{-n})

t = the release time

Q = the amount of material flowing through a unit cross section of barrier (g/cm^2) in unit time, t (s)

C_0 = the initial drug concentration in the film (g/cm^3)

D = the diffusion coefficient of a drug (cm^2/s)

The diffusion coefficient was calculated from the slope of the plot of the amounts of IN permeated from IN-loaded DCNR at time t versus square root of time.

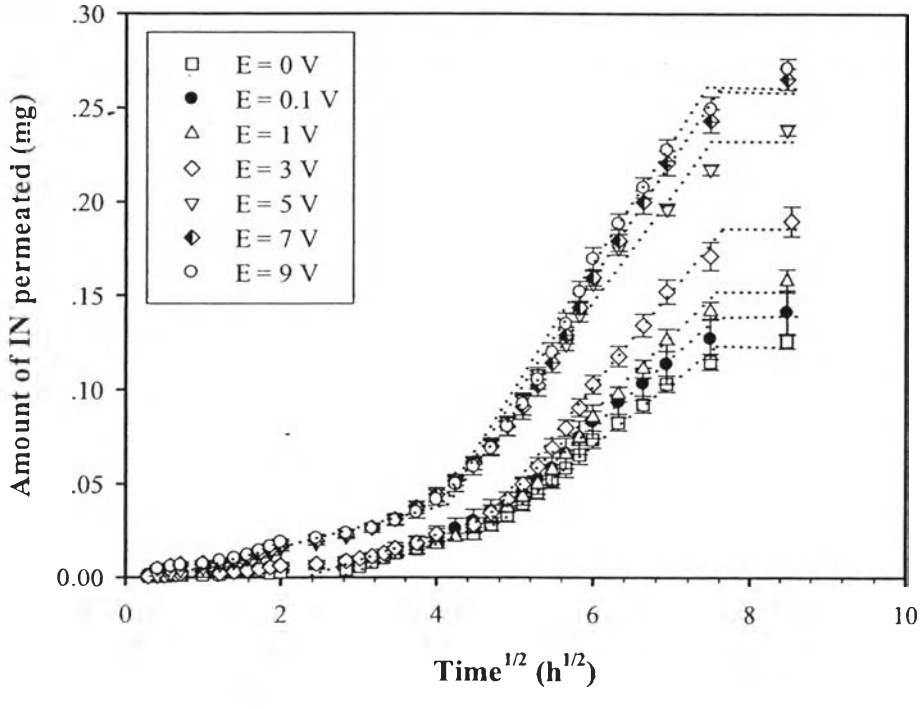

Figure O2 Amounts of IN permeated from IN-loaded DCNR film versus time$^{1/2}$ with various electric field strengths at 0.0032 crosslink ratio, pH 7.4, 37 °C.

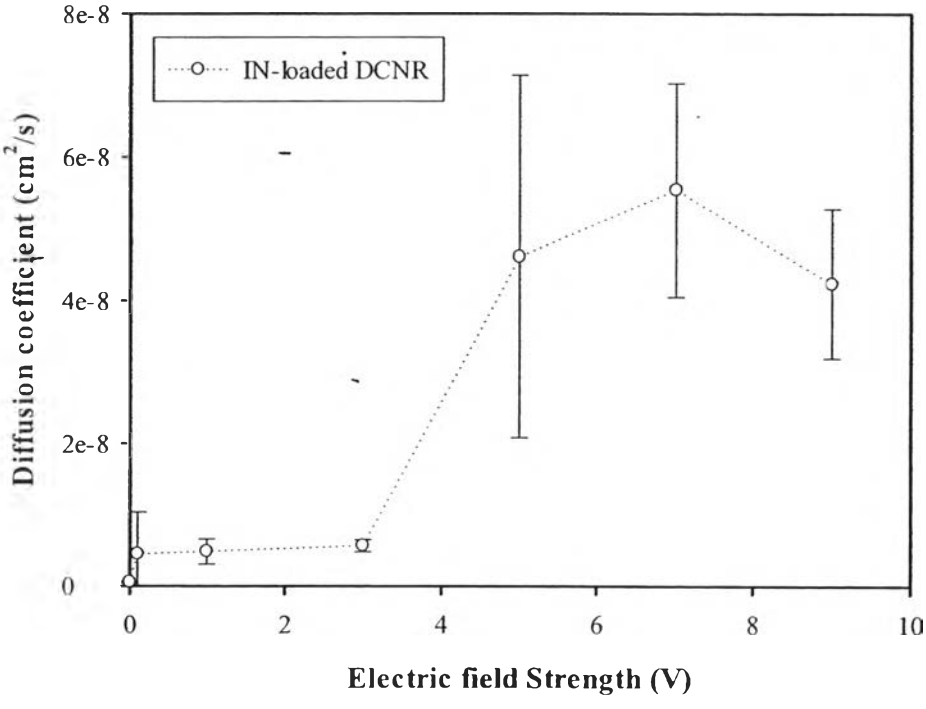

Figure O3 Diffusion coefficients (n_1) of IN permeated from IN-loaded DCNR film versus time$^{1/2}$ with various electric field strengths at 0.0032 crosslink ratio, pH 7.4, 37 °C.

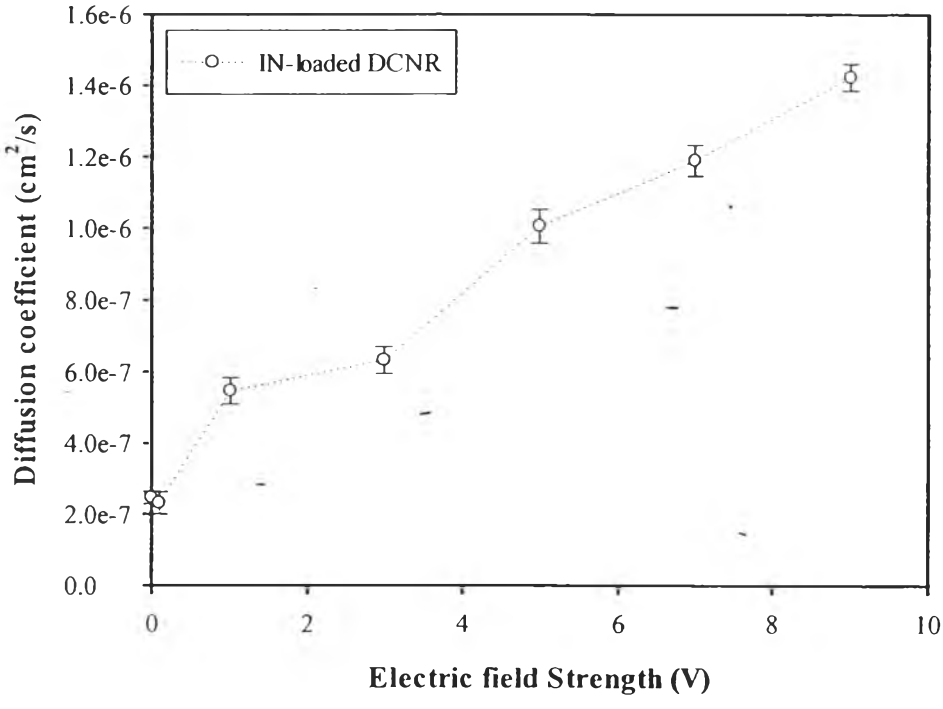

Figure O4 Diffusion coefficients (n_2) of IN permeated from IN-loaded DCNR film versus time$^{1/2}$ with various electric field strengths at 0.0032 crosslink ratio, pH 7.4, 37 °C.

Table O8 The diffusion coefficients (D_I) of IN permeated from the IN-loaded DCNR films with various electric field strengths at 0.0032 crosslink ratio, pH 7.4 at 37 °C

Electric field strength (V)	Slope	Diffusion coefficient (cm^2/h)	Diffusion coefficient (cm^2/s)	Average (cm^2/s)	SD
0	0.0019	2.47E-06	6.86E-10	5.74E-10	1.02E-10
	0.0016	1.75E-06	4.86E-10		
	0.0017	1.98E-06	5.50E-10		
0.1	0.0023	3.62E-06	1.01E-09	4.49E-09	5.87E-09
	0.0077	4.06E-05	1.13E-08		
	0.0025	4.28E-06	1.19E-09		
1	0.0047	1.51E-05	4.19E-09	4.86E-09	1.76E-09
	0.0043	1.27E-05	3.52E-09		
	0.006	2.47E-05	6.86E-09		
3	0.0058	2.30E-05	6.39E-09	5.70E-09	8.51E-10
	0.0056	2.15E-05	5.87E-09		
	0.005	1.71E-05	4.75E-09		
5	0.0126	1.09E-04	3.03E-08	4.61E-08	2.53E-08
	0.0199	2.71E-04	7.53E-08		
	0.0131	1.18E-04	3.28E-08		
7	0.0147	1.48E-04	4.11E-08	5.55E-08	1.49E-08
	0.0193	2.55E-04	7.08E-08		
	0.0169	1.96E-04	5.44E-08		
9	0.0138	1.30E-04	3.61E-08	4.24E-08	1.04E-08
	0.0169	1.96E-04	5.44E-08		
	0.0139	1.32E-04	3.67E-08		

Table O9 The diffusion coefficients (n_2) of IN permeated from the IN-loaded DCNR films with various electric field strengths at 0.0032 crosslink ratio, pH 7.4 at 37 °C

Electric field strength (V)	Slope	Diffusion coefficient (cm^2/h)	Diffusion coefficient (cm^2/s)	Average (cm^2/s)	SD
0	0.0357	8.73E-04	2.43E-07	2.46E-07	1.75E-08
	0.0373	9.53E-04	2.65E-07		
	0.0348	8.29E-04	2.30E-07		
0.1	0.0356	8.68E-04	2.41E-07	2.32E-07	3.18E-08
	0.0368	9.27E-04	2.56E-07		
	0.0321	7.06E-04	1.96E-07		
1	0.0540	2.00E-03	5.56E-07	5.46E-07	3.70E-08
	0.0515	1.82E-03	5.06E-07		
	0.0551	2.08E-03	5.78E-07		
3	0.0557	2.12E-03	5.89E-07	6.32E-07	3.77E-08
	0.0587	2.36E-03	6.56E-07		
	0.0586	2.35E-03	6.53E-07		
5	0.0719	3.54E-03	9.83E-07	1.00E-06	4.43E-08
	0.0745	3.80E-03	1.06E-06		
	0.0716	3.51E-03	9.75E-07		
7	0.0784	4.21E-03	1.17E-06	1.19E-06	4.34E-08
	0.0808	4.47E-03	1.24E-06		
	0.0782	4.19E-03	1.16E-06		
9	0.0870	5.18E-03	1.44E-06	1.42E-06	3.83E-08
	0.0874	5.23E-03	1.45E-06		
	0.0852	4.97E-03	1.38E-06		

Appendix P Determination of Amounts and Diffusion Coefficient of IN Permeated from IN-loaded DCNR Film at Crosslinking Ratio = 0.0032 at various Electrode Polarities

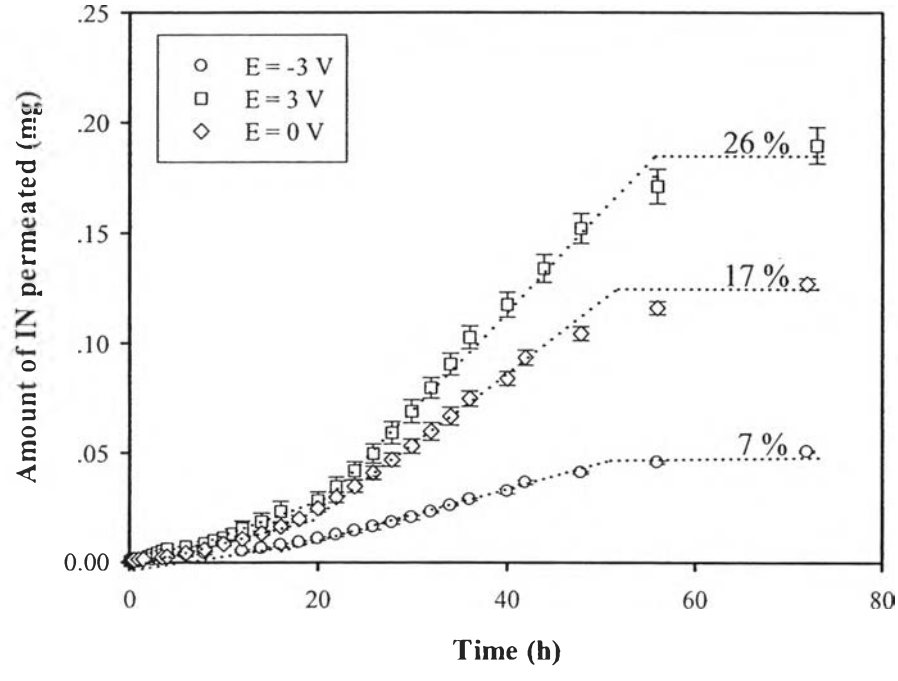

Figure P1 Amount of IN permeated from crosslinked DCNR film at 0.0032 crosslink ratio versus time t under the cathode, the anode, and the absence of electric field, pH 7.4, 37 °C.

The total amounts of IN permeated from the DCNR film connected to the cathode at 0 and 3 V and the anode at 3 V of electric field strength are 0.118 (17 %), 0.186 (26 %), and 0.049 (7 %) mg, respectively. The amount of IN permeated under the negatively charged electrode (cathode in the donor part) is higher than the others under the cathode without the electric field and under the anode, respectively. The electrorepulsion between the negative charge of drug and the negative charge of cathode promotes a faster drug release through the membrane. Without the electric field, drug concentration gradient drives the drug permeation. Under the anode, the electroattractive force between the negative charge of drug and the positive charge of

anode delays the permeation of IN through the films into a PBS buffer which results in the lowest amount of IN permeated (Juntanon *et al.*, 2008).

Release Kinetics of Model Drug from IN-loaded Crosslinked DCNR Films

The appearance of two steps of IN permeation from all crosslinked DCNR films in figure P1, was investigated for a transport behavior using Korsmeyer-Peppas equation:

$$\frac{M_t}{M_\infty} = kt^n \quad \text{(P1)}$$

where M_t and M_∞ = the amount of drug released from DCNR film at time t and the total amount of drug release, respectively (mg),

k = the kinetic constant (h^{-n}),

t = time (h),

n = the diffusion scaling exponent.

Then, the log value of M_t/M_∞ was plotted against log time to calculate the release exponent, n according to Eq. (P2)

$$\log\left(\frac{M_t}{M_\infty}\right) = \log k + n \log t \quad \text{(P2)}$$

The release mechanism is force-fitted to the Higuchi equation (n = 0.5) and then the diffusion coefficient of IN from a crosslinked DCNR film can be calculated by Eq. (P3), Eq. (P4), and Eq. (P5):

$$\frac{M_t}{M_\infty} = kt^{1/2} \quad \text{(P3)}$$

$$Q = \frac{M_t}{A} = 2C_0\left(\frac{Dt}{\pi}\right)^{1/2} \quad \text{(P4)}$$

$$M_t = k_H M_\infty t^{1/2} = 2C_0 \left(\frac{D^{1/2}}{\pi^{1/2}}\right) A\, t^{1/2} \quad \text{(P5)}$$

where M_t/M_∞ = the fractional drug release

k_H = a kinetic constant (with the unit of t^{-n})

t = the release time

Q = the amount of material flowing through a unit cross section of barrier (g/cm^2) in unit time, t (s)

C_0 = the initial drug concentration in the film (g/cm^3)

D = the diffusion coefficient of a drug (cm^2/s)

The diffusion coefficient was calculated from the slope of the plot of the amounts of IN permeated from IN-loaded DCNR at time t versus square root of time.

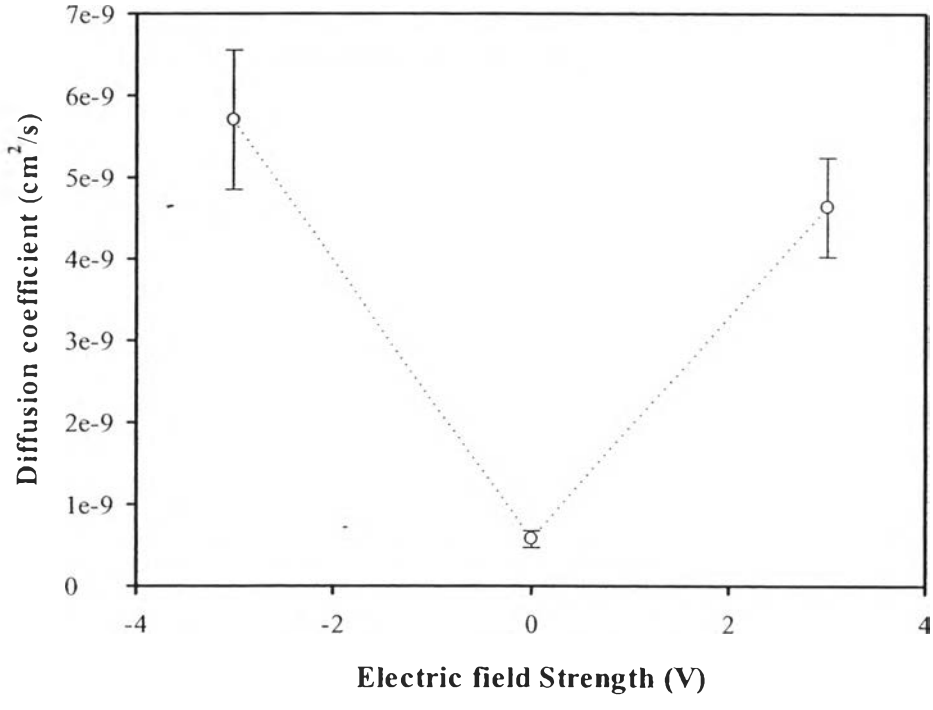

Figure P2 The diffusion coefficients (D_2) of IN permeated from IN-loaded DCNR film versus $time^{1/2}$ with 0.0032 crosslink ratio under the cathode, the anode, and the absence of electric field, pH 7.4, 37 °C.

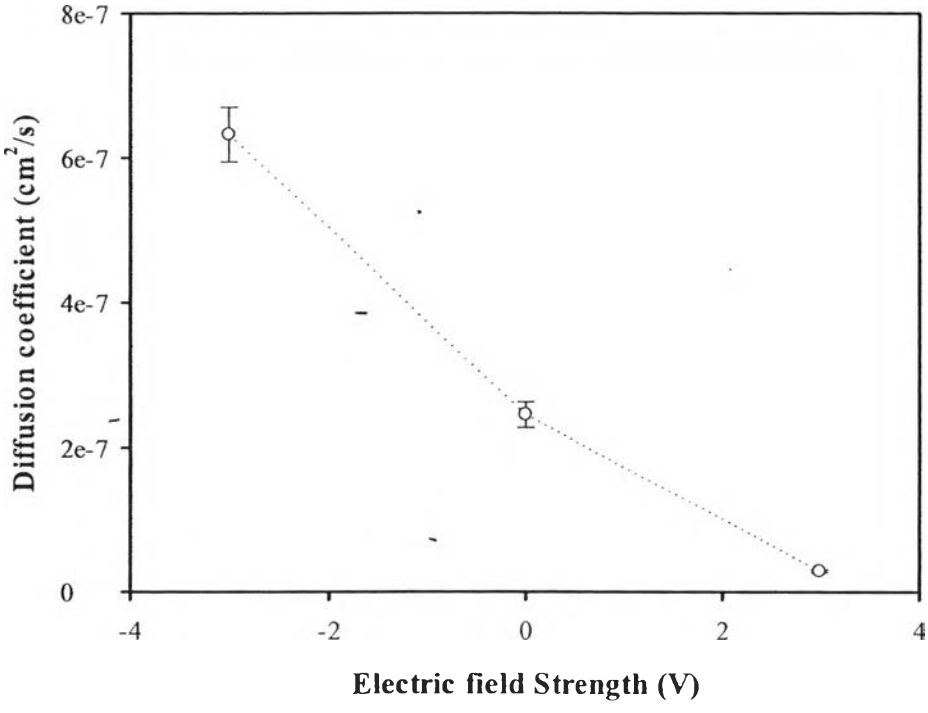

Figure P3 The diffusion coefficients (n_2) of IN permeated from IN-loaded DCNR film versus time$^{1/2}$ with 0.0032 crosslink ratio under the cathode, the anode, and the absence of electric field, pH 7.4, 37 °C.

Table P1 The diffusion coefficients (n_1) of IN permeated from crosslinked DCNR films under the cathode, the anode, and the absence of electric field, pH 7.4 at 37 °C

Electric field strength (V)	Slope	Diffusion coefficient (cm^2/h)	Diffusion coefficient (cm^2/s)	Average (cm^2/s)	SD
0	0.0019	2.47E-06	6.86E-10	5.74E-10	1.02E-10
	0.0016	1.75E-06	4.86E-10		
	0.0017	1.98E-06	5.5E-10		
3 (cathode)	0.0058	2.30E-05	6.39E-09	5.70E-09	8.52E-10
	0.0056	2.15E-05	5.97E-09		
	0.0050	1.71E-05	4.75E-09		
3 (anode)	0.0047	1.51E-05	4.19E-09	4.64E-09	6.09E-10
	0.0048	1.58E-05	4.39E-09		
	0.0053	1.92E-05	5.33E-09		

Table P2 The diffusion coefficients (n_2) of IN permeated from crosslinked DCNR films under the cathode, the anode, under the absence of electric field, pH 7.4 at 37 °C

Electric field strength (V)	Slope	Diffusion coefficient (cm^2/h)	Diffusion coefficient (cm^2/s)	Average (cm^2/s)	SD
0	0.0357	8.73E-04	2.43E-07	2.46E-07	1.74E-08
	0.0373	9.53E-04	2.65E-07		
	0.0348	8.29E-04	2.30E-07		
3 (cathode)	0.0557	2.12E-03	5.89E-07	6.32E-07	3.77E-08
	0.0587	2.36E-03	6.56E-07		
	0.0586	2.35E-03	6.53E-07		
3 (anode)	0.0127	1.10E-04	3.06E-08	2.89E-08	1.82E-09
	0.0119	9.70E-05	2.69E-08		
	0.0124	1.05E-04	2.92E-8		

Appendix Q Determination of Amounts and Diffusion Coefficient of IN Released from IN-loaded PCz/DCNR Blend Film at Crosslinking Ratio = 0.0032 with Various Electric Field Strengths under Cathode

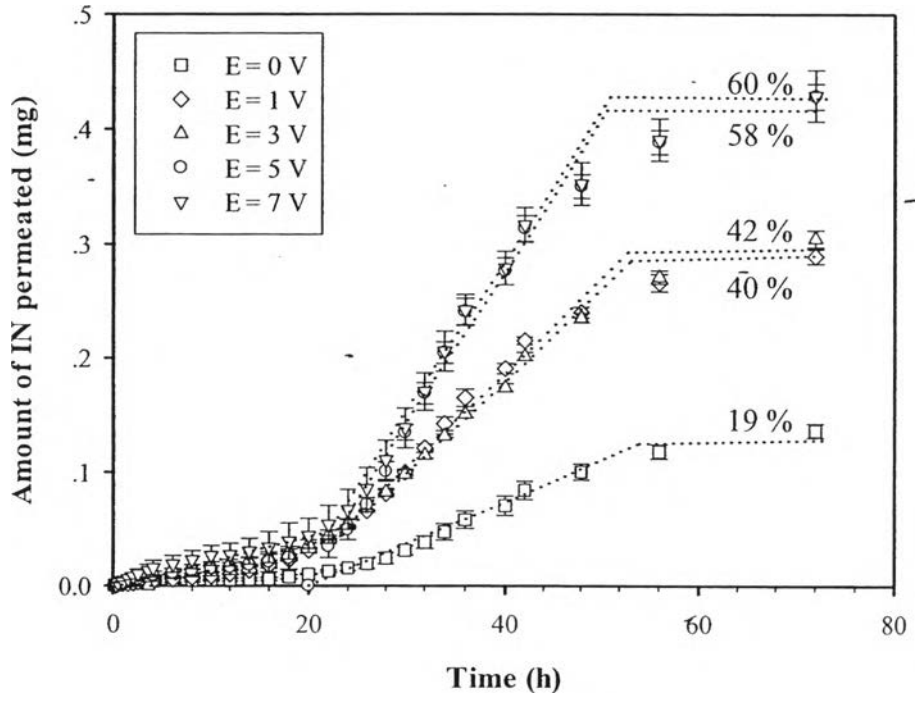

Figure Q1 Amount of IN permeated from PCz/DCNR blend film at 0.0032 crosslink ratio versus time t at various electric field strengths, pH 7.4, 37 °C.

Release Kinetics of Model Drug from IN-doped PCz/DCNR Films

The appearance of two steps of IN permeation from all crosslinked DCNR films in figure Q1, was investigated for a transport behavior using the Korsmeyer-Peppas equation:

$$\frac{M_t}{M_\infty} = kt^n \qquad \text{(Q1)}$$

where M_t and M_∞ = the amount of drug released from DCNR film at time t and the total amount of drug release, respectively (mg),

k = the kinetic constant (h^{-n}),

t = time (h),

n = the diffusion scaling exponent.

Then, the log value of M_t/M_∞ was plotted against log time to calculate the release exponent, n according to Eq. (Q2)

$$\log\left(\frac{M_t}{M_\infty}\right) = \log k + n \log t \quad \text{(Q2)}$$

The release mechanism is force-fitted to the Higuchi equation (n = 0.5) and then the diffusion coefficient of IN from a crosslinked DCNR film can be calculated by Eq. (Q3), Eq. (Q4), and Eq. (Q5):

$$\frac{M_t}{M_\infty} = kt^{1/2} \quad \text{(Q3)}$$

$$Q = \frac{M_t}{A} = 2C_0\left(\frac{Dt}{\pi}\right)^{1/2} \quad \text{(Q4)}$$

$$M_t = k_H M_\infty t^{1/2} = 2C_0 \left(\frac{D^{1/2}}{\pi^{1/2}}\right) A\, t^{1/2} \quad \text{(Q5)}$$

where M_t/M_∞ = the fractional drug release

k_H = a kinetic constant (with the unit of t^{-n})

t = the release time

Q = the amount of material flowing through a unit cross section of barrier (g/cm^2) in unit time, t (s)

C_0 = the initial drug concentration in the film (g/cm^3)

D = the diffusion coefficient of a drug (cm^2/s)

The diffusion coefficient was calculated from the slope of the plot of the amounts of IN permeated from IN-loaded DCNR at time t versus square root of time.

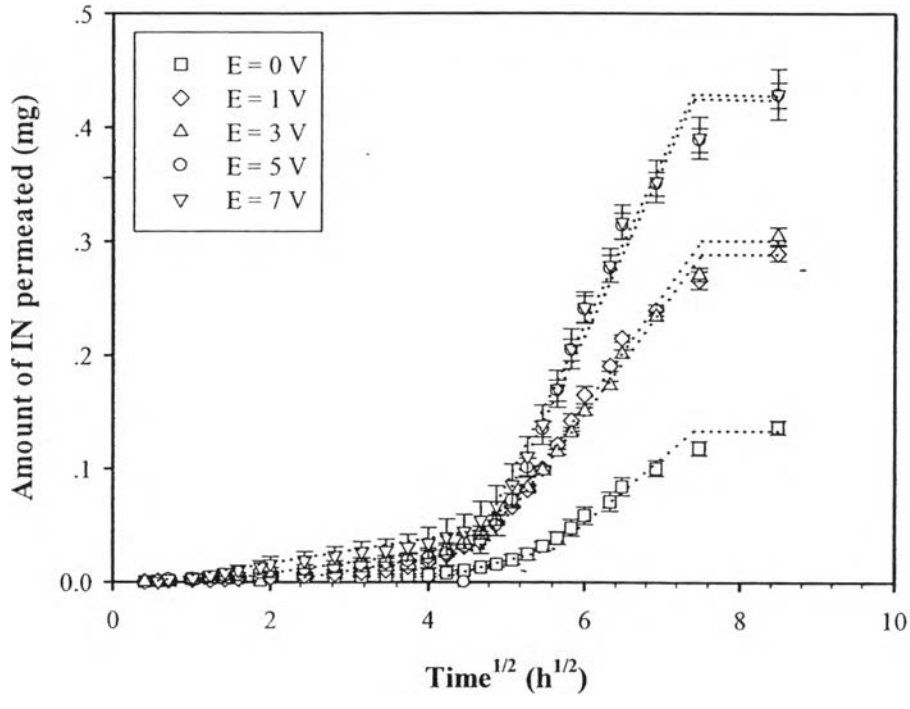

Figure Q2 Amounts of IN permeated from IN-doped PCz/DCNR film versus time$^{1/2}$ with 0.0032 crosslink ratio at various electric field strengths, pH 7.4, 37 °C.

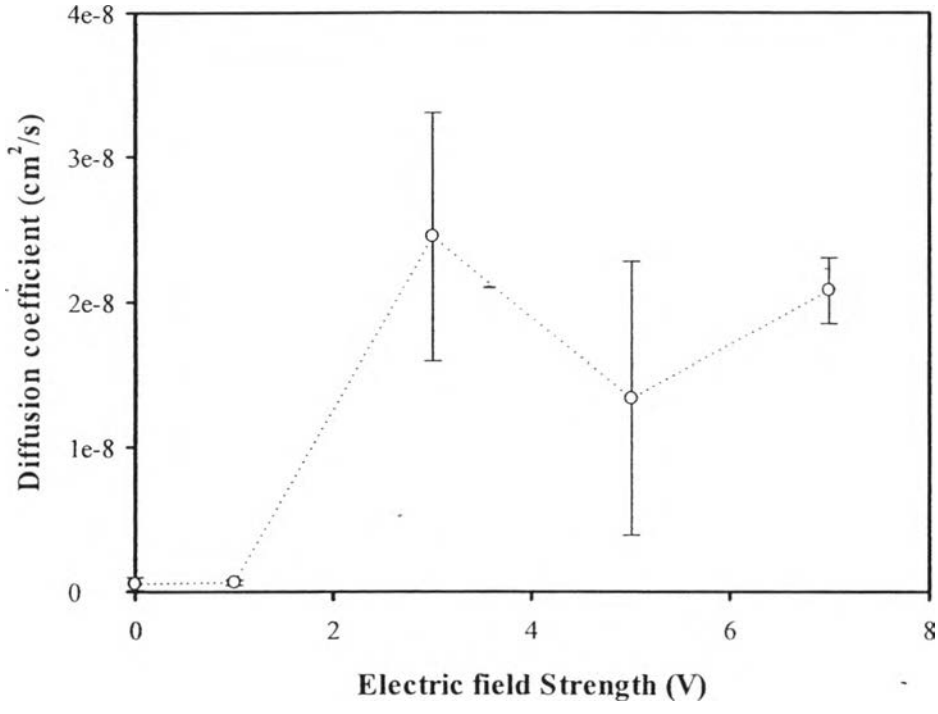

Figure Q3 Diffusion coefficients (D_I) of IN permeated from IN-doped PCz/DCNR blend film versus time$^{1/2}$ at various electric field strengths using 0.0032 crosslink ratio, pH 7.4, 37 °C.

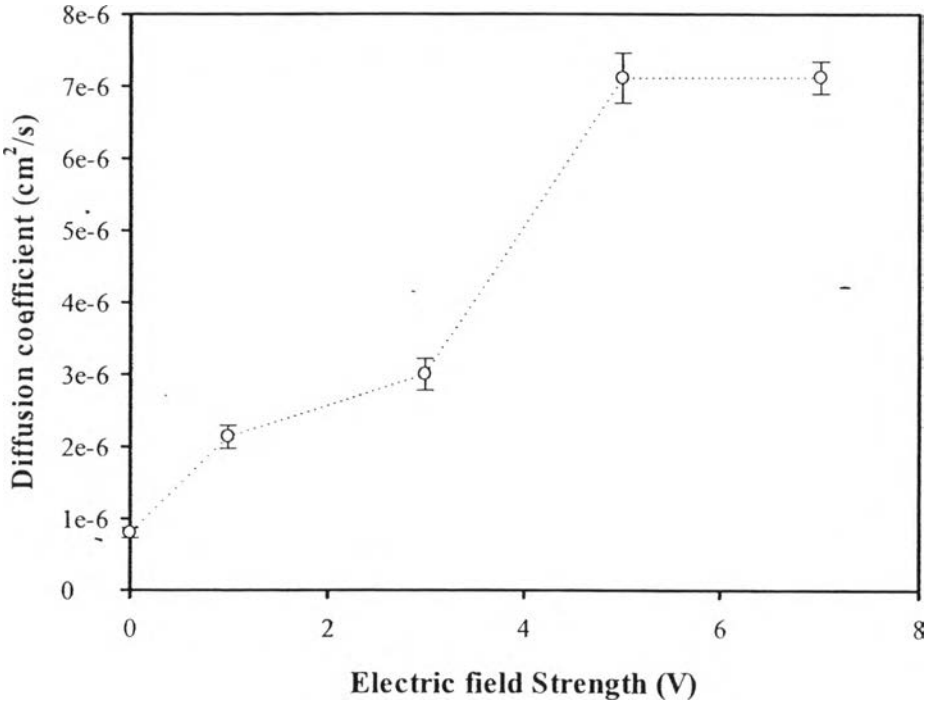

Figure Q4 Diffusion coefficients (D_2) of IN permeated from IN-doped PCz/DCNR blend film versus time$^{1/2}$ with various electric field strengths at 0.0032 crosslink ratio, pH 7.4, 37 °C.

Table Q1 The diffusion coefficients (D_1) of IN permeated from PCz/DCNR blend films under the cathode, the anode, and the absence of electric field, pH 7.4 at 37 °C

Electric field (V)	Slope	Diffusion coefficient (cm^2/h)	Diffusion coefficient (cm^2/s)	Average (cm^2/s)	SD
0	0.0010	7.04E-07	1.96E-10	5.38E-10	4.41E-10
	0.0023	3.73E-06	1.04E-09		
	0.0014	1.38E-06	3.83E-10		
1	0.0015	1.58E-06	4.39E-10	6.43E-10	1.81E-10
	0.0020	2.82E-06	7.83E-10		
	0.0019	2.54E-06	7.06E-10		
3	0.0109	8.37E-05	2.33E-08	2.45E-08	8.59E-09
	0.0131	1.21E-04	3.36E-08		
	0.0092	5.96E-05	1.66E-08		
5	0.0106	7.91E-05	2.20E-08	1.34E-08	9.43E-09
	0.0087	5.33E-05	1.48E-08		
	0.0041	1.18E-05	3.28E-09		
7	0.0099	6.90E-05	1.92E-08	3.81E-08	3.01E-08
	0.0193	2.62E-04	7.28E-08		
	0.0107	8.06E-05	2.24E-08		

Table Q2 The diffusion coefficients (D_2) of IN permeated from PCz/DCNR blend films under the cathode, the anode, and the absence of electric field, pH 7.4 at 37 °C

Electric field (V)	Slope	Diffusion coefficient (cm^2/h)	Diffusion coefficient (cm^2/s)	Average (cm^2/s)	SD
0	0.0610	2.62E-03	7.28E-07	8.01E-07	6.97E-08
	0.0643	2.91E-03	8.08E-07		
	0.0666	3.12E-03	8.67E-07		
1	0.1085	8.29E-03	2.30E-06	2.14E-06	1.60E-07
	0.1007	7.14E-03	1.98E-06		
	0.1043	7.66E-03	2.13E-06		
3	0.1194	1.00E-02	2.78E-06	3.00E-06	2.22E-07
	0.1240	1.08E-02	3.00E-06		
	0.1282	1.16E-02	3.22E-06		
5	0.1863	2.44E-02	6.78E-06	7.11E-06	3.48E-07
	0.1902	2.55E-02	7.08E-06		
	0.1956	2.69E-02	7.47E-06		
7	0.1876	2.48E-02	6.89E-06	7.12E-06	2.23E-07
	0.1909	2.57E-02	7.14E-06		
	0.1935	2.64E-02	7.33E-06		

Appendix R Determination of Amounts and Diffusion Coefficient of IN Released from IN-loaded DCNR Film at Crosslinking Ratio = 0.0048 without Electric Field

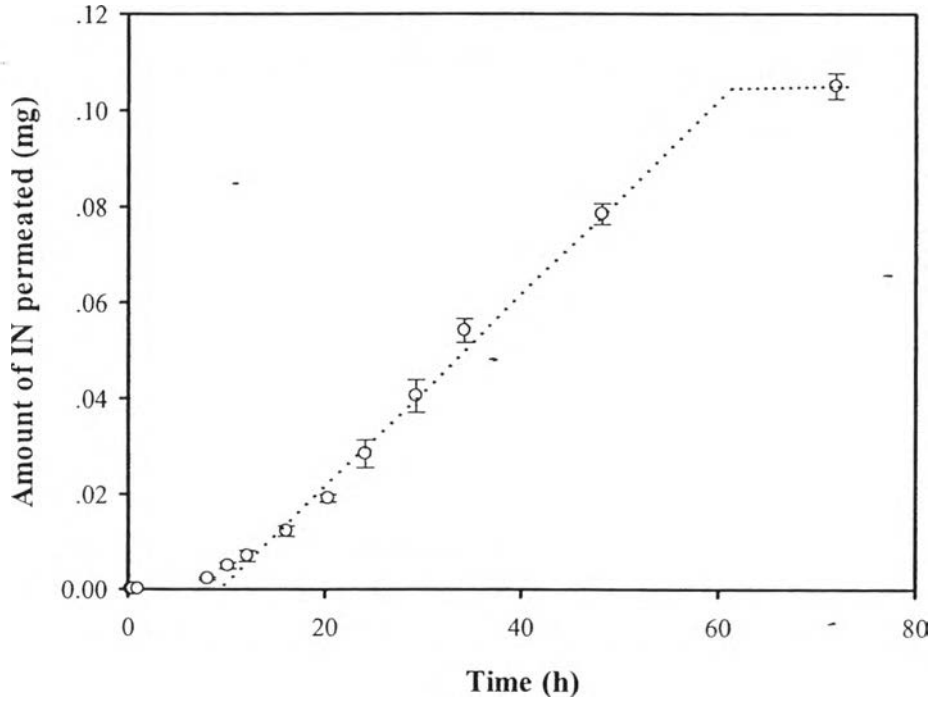

Figure R1 Amount of IN released from DCNR film at 0.0048 crosslink ratio versus time t without electric field, pH 7.4, 37 °C.

Release Kinetics of Model Drug from IN-loaded DCNR Films

The appearance of one step of IN release from all crosslinked DCNR films in figure R1, was investigated for a transport behavior using the Korsmeyer-Peppas equation:

$$\frac{M_t}{M_\infty} = kt^n \quad \text{(R1)}$$

where M_t and M_∞ = the amount of drug released from DCNR film at time t and the total amount of drug release, respectively (mg),

k = the kinetic constant (h^{-n}),

t = time (h),

n = the diffusion scaling exponent.

Then, the log value of M_t/M_∞ was plotted against log time to calculate the release exponent, n according to Eq. (R2)

$$\log\left(\frac{M_t}{M_\infty}\right) = \log k + n \log t \quad \text{(R2)}$$

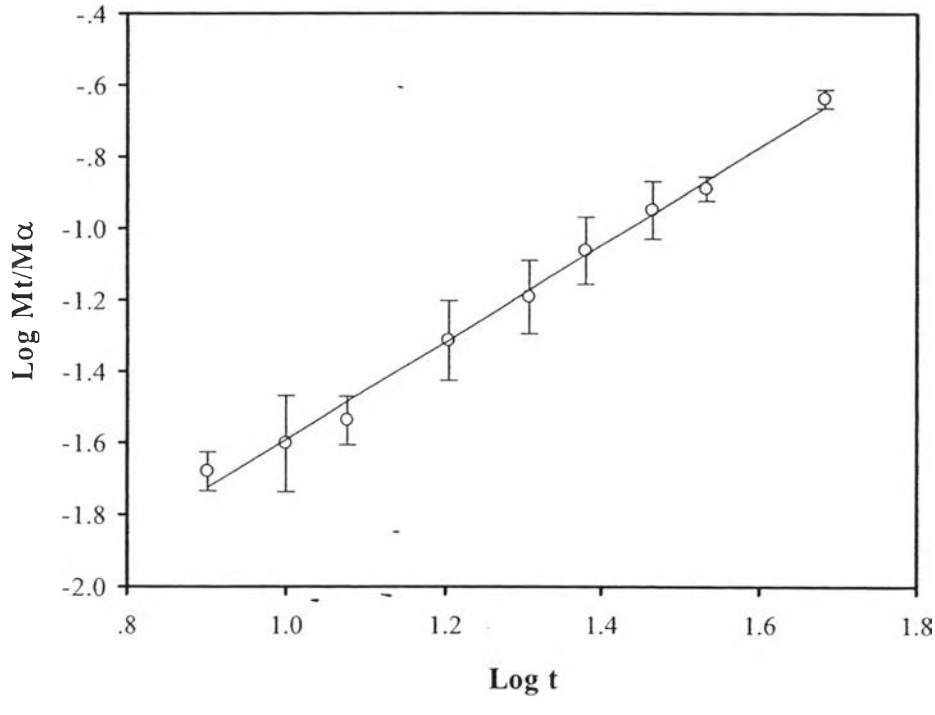

Figure R2 Log (M_t/M_∞) versus log time.

The release mechanism was force-fitted to the Higuchi equation (n = 0.5) and then the diffusion coefficient of IN from a crosslinked DCNR film was calculated by Eq. (R3), Eq. (R4), and Eq. (R5):

$$\frac{M_t}{M_\infty} = kt^{1/2} \quad \text{(R3)}$$

$$Q = \frac{M_t}{A} = 2C_0\left(\frac{Dt}{\pi}\right)^{1/2} \quad \text{(R4)}$$

$$M_t = k_H M_\infty t^{1/2} = 2C_0 \left(\frac{D^{1/2}}{\pi^{1/2}}\right) A\, t^{1/2} \quad \text{(R5)}$$

where M_t/M_∞ = the fractional drug release

k_H = a kinetic constant (with the unit of t^{-n})

t = the release time

Q = the amount of material flowing through a unit cross section of barrier (g/cm^2) in unit time, t (s)

C_0 = the initial drug concentration in the film (g/cm^3)

D = the diffusion coefficient of a drug (cm^2/s)

The diffusion coefficient was calculated from the slope of the plot of the amounts of IN released from IN-loaded DCNR at time t versus square root of time.

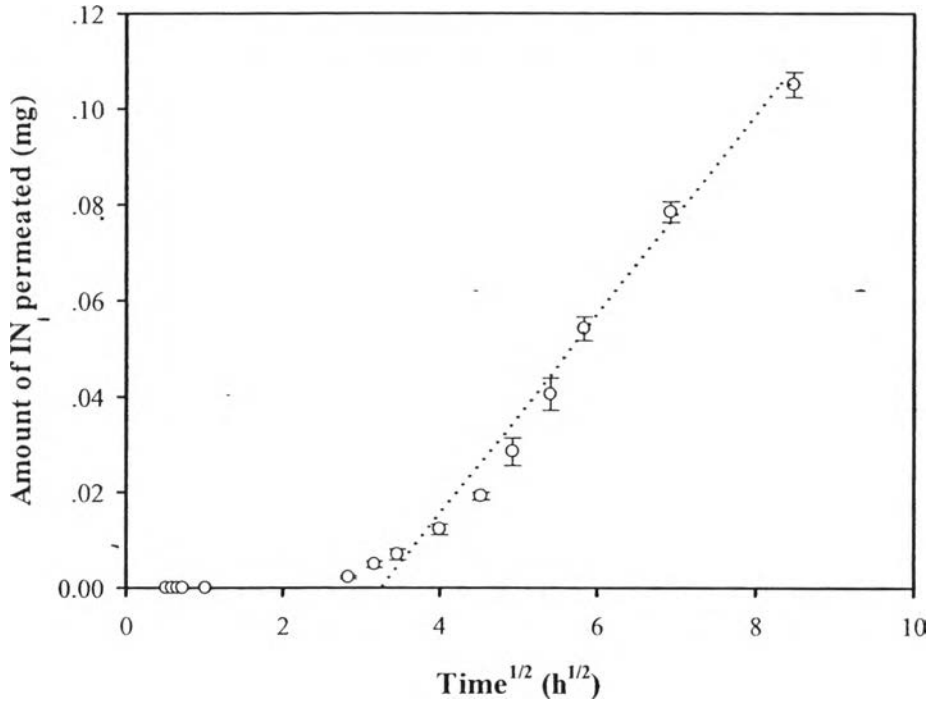

Figure R3 Amounts of IN released from IN-loaded DCNR film versus time$^{1/2}$ with 0.0048 crosslink ratio without electric field, pH 7.4, 37 °C.

The total amount of IN released from the DCNR film is 0.1067 mg. The diffusional exponent and kinetic factor are 1.367 and 0.0110 t^{-n}, respectively. The result provides only one-stage transport of drug and indicates the drug transport mechanism as the Super Case II transport. The diffusion coefficient of IN released from DCNR film at 0.0048 crosslink ratio is $4.00 \pm 0.75 \times 10^{-9}$ cm^2/s.

Appendix S The Permeation and Release Times

A time region in the permeation behavior of IN through a rubber matrix and a pig skin can be divided into three regimes. In the first regime, the amount of IN permeation is nearly independent of square root of time so called the permeation time. The permeation time occurred from the natures of the DCNR matrix (mostly) and the pig skin which affect to delay the IN release and permeation. In the the second region, IN permeated through the film and the pig skin by the diffusion into the PBS buffer providing an increasing amount of IN release and permeation as a function of time, the so called the releaseduration1. For the third regime, the IN permeated through the DCNR matrix with erosion and through the pigskin, the so called the release duration 2.

Table S1 Permeation and release times of IN permeated from IN-loaded DCNR films and PCz/DCNR blend films

Matrix	E (V)	CL	Permeation time (h)	Release duration 1 (h)	Release duration 2 (h)	Release and permeation time (h)
NR	0	0.0008	6.31	20.52	35.88	56.40
NR	0	0.0032	6.89	13.18	43.67	56.85
NR	0	0.0064	7.56	12.16	43.50	55.65
NR	0.1	0.0032	9.08	11.80	45.20	57.00
NR	1	0.0032	9.36	13.68	42.87	56.55
NR	3	0.0032	7.46	14.63	42.67	57.30
NR	5	0.0032	2.99	18.54	40.29	58.83
NR	7	0.0032	0.50	18.42	37.53	55.95
NR	9	0.0032	0.23	18.87	38.13	57.00
PCz/NR	0	0.0032	11.29	16.59	38.17	54.76
PCz/NR	1	0.0032	6.25	17.66	38.89	56.55
PCz/NR	3	0.0032	2.28	20.00	36.25	56.25
PCz/NR	5	0.0032	0.42	21.86	33.20	55.06
PCz/NR	7	0.0032	0.36	21.64	33.57	55.20

Appendix T Effect of Amount of IN-loaded into the DCNR Film

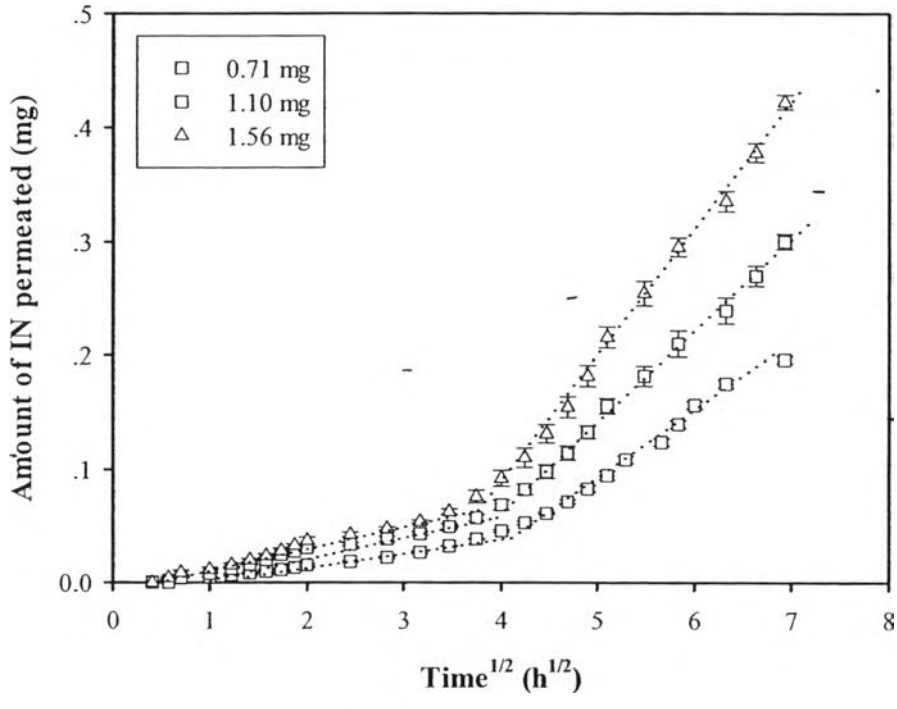

Figure T1 Amount of IN permeated from IN-loaded DCNR film at various amount of drug loading under an applied electric field strength of 5 V.

Amounts of IN permeated from the DCNR film was significantly influenced by the drug-loaded quantity as shown in Figure T1. The amount of IN permeated through the film and the pig skin after 48 hour increases from 0.206 (29 %)mg to 0.301 (27 %) mg and 0.425 (27 %) mg when the amounts of drug loaded varies from 0.71 mg to 1.10 mg and 1.56 mg, respectively.

Appendix U Pore Area to Film Area Ratio

The pore area to film area ratios of the IN-loaded DCNR film with 0 and 3 V of electric field strength generally increase with time until reaching constant values, as shown in Figure U1. The film with an applied electric field at a given time possesses a higher pore area to film area ratio than that without electric field. Moreover the DCNR film without the drug loaded slightly generates pores throughout the film after the permeation study with or without applied electric field, as shown in Figure U2. Thus it appears that the presence of the drug caused the formation of pores, regardless of electric field was applied or not. The pore formation on the matrix surface without the drug loaded occurred as a DCNR surface degradation but at a smaller degree.

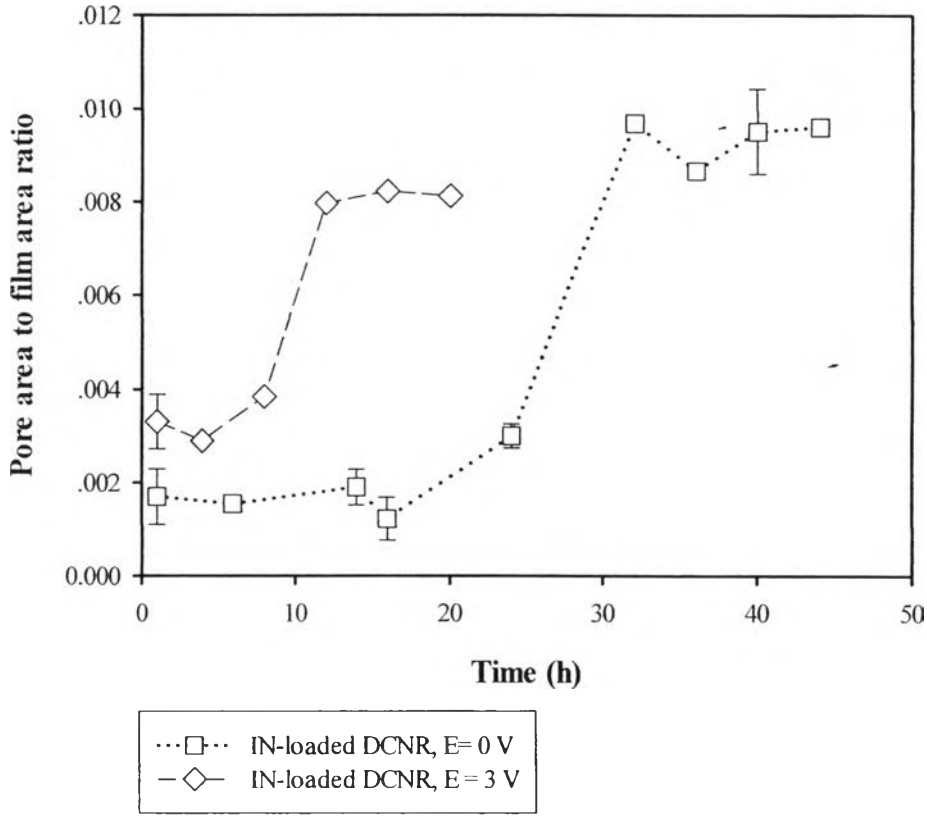

Figure U1 Pore area to film area ratio versus time of IN-loaded DCNR film under 0 and 3 V of the electric field strength.

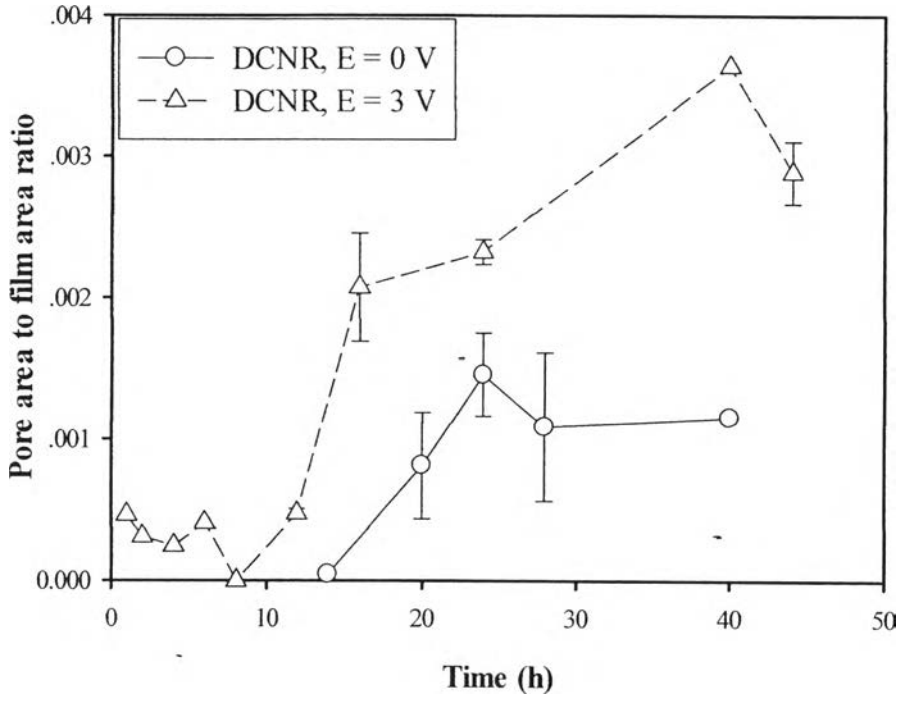

Figure U2 Pore area to film area ratio versus time of DCNR film under 0 and 3 V of the electric field strength.

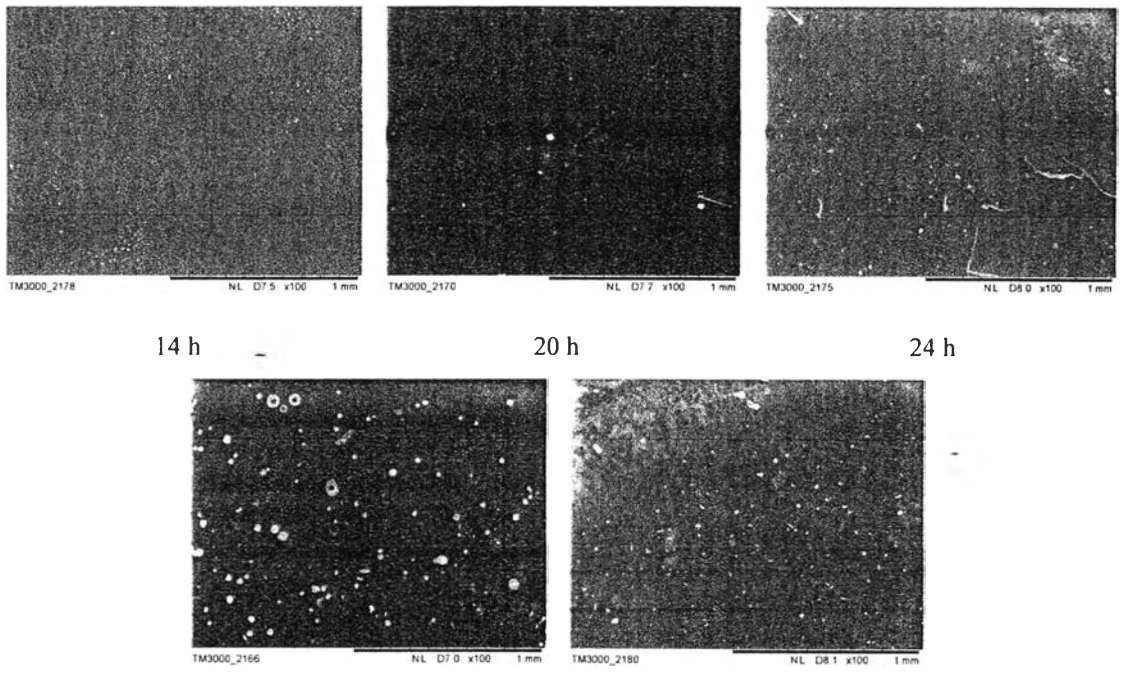

Figure U3 SEM images of DCNR film after the permeation study without an electric field at 100 magnification.

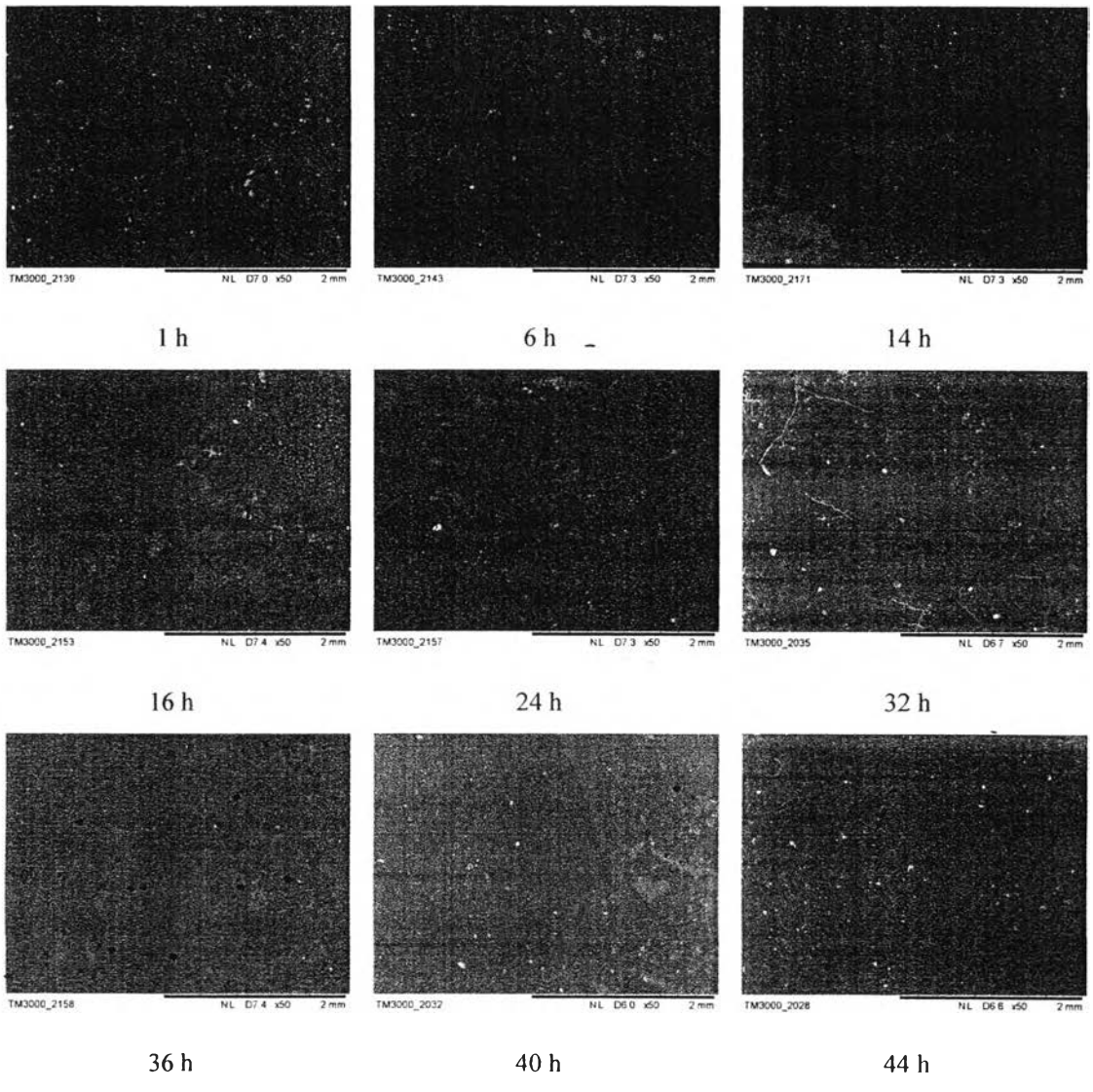

Figure U4 SEM images of IN-loaded DCNR film after the permeation study without an electric field at 50 magnification.

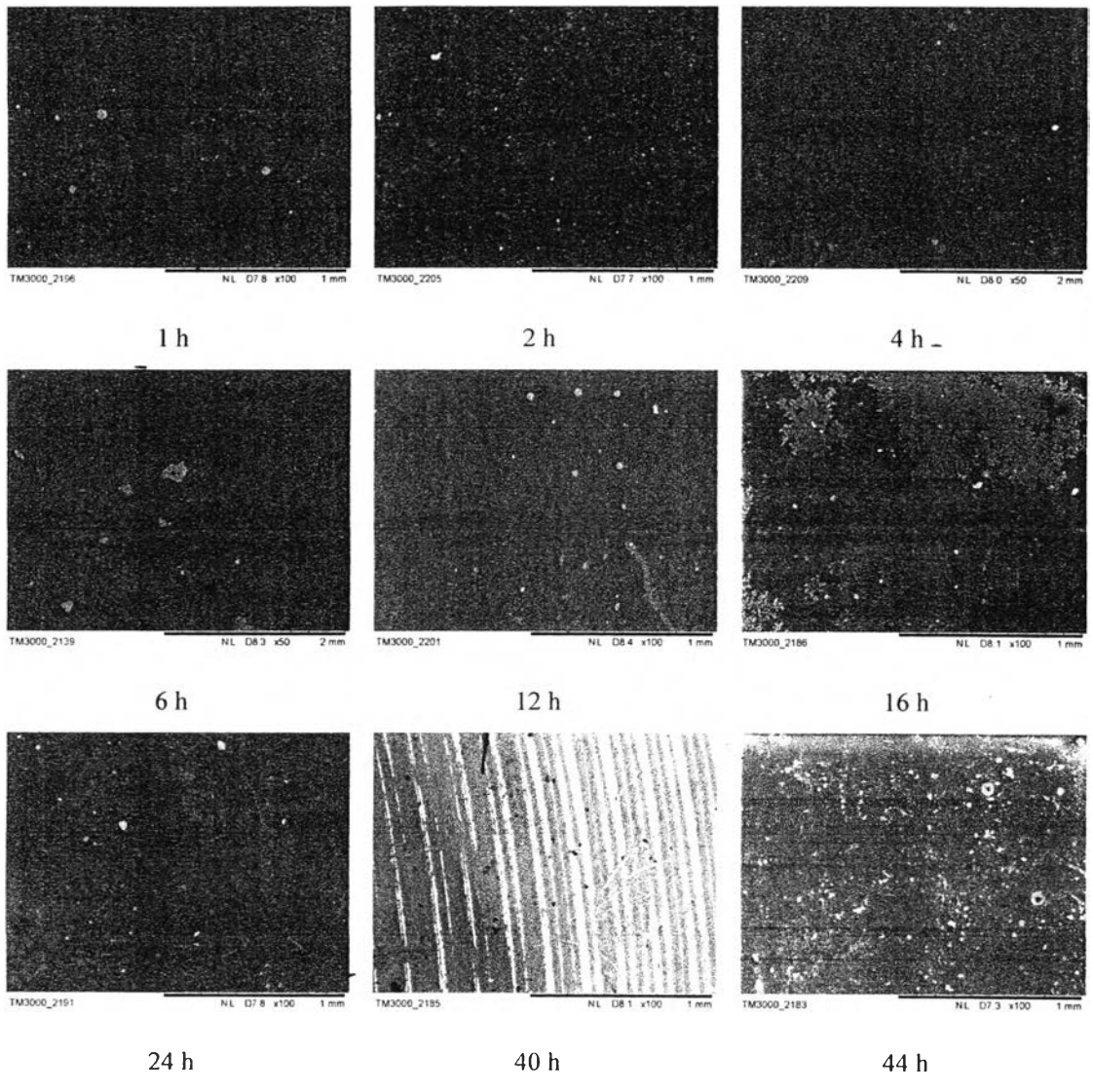

Figure U5 SEM images of DCNR film after the permeation study with an electric field (E = 3 V) at 100 magnification.

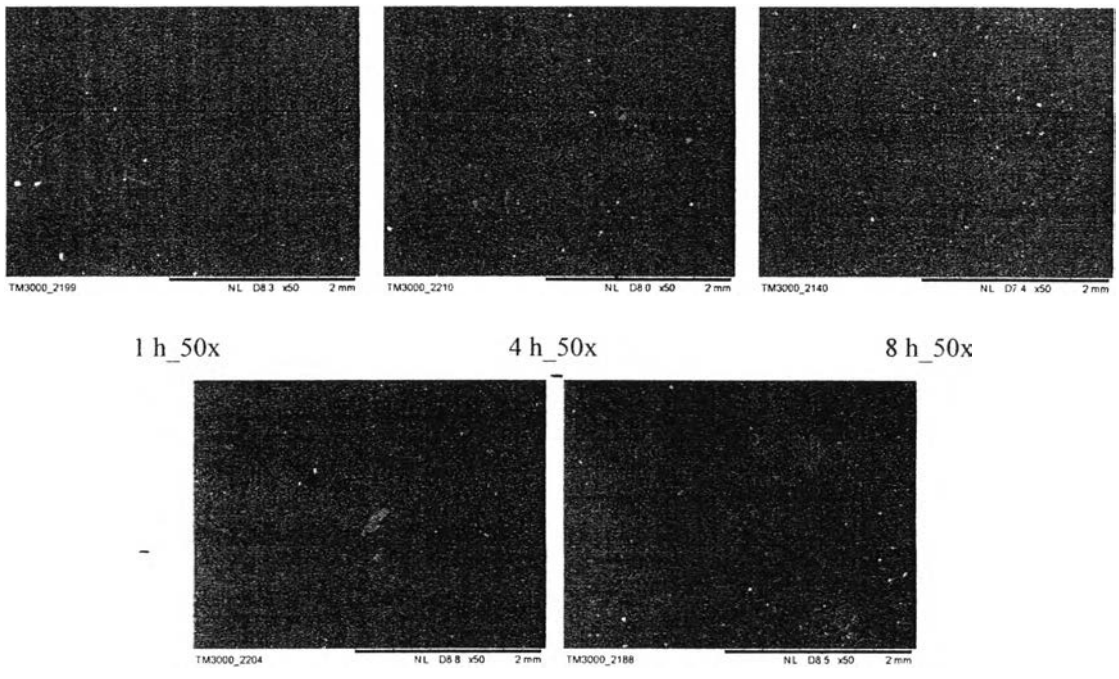

Figure U6 SEM images of IN-load DCNR film after the permeation study with an electric field (E = 3 V).

ต้นฉบับ หน้าขาดหาย

CURRICULUM VITAE

Name: Miss Pornwalai Thorngkham

Date of Birth: July 18, 1990

Nationality: Thai

University Education:

2008–2012 Bachelor Degree of Chemistry Science, Faculty of Science, Chiang Mai University, Chiangmai, Thailand

Proceedings:

1. Thorngkham, P.; and Sirivat, A. (2014, April 22) Permeation Study of Indomethacin from Polycarbazole/Natural Rubber Blend Film under Electric Field. Proceedings of The 5th Research Symposium on Petrochemical and Materials Technology and The 20th PPC Symposium on Petroleum, Petrochemicals, and Polymers, Bangkok, Thailand.

Presentations:

1. Thorngkham, P.; and Sirivat, A. (2014, April 22) Permeation Study of Indomethacin from Polycarbazole/Natural Rubber Blend Film under Electric Field. Paper presented at The 5th Research Symposium on Petrochemical and Materials Technology and The 20th PPC Symposium on Petroleum, Petrochemicals, and Polymers, Bangkok, Thailand.
2. Thorngkham, P.; and Sirivat, A. (2014, May 15-18) Electrically Controlled Release of Indomethacin from Polycarbazole/Natural Rubber Blend Film. Paper presented at The 15th European Biotechnology Congress, Lecce, Italy.